

*Dr. Deij
ontv. 12/6/68*

MEDEDELINGEN EN VERHANDELINGEN

No. 91

P. J. RIJKOORT

**THE INCREASE OF MEAN WIND SPEED WITH HEIGHT
IN THE SURFACE FRICTION LAYER**

1968

Prijs f. 15,50

**THE INCREASE OF MEAN WIND SPEED WITH
HEIGHT IN THE SURFACE FRICTION LAYER**

KONINKLIJK NEDERLANDS METEOROLOGISCH INSTITUUT
MEDEDELINGEN EN VERHANDELINGEN

No. 91

P. J. RIJKOORT

THE INCREASE OF MEAN WIND SPEED WITH HEIGHT
IN THE SURFACE FRICTION LAYER

1968

STAATSDRUKKERIJ/'S-GRAVENHAGE

PUBLIKATIENUMMER K.N.M.I. 102-91

U.D.C.: 551.554

PREFACE

The increase of the mean wind speed with height in dependency of atmospheric stability is a main problem in the theory of the boundary layer. The solution of this problem is of great importance from a theoretical as well as from a practical point of view.

If a reliable formula describing this increase with height was available, important information could be given for a number of practical problems, viz.: air pollution, wind-load on buildings, wind shear for aviation, etc.

A large number of studies exists in meteorological literature in which a solution for this problem is attempted. As a complete physical and mathematical description of the boundary layer processes is very complicated and not yet available, solutions have been sought with the aid of dimensional considerations and ad hoc assumptions. The result is a confused situation featuring a large number of rather different wind profile descriptions.

It is the aim of the present study to bring some sort of order into this rather confused situation. It has turned out to be possible to derive a mathematical system which contains most of the existing formulae.

A method of testing these formulae was indicated, using results of observations.

This study has also been accepted by the Faculty of Natural Sciences of the University of Utrecht as a thesis for the degree of doctor.

*The Director in Chief of the
Royal Netherlands Meteorological Institute*

DR. M. W. F. SCHREGARDUS

VOORWOORD

Een belangrijk probleem in de grenslaagmeteorologie is de toename van de windsnelheid met de hoogte in afhankelijkheid van de atmosferische stabiliteit. Een oplossing van dit probleem is zowel uit theoretisch als uit praktisch oogpunt van groot belang.

Indien een betrouwbare formule beschikbaar zou komen om deze hoogte-afhankelijkheid te beschrijven, zou daarmee belangrijke informatie voor een aantal praktijkproblemen zoals: luchtverontreiniging, windbelasting op constructies, windschering voor de luchtvaart, enz., worden gegeven.

Er bestaan in de meteorologische literatuur een groot aantal studies waarin gepoogd wordt een oplossing voor deze afhankelijkheid te vinden. Aangezien een volledige fysisch-mathematische beschrijving van de processen in de atmosferische grenslaag zeer ingewikkeld is en vooralsnog niet beschikbaar, zijn oplossingen gezocht met behulp van dimensiebeschouwingen en ad hoc onderstellingen. Het gevolg is dat een onoverzichtelijk geheel van een groot aantal zeer verschillende formules is ontstaan.

Het doel van de thans gepubliceerde studie is enige orde te scheppen in deze materie. Het is daarbij mogelijk gebleken een mathematisch systeem af te leiden waarin de meeste formules voorkomen. Met behulp van waarnemingsresultaten wordt aangegeven op welke wijze toetsing van de formules het beste zou kunnen worden uitgevoerd.

Deze studie is tevens aanvaard als dissertatie door de Faculteit der Wiskunde en Natuurwetenschappen van de Universiteit van Utrecht.

De Hoofddirecteur van het
Kon. Nederl. Meteorol. Instituut,
DR. M. W. F. SCHREGARDUS

CONTENTS

Nomenclature

page

11	0	General Introduction
13	1	Theory of wind profile formulae
13	1.1	Introduction
14	1.2	Survey of wind profile formulae
23	1.3	Generalizations
23	1.3.1	Generalization of the derivation of the KEYPS profile
25	1.3.2	Generalization of Businger's derivation of profile formulae
26	1.3.3	A formal overall generalization and its solution
27	1.4	Special cases
27	1.4.1	Special cases of the Plus group
30	1.4.2	Special cases of the Minus group
31	1.4.3	Tables and figures illustrating the Plus and Minus groups
31	1.4.4	Two other groups
37	1.5	The Swinbank formula
37	1.5.1	The relation to the Plus group; its equivalent in the Minus group
39	1.5.2	A by-path: Generalization of the Swinbank formula
41	1.6	The wind speed difference ratio as a function of stability
47	1.7	General comments on the theoretical results
48	2	Applications of profile formulae to numerical results of observations
48	2.0	Introduction
49	2.1	Objections to the $(S, z/L)$ diagram
52	2.2	Application of some of the wind profile formulae to O'Neill data (Great Plains Turbulence Field Program)
52	2.2.0	Introduction
52	2.2.1	The $(\zeta, z/L)$ diagram
63	2.2.2	Probability distribution of V -values as a rough method of selection
66	2.3	Application of some of the wind profile formulae to wind speed observations from Project Prairie Grass
66	2.3.0	Introduction
67	2.3.1	General results
67	2.3.2	The wind speed difference ratios
69	2.3.3	Least squares estimates of the parameters of different wind profile formulae

74	2.3.4	The standard deviation values
76	2.3.5	The stability parameter values
77	2.3.6	The friction velocity values
80	2.3.7	The roughness parameter values
87	3	The value of the power profile exponent as a function of stability
87	3.0	Introduction
88	3.1	Values of the power profile exponent from wind speed measurements at Lopik
89	3.2	The night hours observations
89	3.2.1	Graphical representation of the observations
89	3.2.2	The theoretical variation of the power profile exponent as derived from the Holzman profile
94	3.3	The day-time observations
96	3.4	The variation of z_0 as derived from the variation of p
99		Appendices
99	I.	Standard deviation of $V = \frac{u_3 - u_2}{u_3 - u_1}$ (par. 2.2.1)
100	II.	Regression lines for the $(\zeta, z/L)$ relation (par. 2.2.1)
101	III.	Normality test by means of the χ^2 test (par. 2.2.2)
102	IV.	Testing whether V is dependent on height or not with the aid of the binomial distribution (par. 2.3.2)
102	V.	The method of least squares (par. 2.3.3)
103	VI.	The method of m -rankings (par. 2.3.4)
104	VII.	Kendall's rank correlation test (par. 2.3.7)
105	VIII.	Fitting theoretical p curves to power profile exponent values from Lopik wind speed observations (par. 3.2.2)
106		References
110		Summary
113		Samenvatting

NOMENCLATURE

t	time	t
z	height	l
u	wind speed	lt^{-1}
T	air temperature	deg
θ	potential temperature	deg
u'	horizontal wind speed fluctuation	lt^{-1}
w'	vertical wind speed fluctuation	lt^{-1}
T'	temperature fluctuation	deg
τ	shearing stress	$ml^{-1}t^{-2}$
ρ	air density	ml^{-3}
c_p	specific heat of air at constant pressure	$l^2t^{-2}deg^{-1}$
g	acceleration due to gravity	lt^{-2}
u_*	friction velocity	lt^{-1}
k	von Kármán's constant	—
z_0	roughness parameter	l
E	total turbulent energy per unit mass	l^2t^{-2}
H	vertical flux of heat	mt^{-3}
K_M	coefficient of eddy viscosity	l^2t^{-1}
K_H	coefficient of eddy conductivity	l^2t^{-1}
K	coefficient of eddy transfer (stated : $K_M = K_H$)	l^2t^{-1}
K_f	coefficient of eddy transfer (if all turbulence were mechanical)	l^2t^{-1}
l	mixing length (under diabatic conditions)	l
l_f	mixing length (if all turbulence were mechanical)	l
ν	kinematic viscosity	l^2t^{-1}
ε	total dissipation of turbulent energy per unit mass	l^2t^{-3}
S	non-dimensional wind shear	—
L	Monin-Obukhov stability length	l
β	Deacon's stability parameter	—
B	$1 - \beta$	—
Ri	Richardson number	—
Rf	Richardson flux number ($\equiv (K_H/K_M)Ri$)	—
ζ	stability height parameter	—
η	auxiliary function	—
φ	universal function	—
f	non-dimensional profile function	—
X	Swinbank's diabatic measure of height	l
$\underline{\underline{d}}$	definition symbol	—
$\underline{\underline{\xi}}$	$\frac{d}{d} X/z$	—
$\underline{\underline{\omega}}$	$\frac{d}{d} \xi S$	—

γ	temperature lapse rate	deg l ⁻¹
Γ	potential temperature lapse rate	deg l ⁻¹
λ	measure of size of the largest eddies	l
Δu	velocity difference over the length λ	lt ⁻¹
V	wind speed difference ratio	—
$a..$	different empirical constants	—
p	power profile exponent	—
a	} general exponents	---
b		
q		
A	} different constants	—
C		
c		
\wedge	} symbols indicating adiabatic stratification	
\wedge		
\wedge		

Statistical symbols (Appendices)

σ_x	population standard deviation of variable x
s_x	sample standard deviation of variable x
α_r	} regression coefficients
β_r	
E	expectation symbol
ε	measuring error
Q_t	fraction
ν	number of degrees of freedom
χ^2	chi square statistic
P	probability
r_i	rank order number
h	statistic for the method of m rankings
T	statistic for Kendall's rank correlation test
—	symbol for mean values
~	symbol for estimates or for smoothed values
*	symbol for "true" values

0. GENERAL INTRODUCTION

There are a large number of papers in the literature on meteorology dealing with the problem of the increase of mean wind speed with increasing height.

In considering the flow of air over the earth's surface there is a tendency in the first instance to draw a comparison with hydrodynamics. However, there are important differences between the flow of air in the atmosphere and the flow of liquids as considered in laboratory hydrodynamics.

In the first place, in addition to an increase of speed with increasing height, there is the effect of the Coriolis force, resulting from the rotation of the earth, which causes the wind to change direction with increasing height.

This effect will be ignored in the present study of wind profile formulae. But this means that the height Z , for which a given profile will hold, will be limited to a certain value. This value of Z is not quite constant, as it depends on stability, but is of the order of 50 m (see MONIN and OBUKHOV, 1958). The height Z marks the top of the surface friction layer.

The problem in this layer is reduced to a two-dimensional one. The coordinates x and z will be used, x being assumed to correspond to mean wind direction and z to represent the vertical.

A second important question is the influence of the thermal stratification of the friction layer. This is in fact the complication that creates the problem of the wind speed profile which we are studying. As a result of heating or cooling of the earth's surface, the thermal stratification can change from very unstable through neutral (adiabatic) to very stable, and a quantity therefore has to be introduced to act as a stability parameter.

The well-known formulae for the wind speed profile, the power "law" and the logarithmic "law", are inadequate to describe completely the increase of wind speed with height. However, they are often used in papers on practical meteorological problems, and they may often prove useful.

It is customary to speak of the power "law" and the logarithmic "law". It seems to me that the word "law" is too weighty. To speak of any relation as a "law" supposes its general validity. The power "law" is only an empirical formula that can be used as a very rough approximation but without any physical basis of proof. The logarithmic profile could be called a law, even though it holds only for the neutral state, because a generally accepted physical basis is present. For the sake of consistency I propose to speak of profile formulae, or, profiles for short, in all cases.

Stationarity of the atmospheric processes is an important prerequisite for the theoretical derivation of wind profile formulae. The concept of stationarity can be defined in two different but equivalent ways, statistically and physically.

The statistical definition of stationarity is based on the variation of the considered quantity x (speed, temperature, etc.) as a function of time t , written $x(t)$, or as a

result of a stochastic (random) process. A stochastic process is called stationary if the multivariate distribution of $x(t_1), \dots, x(t_n)$ is the same as the distribution of $x(t_1 + t_*), \dots, x(t_n + t_*)$ for every t_* and every group of arguments t_1, \dots, t_n .

To define stationarity physically we must look at the phenomenon of turbulence. By turbulence is understood the irregular variations of speed and temperature that are superimposed on a time average. They comprise a certain amount of energy (E). A situation is stationary if the variation of the total turbulent energy is zero ($dE/dt = 0$), (and the form of the energy spectrum is constant).

The stationarity requirement limits the time interval for which the profile formulae will obtain. On the one hand this interval cannot be too short or the random fluctuations will not cancel out; the lower limit is about 10 minutes. On the other hand the interval cannot be too long, because otherwise factors such as long-period fluctuations or trends (e.g. the daily temperature range) may come into play. The upper limit is usually one hour, but may be more depending on the kind of long-period fluctuations present.

Turbulence may be divided into mechanical and thermal, or convective, turbulence. Mechanical turbulence is the result of the motion of the air over the rough surface of the earth; thermal turbulence is caused by heating and cooling of the earth's surface owing to incoming and outgoing radiation, which may result in instability of the lower layers, leading to rising and descending motions of air parcels.

It is the aim of the present study to review the different profile formulae which have been discussed in the literature on the subject and to combine them into a general system, so as to facilitate comparison between them. As we shall see, the introduction of this general system makes it possible to create an unlimited number of new formulae.

Observations from the "GREAT PLAINS TURBULENCE FIELD PROGRAM" undertaken in 1953 and the "PROJECT PRAIRIE GRASS" in 1956, both in O'NEILL—NEBRASKA, will be used to illustrate the value of the various profile formulae. Definite conclusions cannot be drawn from these observations, unfortunately, since they are too few and too inaccurate.

The power "law" as it is termed, being in fact a simple formula often used for practical purposes, will be studied in a separate chapter. The variability of the power profile exponent will be investigated, both theoretically, using one of the formulae for the diabatic case and empirically, using observations recorded at television and radio transmission towers in the central Netherlands (Lopik).

1. THEORY OF WIND PROFILE FORMULAE

1.1 Introduction

The basic equations used in theoretical derivations of wind profile formulae are the well-known transfer equations:

$$K_M \frac{du}{dz} = \frac{\tau}{\rho} = u_*^2 \quad (1.1.1)$$

$$K_H \frac{d\theta}{dz} = - \frac{H}{c_p \rho} \quad (1.1.2)$$

where τ is the shearing stress defined by:

$$\tau = - \rho \overline{u'w'} \quad (1.1.3)$$

and H is the heat flux defined by:

$$H = c_p \rho \overline{w'T'}. \quad (1.1.4)$$

K_M and K_H are the coefficients of eddy viscosity and conductivity, respectively. They are both functions of z and we formally fix the zero level of z by requiring that $K_M = K_H = 0$ where $z = 0$.

The meaning of the symbols and the dimensions belonging to them are given in the nomenclature (p. 9).

A dash over a symbol indicates that it represents an average over a certain period of time.

It is usual to replace the shearing stress τ as a parameter by the friction velocity u_* defined by:

$$u_* = \sqrt{\frac{\tau}{\rho}} \quad (1.1.5)$$

as was already introduced in (1.1.1).

The stability parameter referred to in the general introduction is a function of u_* and H (see the derivation of the Monin-Obukhov profile (VIII)), and is defined by:

$$L = \frac{d}{k} \frac{u_*^3}{\frac{g}{T} \frac{H}{c_p \rho}}, \quad (1.1.6)$$

L is known as the Monin-Obukhov length.

To simplify the problem, variations of density and deviations of temperature from the mean absolute temperature T will be ignored in (1.1.6); in other words: ρ is constant and T is constant.

Two relevant parameters have now been introduced viz.: u_* and L .

A third parameter, z_0 , is connected with the roughness of the surface. It is fixed by the requirement:

$$u(z_0) = 0 \quad (1.1.7)$$

Finally there is one more requirement, the homogeneity of the surface. It is obvious that a sudden change in the surface roughness will influence the build-up of the atmospheric boundary layer. The detailed effect of inhomogeneity has been studied (e.g. TOWNSEND, 1965) but will be ignored in the present study.

Homogeneity of the surface over a sufficient distance in front of the measuring station is therefore an essential requirement here. The actual distance required depends on the height to which it is desired to measure the wind speed and on atmospheric stability. As a rough estimate a ratio of 100 : 1 between the length of the up-wind area and the maximum measuring height could be taken (see BUSINGER 1954, p. 45). We have to realize that this is a very rigorous requirement, and it can seldom be completely fulfilled in practice.

Apart from the parameters already mentioned two constants also appear in the formulae, viz. a "universal" constant k (von Kármán's constant, numerical value generally taken as 0.4) and a constant α which has to be determined empirically.

A number of different notations for the quantities used are to be found in the large number of papers dealing with the development of wind profile formulae.

In this study we shall use symbols which have been common since the work of MONIN and OBUKHOV, notably:

The non-dimensional wind shear parameter:

$$S \equiv \frac{d}{u_*} \frac{kz}{dz} \frac{du}{dz} \equiv \frac{k}{u_*} \frac{du}{d \ln z} \quad (1.1.8)$$

and a non-dimensional parameter ζ which is proportional to z/L .

$$\zeta \sim z/L. \quad (1.1.9)$$

The proportionality constant will be introduced in a subsequent paragraph. ζ can be considered as a combined height and stability parameter.

We shall try to express all formulae by means of these symbols.

1.2 Survey of wind profile formulae

Table 1.2.1 shows the different formulae which have been proposed throughout the literature on the subject. The original notation has in some cases been changed for the sake of uniformity. We shall use u as the symbol for wind velocity. This is considered as a mean value, averaged over an interval of about an hour, to eliminate turbulent velocity fluctuations.

In the Monin-Obukhov profile the roughness parameter z_0 is sometimes omitted in the linear term. This is in contrast to our formulation, which takes into account formula (1.1.7).

No empirical constant α was introduced by the authors in the Swinbank, Businger

and Su formulae. It became necessary to add this constant in the formulae of table 1.2.1 in order to obtain a general and uniform system. We have added an index to α , to indicate that α takes different values for the different profile formulae.

GOPTAREV has used in his formula only a "constant" a ; this "constant" may be identified with α/L .

In the Deacon formula a parameter β occurs which has to be considered as a stability parameter.

TABLE 1.2.1 *Survey of wind profile formulae*

I. Power profile.

$$u = Az^p$$

(where $A = u_1/z_1^p$ and z_1 is any standard height)

II. Logarithmic profile.

$$u = \frac{u_*}{k} \ln \frac{z}{z_0}$$

III. Deacon profile.

$$u = \frac{u_*}{k(1-\beta)} \left\{ \left(\frac{z}{z_0} \right)^{1-\beta} - 1 \right\}$$

IV. Rossby-Montgomery profile.

$$u = \frac{u_*}{k} \left\{ 3(\eta - \eta_0) + \ln \frac{\eta - 1}{\eta + 1} \frac{\eta_0 + 1}{\eta_0 - 1} \right\}$$

with $\frac{1}{2}(\eta^3 - \eta) = \alpha_{RM} z/L$ and $\frac{1}{2}(\eta_0^3 - \eta_0) = \alpha_{RM} z_0/L$

V. Holzman profile.

$$u = \frac{u_*}{k} \left\{ \ln z/z_0 + \alpha_H(z - z_0)/L + \sqrt{1 + \alpha_H^2 z^2/L^2} - \sqrt{1 + \alpha_H^2 z_0^2/L^2} \right. \\ \left. - \ln \frac{1 + \sqrt{1 + \alpha_H^2 z^2/L^2}}{1 + \sqrt{1 + \alpha_H^2 z_0^2/L^2}} \right\}$$

VI. Businger's first profile.

$$u = \frac{u_*}{k} \left\{ \ln \frac{\sqrt{1 - \alpha_{BIZ}/L} - 1}{\sqrt{1 - \alpha_{BIZ}/L} + 1} \cdot \frac{\sqrt{1 - \alpha_{BIZ_0}/L} + 1}{\sqrt{1 - \alpha_{BIZ_0}/L} - 1} \right. \\ \left. + 2 \frac{\sqrt{1 - \alpha_{BIZ}/L}}{\{1 + \sqrt{1 - \alpha_{BIZ}/L}\}^2} - 2 \frac{\sqrt{1 + \alpha_{BIZ_0}/L}}{\{1 + \sqrt{1 - \alpha_{BIZ}/L}\}^2} \right\}$$

VII. Businger's second profile.

$$u = \frac{u_*}{k} \left\{ \ln z/z_o - \ln \left| \frac{1 - \alpha_{BII} z/L}{1 - \alpha_{BII} z_o/L} \right| \right\}$$

VIII. Monin-Obukhov profile.

$$u = \frac{u_*}{k} \left\{ \ln z/z_o - \alpha_{MO} (z - z_o)/L \right\}$$

IX. KEYPS profile.

$$u = \frac{u_*}{k} \left\{ \frac{\eta_o - \eta}{\eta \eta_o} + 2 \operatorname{arctg} \frac{\eta - \eta_o}{1 + \eta \eta_o} + \ln \frac{(1 + \eta_o)(1 - \eta)}{(1 - \eta_o)(1 + \eta)} \right\}$$

with $(1 - \eta^4)/\eta = \alpha_K z/L$ and $(1 - \eta_o^4)/\eta_o = \alpha_K z_o/L$

X. Su profile.

$$u = \frac{u_*}{k} \left\{ \frac{1}{2} \ln z/z_o + \sqrt{1 + \alpha_{Su} z/L} - \sqrt{1 + \alpha_{Su} z_o/L} \right. \\ \left. + \frac{1}{2} \ln \frac{\sqrt{1 + \alpha_{Su} z/L} - 1}{\sqrt{1 + \alpha_{Su} z/L} + 1} \frac{\sqrt{1 + \alpha_{Su} z_o/L} + 1}{\sqrt{1 + \alpha_{Su} z_o/L} - 1} \right\}$$

XI. Goptarev profile

$$u = \frac{u_*}{k} \left\{ \ln z/z_o + \sum_{n=1}^{\infty} \frac{\alpha_G^n (z^n - z_o^n)}{L^n n n!} \right\}$$

XII. Swinbank profile.

$$u = \frac{u_*}{k} \ln \frac{\exp(\alpha_S z/L) - 1}{\exp(\alpha_S z_o/L) - 1}$$

XIII. Pandolfo profile.

$$u = \begin{cases} \frac{u_*}{k} \{ \ln z/z_o + \alpha_P (z - z_o)/L \} & \text{if } -\frac{1}{7\alpha_P} < z/L < 0 \\ -\frac{6^2}{7^{1\frac{1}{6}}} \frac{u_*}{k} \{ |z_o/L|^{-\frac{1}{6}} - |z/L|^{-\frac{1}{6}} \} & \text{if } z/L < -\frac{1}{7\alpha_P} \end{cases}$$

The full derivation of these formulae can be found in the original papers. For completeness' sake and because we shall use the derivation of KEYPS and the Businger formulae as a basis for our system, we shall now review the various derivations (shortly in most cases, but more extensively on VI, VII, VIII and IX).

I. The power profile originates from hydrodynamics. If we study the flow of fluids through cylindrical pipes we find that the speed increases from the wall to the axis of the pipe according to a power profile. The formula also holds good for the

flow in canals, etc. where the range of values of the Reynolds number¹⁾ is limited. The exponent appears from experiment to be $1/7$, for fully turbulent flow (SCHUBAUER AND TCHEN, 1961). The power profile is often used in meteorology because it is so very simple and a relatively large number of observations prove to conform to it. It is not, however, very accurate. An examination of the exponent p shows that it may vary over a fairly wide range of values and this variation proves to be related to the stability of the atmospheric layer (see chapter 3).

II. The logarithmic profile holds good in an adiabatically layered atmosphere. This fact is generally accepted and is supported by a large number of observations. All formulae which have been proposed to describe "diabatic" situations change into the logarithmic profile formula if the stability parameter is given its value for the adiabatic case.

The logarithmic profile can be derived in different ways. In older papers the concept of the mixing length of Prandtl is used (see SUTTON 1953 p. 72 etc.). A very short derivation is possible with the aid of Monin-Obukhov's similarity hypothesis (1954), (see also KLUG, 1963).

In the adiabatic case expressed in the general symbols S and L , we have:

$$z/L = 0 \text{ and } S = 1 \quad (1.2.1)$$

III. Deacon's profile (1959) is based exclusively on the empirical fact that, if observations of wind speed u are plotted on a graph against the logarithm of height ($\ln z$), a curve is produced which is concave towards the wind speed axis in stable situations and convex in unstable situations.

DEACON states that the curvature can be represented by:

$$\frac{du}{dz} = az^{-\beta} \quad (1.2.2)$$

with $\beta > 1$ for stable situations.

$\beta = 1$ for neutral situations, in which the logarithmic profile results.

$\beta < 1$ for unstable situations.

Incidentally, Deacon's profile cannot be expressed in the S , L or ζ symbols (see 1.5 and 2.3.2).

IV. ROSSBY and MONTGOMERY derived a balance equation for stable and neutral situations. They equated the total turbulent kinetic energy per unit mass in the stable case to the turbulent kinetic energy that would be present if the rate of shear were the

1) The Reynolds number (ul/ν) indicates whether the viscosity effects or the inertia effects dominate in a flowing medium; u is a characteristic speed and l is a characteristic length of the system, ν is the kinematic viscosity.

same but the lapse rate adiabatic, less the potential energy due to the deviation of the temperature lapse rate from the adiabatic rate.

Their equation is written in the following form:

$$l^2 \left(\frac{du}{dz} \right)^2 = l_f^2 \left(\frac{du}{dz} \right)^2 - \frac{g}{T} l^2 \frac{d\theta}{dz} \quad (1.2.3)$$

where l is the mixing length under diabatic conditions and l_f is the equivalent quantity, if all turbulence were of mechanical origin ($l_f = k(z + z_o)$), T is the absolute air temperature. The notation used here is BUSINGER'S (1954).

By assuming $l \frac{du}{dz} = u_*$, which results in:

$$l_f \frac{du}{dz} = u_* \sqrt{1 + \frac{\frac{\alpha g}{T} \frac{d\theta}{dz}}{\left(\frac{du}{dz} \right)^2}} \quad (1.2.4)$$

ROSSBY and MONTGOMERY were able to solve the differential equation for $u(z)$, but their solution, given on p. 49 in their 1935 paper (formula 100), is not quite correct because they introduced a symbol $\kappa^2 = \frac{\alpha g}{T} \frac{d\theta}{dz}$ and proceeded as if it were a constant, while in fact κ^2 is a function of z .

The solution IV (RM profile) which is given in table 1.2.1 therefore differs from Rossby and Montgomery's formula (100).

To be able to express (1.2.3) in terms of S and z/L we have to replace $l_f = k(z + z_o)$ by $l = kz$. This is required in connection with the introduction of z_o as a result of the boundary condition $u(z_o) = 0$, while in the Prandtl formulation $u(0) = 0$ holds.

If we assume $K_H = K_M$ it follows from (1.1.1) and (1.1.2) that $\frac{d\theta}{dz} \frac{du}{dz} = \frac{-H}{c_p \rho u_*^2}$ and with (1.1.6): $\frac{d\theta}{dz} \frac{du}{dz} = \frac{u_*}{k \frac{g}{T} L}$. Using the definition of the symbol S (1.1.8) and after

introduction of a constant, α_{RM} , formula (1.2.3) becomes:

$$S^3 = S + \alpha_{RM} z/L. \quad (1.2.5)$$

V. HOLZMAN made use of Rossby and Montgomery's equation (1.2.4) in 1943 in a study on evaporation. Because, he writes, this equation produces a number of "disagreeable integrals", he replaced it by:

$$l_f \frac{du}{dz} \sqrt{1 - \frac{\frac{\alpha g}{T} \frac{d\theta}{dz}}{\left(\frac{du}{dz} \right)^2}} = u_* \quad (1.2.6)$$

which in fact is no more than an approximation of (1.2.4) for low values of $\frac{\alpha g}{T} \frac{d\theta}{dz}$.

If (1.2.5) is written:

$$S = (1 + (\alpha_{RM}z/L) S^{-1})^{\frac{1}{2}} \quad (1.2.7)$$

the approximation which HOLZMAN makes is equivalent to changing formula (1.2.7) into:

$$S = (1 - (\alpha_{RM}z/L) S^{-1})^{-\frac{1}{2}}$$

or:

$$S^{-2} + (\alpha_{HZ}/L) S^{-1} = 1, \quad (1.2.8)$$

the index RM of the constant α having been replaced by H to indicate that the change is due to HOLZMAN.

The solution is given under V in table 1.2.1.

VI and VII. In his thesis (1954) BUSINGER derived two wind profile formulae based on the formulation of a balance equation as given by ROSSBY and MONTGOMERY (1935), see formula (1.2.3), and by LETTAU (1949).

Although BUSINGER dealt with more advanced theories concerning wind profiles in 1959 and 1961, producing some rather complicated profile formulae, we nevertheless give the derivation and solutions of his earlier formulae. The reason will be explained in the next chapter.

BUSINGER uses the concepts of mixing lengths already mentioned in connection with the derivation of the Rossby-Montgomery profile IV. Furthermore, he defines K_f as the transfer coefficient for purely mechanical turbulence and K as the equivalent quantity for the total turbulence. He also assumes $K_M = K_H = K$.

He then states that:

$$\frac{K}{K_f} = \left(\frac{l}{l_f}\right)^2. \quad (1.2.9)$$

BUSINGER expresses the turbulent balance equation in two ways. First in terms of turbulent acceleration:

$$\frac{K^2}{l^3} = \frac{K_f^2}{l_f^3} - l \frac{g}{T} \frac{d\theta}{dz} \quad (1.2.10)$$

and then in terms of turbulent energy per unit mass:

$$\frac{K^2}{l^2} = \frac{K_f^2}{l_f^2} - l^2 \frac{g}{T} \frac{d\theta}{dz}. \quad (1.2.11)$$

By substitution:

$$K_f = ku_*z \text{ and } l_f = kz \quad (1.2.12)$$

we can transform these equations into expressions in the non-dimensional quantities S and z/L .

(1.2.10) becomes:

$$\frac{u_*^2}{kzS^\dagger} = \frac{u_*^2}{kz} - \frac{u_*^2}{kz} S^\dagger z/L \text{ or (after insertion of a constant } \alpha_{BI}):$$

$$S^\dagger - (\alpha_{BI}z/L)S = 1 \quad (1.2.13)$$

and (1.2.11) becomes:

$$u_*^2 S^{-1} = u_*^2 - u_*^2 (z/L) \text{ or (after insertion of a constant } \alpha_{BII}):$$

$$S - (\alpha_{BII}z/L)S = 1. \quad (1.2.14)$$

The solution of (1.2.13) is given in formula VI, table 1.2.1 and the solution of (1.2.14) in formula VII.

VIII. In the Monin-Obukhov theory a stability measure L (with the dimension of length) is introduced. Its definition is given in formula (1.1.6). Compared with the stability measure Ri introduced by RICHARDSON and defined by:

$$Ri = \frac{d}{T} \frac{g}{dz} \left| \left(\frac{du}{dz} \right)^2 \right|, \quad (1.2.15)$$

L has the advantage of being independent of height (in the friction layer), while Ri is not.

If the non-dimensional wind shear parameter, defined by (1.1.8), is used, Monin and Obukhov's similarity hypothesis¹⁾ leads to the conclusion that S is a function of z/L only:

$$S = \phi(z/L) \quad (1.2.16)$$

where ϕ is assumed to be a universal function.

Since (1.2.1) should still obtain, the simplest form of ϕ that can be used, and that satisfies (1.2.1) is:

$$\phi = 1 + \alpha z/L. \quad (1.2.17)$$

Formula VIII, known as the Monin-Obukhov profile (MO profile) provides a solution for the equations (1.1.8), (1.2.16) and (1.2.17).

IX. KAZANSKY and MONIN (1956), ELLISON (1957), YAMAMOTO (1959), PANOFSKY (1961) and SELLERS (1962) have all developed theories that resulted in a wind profile for the diabatic case. The well-known transfer equations (1.1.1) and (1.1.2) are used to derive these profile formulae. The derivation is based on an equation for the turbulent energy balance. In this equation the total turbulent energy variation is equated to the sum of the rate of variation of mechanical and convective energies, the divergence of potential and kinetic turbulent energy and the rate of dissipation of energy by molecular forces. The mathematical expression of this equation is derived from

1) This hypothesis states that the characteristic statistical quantities of the relative motions of the flow are invariant under the transformation $x' = kx$; $y' = ky$; $z' = kz$ and $t' = kt$.

the Navier-Stokes equation by CALDER (1949) and by HOLLMANN (1961) (see also KLUG, 1963). We already pointed out in the introduction that the condition of stationarity must be fulfilled; this means that the total energy variation must be zero. If a number of simplifying assumptions (see KLUG, 1963) are made regarding the divergence of potential and kinetic energy, the balance equation can be stated in the following form:

$$K_M \left(\frac{du}{dz} \right)^2 - \alpha \frac{g}{T} K_H \frac{d\theta}{dz} = \varepsilon \quad (1.2.18)$$

where the first term represents the mechanical turbulent energy, the second term the convective turbulent energy and ε the total dissipated energy per unit time and unit mass.

Unfortunately attempts to obtain a direct theoretical derivation of an expression for ε in known terms have not yet been successful.

In order to obtain a solution in spite of this difficulty, dimensional considerations have to be used together with the requirement that in the adiabatic case ($d\theta/dz = 0$) the logarithmic profile holds good.

The reasoning is as follows: (see KLUG, 1963).

Because the dissipated energy ε originates from the largest eddies, ε has to be a function of the quantities which characterize these, namely: density ρ , the dimension λ and the change of the mean turbulent velocity (Δu) over the distance λ . From dimensional considerations it follows that ρ cannot be contained in this function. The only remaining possibility then is:

$$\varepsilon = \frac{(\Delta u)^3}{\lambda} = \frac{(\Delta u \cdot \lambda)^3}{\lambda^4} \quad (1.2.19)$$

The dimension of $\Delta u \cdot \lambda$ (which is $l^2 t^{-1}$) is that of a kinematic viscosity. The logical conclusion is that this must be the turbulent kinematic viscosity K_M . If, moreover, λ is assumed to be proportional to the height z , we can rewrite (1.2.18) as:

$$K_M \left(\frac{du}{dz} \right)^2 - \alpha \frac{g}{T} K_H \frac{d\theta}{dz} = C \cdot \frac{K_M^3}{z^4} \quad (1.2.20)$$

The constant C is determined as follows:

Let us consider the adiabatic case ($d\theta/dz = 0$), assuming that (1.2.20) obtains in all situations with the same C . Then from profile II, table 1.2.1, it follows that $du/dz = u_* / kz$, and from (1.1.1) that $K_M = kz u_*$. Substitution in (1.2.20) gives: $C = k^{-4}$.

If the non-dimensional quantities S and z/L and the transfer equations (1.1.1) and (1.1.2) are used, (1.2.20) can be written as:

$$S^4 - (\alpha z/L) S^3 = 1. \quad (1.2.21)$$

This is the equation referred to in most literature on wind profiles of recent date. The solution of (1.2.21) is given in formula IX in table 1.2.1; so that α in (1.2.21) is

α_K in IX. The profile is called the KEYPS profile, the name being formed from the initial letters of KAZANSKY, ELLISON, YAMAMOTO, PANOFSKY and SELLERS.

X. Su's derivation of his wind profile formula (see NAITO, 1964) is also based on the Rossby-Montgomery equation (1.2.3), but he changes it into:

$$K_f \left(\frac{du}{dz} \right)^2 - K \left(\frac{du}{dz} \right)^2 = \alpha_{Su} K_T^g \frac{d\theta}{dz}. \quad (1.2.22)$$

In the $S, z/L$ symbols:

$$S - (\alpha_{Su} z/L) S^{-1} = 1 \quad (1.2.23)$$

the solution being given in formula X.

XI. The Goptarev profile results from the purely mathematical statement that the curvature of the $(u, \ln z)$ relation can be expressed by:

$$\frac{du}{dz} = \frac{u_*}{kz} e^{az}. \quad (1.2.24)$$

We have replaced the exponent $a(z + z_0)$ which GOPTAREV used (GOPTAREV 1960, also ROLL 1965) by az , for the same reason that we replaced $l_f = k(z + z_0)$ by $l_f = kz$ in IV (p. 18).

If a is assumed to be proportional to L^{-1} the $(S, z/L)$ expression is:

$$S = e^{a_G(z/L)} \quad (1.2.25)$$

XII. SWINBANK (1964) introduced a quantity X with the dimension of length and having properties such that the expression:

$$\frac{du}{dz} = \frac{u_*}{kz}$$

for the adiabatic situation can be generalized to become:

$$\frac{du}{dX} = \frac{u_*}{kX} \quad (1.2.26)$$

for the general diabatic situation.

He also uses (1.2.18) and states:

$$\varepsilon = u_*^2 \frac{du}{dX} \quad (1.2.27)$$

because in the adiabatic case (1.2.18) becomes:

$$K_M \left(\frac{du}{dz} \right)^2 = u_*^2 \frac{du}{dz} = \varepsilon.$$

So (1.2.27) may be considered as a generalization of the latter relation.

The $(S, z/L)$ expression proves to be:

$$S = \frac{(\alpha_S z/L) \exp \alpha_S z/L}{\exp (\alpha_S z/L) - 1} \quad (1.2.28)$$

(see section 1.5).

SWINBANK derived his formula without introducing a constant α , but for reasons of uniformity we have added a constant α_S .

The solution of (1.2.28) results in profile XII.

XIII. PANDOLFO (1966) assumes that the Monin-Obukhov profile holds good if $(z/L)_T < z/L < 0$. $((z/L)_T$ is a value indicating the point of transition from free to forced convection). He states that if $z/L < (z/L)_T$ the wind profile is analogous to the Priestley temperature profile:

$$\frac{du}{dz} = \frac{u_*}{kz} \frac{C}{3} (z/L)^{-\frac{1}{3}} \frac{K_H}{K_M}. \quad (1.2.29)$$

PANDOLFO assumes: $z/L = Ri$ for unstable conditions, which is supported by observation results. The value of $(z/L)_T$ is fixed by assuming continuity conditions for K_M/K_H and its first derivative with respect to z/L . It is then found that $(z/L)_T = -1/7\alpha_P$.

1.3 Generalizations

1.3.1. Generalizations of the derivation of the KEYPS profile

In the first place we introduce two constants, c and α , and write formula (1.1.9) as:

$$c\zeta = \alpha z/L. \quad (1.3.1)$$

The constant c must be regarded as a scale parameter, the numerical values of which will be specified later (p. 25). α proves to be an empirical constant.

The wind profile formulae can now be written in the most general form as:

$$u = \frac{u_*}{k} \{f(\zeta) - f(\zeta_0)\} \quad (1.3.2)$$

where f may be said to be the non-dimensional profile function.

The requirement (1.1.7) is satisfied by this formula.

The formula (1.1.8) now becomes:

$$S = \zeta \frac{df(\zeta)}{d\zeta}. \quad (1.3.3)$$

It will be useful to introduce a special symbol $\hat{\wedge}$ or $\hat{\sim}$ or $\hat{\wedge}$ for adiabatic quantities to distinguish them from the general diabatic quantities.

We then have:

$$\hat{S} = 1 \text{ (see (1.2.1)) and } \left(\frac{d\hat{u}}{dz} \right) = \frac{\hat{u}_*}{kz}. \quad (1.3.4)$$

From (1.2.18) it follows that

$$\hat{K}_M \left(\frac{du}{dz} \right)^2 = \hat{\varepsilon} \quad (1.3.5)$$

because $\frac{d\theta}{dz} = 0$.

From (1.1.1) and (1.1.8):

$$K_M = \frac{kzu_*}{S} \quad (1.3.6)$$

hence:

$$\hat{K}_M = kz\hat{u}_* \quad (1.3.7)$$

Substituting (1.3.4) and (1.3.7) into (1.3.5) we find:

$$\hat{\varepsilon} = \frac{\hat{u}_*^3}{kz} \quad (1.3.8)$$

But from (1.3.7) we see that:

$$\frac{\hat{K}_M}{kz\hat{u}_*} = 1.$$

So we can generalize (1.3.8) to:

$$\hat{\varepsilon} = \frac{\hat{K}_M^{q-1} \hat{u}_*^{4-q}}{k^q z^q} \quad (1.3.9)$$

where q is any real number.

Let us now generalize (1.3.9) for the diabatic case as follows:

$$\varepsilon = \frac{K_M^{q-1} u_*^{4-q}}{k^q z^q} \quad (1.3.10)$$

With the insertion of the non-dimensional quantities S and ζ equation (1.2.18) becomes:

$$S^q - c\zeta S^{q-1} = 1. \quad (1.3.11)$$

This is in fact the general equation for the wind profile already proposed by KAZANSKY and MONIN (1956).

For $\zeta = 0$ we have $S^q = 1$. Formally equation (1.3.11) has q roots, of which $S = 1$ is one, but this is the only one that is relevant to our problem. So if $\zeta \rightarrow 0$ all formulae contained in (1.3.11) change into the logarithmic profile, valid for the adiabatic case. Let us now require that all formulae behave in the same way as a function of ζ , in near-neutral situations, which can be done because we still have available the value of c . Mathematically this means:

$$\left(\frac{dS}{d\zeta} \right)_{\zeta=0} = \text{constant}. \quad (1.3.12)$$

If, for convenience, we take the value 1 for this constant, (1.3.11) yields: $c = q$, (1.3.11) therefore becomes:

$$S^q - q\zeta S^{q-1} = 1. \quad (1.3.13)$$

It is interesting to note that as a consequence of (1.3.12) in combination with (1.3.4) the power series for S can be written:

$$S = 1 + \zeta + 0(\zeta^2) \quad (1.3.14)$$

and therefore from (1.3.3) the power series for $f(\zeta)$ as:

$$f(\zeta) = \ln |\zeta| + \zeta + 0(\zeta^2) \quad (1.3.15)$$

where $0(\zeta^2)$ represents $C_1\zeta^2 + C_2\zeta^3 + \dots$

1.3.2 Generalization of BUSINGER's derivation of profile formulae

As we have seen on page 19 BUSINGER used in his thesis two formulations of the energy balance equation. The first, (1.2.10), in the dimension of acceleration, the second, (1.2.11), in the dimension of specific energy. The only reason why he introduced (1.2.10) first is, that it is easier to write the convective term in the way it occurs in this equation. But because no conclusive physical argument is available that (1.2.10) is an adequate formulation BUSINGER felt justified in using (1.2.11) as well as (1.2.10).

One wonders however, whether these two formulations are the only possible ones. On the contrary it is easy to introduce the generalized form:

$$\frac{K^2}{l^{4-2q}} = \frac{K_f^2}{l_f^{4-2q}} - l^{2q} \frac{g}{T} \frac{d\theta}{dz} \quad (1.3.16)$$

which becomes (1.2.10) for $q = \frac{1}{2}$ and (1.2.11) for $q = 1$.

In (1.3.16) we have introduced a factor 2 before the numerical parameter q in order to avoid an exponent $\frac{1}{2}q$ in the final result (1.3.17).

If we use (1.1.6), (1.1.8), (1.2.9), (1.2.12) and (1.3.6) and make K equal to K_M , we can express the various quantities in (1.2.10) and (1.2.11) in terms of S and L .

If in addition we introduce:

$$c\zeta = \frac{K_M z}{K_H L} \text{ analogous to (1.3.1), then (1.3.16) becomes:}$$

$$S^q - c\zeta S = 1.$$

If we revert to (1.3.12), and once more make the constant equal to 1, we again find that $c = q$. Hence (1.3.16) can be written:

$$S^q - q\zeta S = 1. \quad (1.3.17)$$

1.3.3 A formal overall generalization and its solution

The two differential equations (1.3.13) and (1.3.17) have been derived from two different formulations of the balance equation describing the mechanical and thermal contributions to the total turbulence. These two equations resemble each other very closely. This becomes even clearer if we write them as:

$$\zeta = \frac{1}{q} (S - S^{1-q}) \quad (1.3.18)$$

and

$$\zeta = \frac{1}{q} (S^{q-1} - S^{-1}). \quad (1.3.19)$$

They become interchangeable by application of the transformation:

$$\text{TR:} \quad \zeta \rightarrow -\zeta; \quad S \rightarrow S^{-1}. \quad (1.3.20)$$

Both formulae suggest the use of a general wind profile differential equation:

$$\zeta = \frac{1}{a-b} (S^a - S^b) \equiv \frac{1}{b-a} (S^b - S^a). \quad (1.3.21)$$

For $a = 1$ and $b = 1 - q$ (or $b = 1$ and $a = 1 - q$) we again obtain (1.3.18), whereas by taking $a = -1$, and $b = q - 1$ (or $b = -1$ and $a = q - 1$) we get formula (1.3.19).

Let us call the formulae contained in (1.3.13) or (1.3.18) the Plus group and the formulae contained in (1.3.17) or (1.3.19) the Minus group.

It is now easy to express $f(\zeta)$ as a function of S .

In order to do so we write:

$$\frac{df}{dS} = \frac{df}{d\zeta} \cdot \frac{d\zeta}{dS}. \quad (1.3.22)$$

From (1.3.3) and (1.3.21) we have:

$$\frac{df}{d\zeta} = \frac{S}{\zeta} = \frac{(a-b)S}{S^a - S^b}$$

and from (1.3.21) alone:

$$\frac{d\zeta}{dS} = \frac{1}{a-b} (aS^{a-1} - bS^{b-1}).$$

Substituting these two relations in (1.3.22) we find:

$$\frac{df}{dS} = \frac{aS^a - bS^b}{S^a - S^b} = a + (a-b) \frac{1}{S^{a-b} - 1}$$

so that:

$$f(\zeta) = aS + (a - b) \int \frac{dS}{S^{a-b} - 1}.$$

Combined with (1.3.21), we have now found a general "formal" solution of the wind profile problem, viz.:

$$\left. \begin{aligned} \zeta &= \frac{1}{a-b} (S^a - S^b) \\ f(\zeta) &= aS + (a-b) \int \frac{dS}{S^{a-b} - 1} \end{aligned} \right\} \quad (1.3.23)$$

1.4 Special cases

1.4.1 Special cases of the Plus group

The general formula of the Plus group is:

$$\left. \begin{aligned} \zeta &= \frac{1}{q} (S - S^{1-q}) \\ f(\zeta) &= S + q \int \frac{dS}{S^q - 1} \end{aligned} \right\} \quad (1.4.1)$$

We now first consider positive integers for q .

$$q = 1: \quad \zeta = S - 1 \text{ or } S = 1 + \zeta \text{ and } f(\zeta) = \zeta + \ln |\zeta| \quad (1.4.2)$$

which is the Monin-Obukhov profile (VIII).

Attention must be drawn to the fact that we have omitted the numerical integration constant in (1.4.2). This has been done because the constant is not relevant. We are not interested in $f(\zeta)$ but in $u(z)$, according to (1.3.2), where, owing to the introduction of ζ_0 or z_0 , for which (1.1.7) holds good, the numerical constant term of $f(\zeta)$ cancels out. For that reason we shall write $f(\zeta)$ in the following without the integration constant.

$$q = 2: \quad \zeta = \frac{1}{2}(S - S^{-1}) \text{ or } S^2 - 2\zeta S = 1 \text{ and } S = \zeta + \sqrt{1 + \zeta^2}$$

(Because where $\zeta = 0$, S must be ± 1 , the solution $S = \zeta - \sqrt{1 + \zeta^2}$ is not applicable).

$$\begin{aligned} f(\zeta) &= \zeta + \sqrt{1 + \zeta^2} + \ln \left| \frac{\zeta - 1 + \sqrt{1 + \zeta^2}}{\zeta + 1 + \sqrt{1 + \zeta^2}} \right| \\ &= \zeta + \sqrt{1 + \zeta^2} + \ln |\zeta| - \ln (1 + \sqrt{1 + \zeta^2}). \end{aligned} \quad (1.4.3)$$

This is Holzman's approximation formula (V). We shall call it simply the Holzman profile.

$$q = 3: \quad \zeta = \frac{1}{3}(S - S^{-2}) \text{ or } S^3 - 3\zeta S^2 = 1$$

$$\text{and } f(\zeta) = S + \ln |S - 1| - \frac{1}{2} \ln(S^2 + S + 1) + \sqrt{3} \operatorname{arctg} \frac{2S + 1}{-\sqrt{3}}. \quad (1.4.4)$$

It is possible to write S explicitly as a function of ζ , but this leads to a rather complicated form; the formula can be applied more easily in the parameter form.

As far as we know, this formula has never been used as a wind profile formula.

$$q = 4: \quad \zeta = \frac{1}{4}(S - S^{-3}) \text{ or } S^4 - 4\zeta S^3 = 1$$

$$f(\zeta) = S + \ln \left| \frac{S-1}{S+1} \right| - 2 \operatorname{arctg} S. \quad (1.4.5)$$

Here, too, the parameter form is clearer than the very complicated explicit solution. This profile formula is the well-known KEYPS profile (IX).

Higher positive values of q do not result in known profile functions as far as we are aware.

Nor is this the case for $q = 0$, but from a purely mathematical point of view this value gives an interesting result. We write (1.4.1) as:

$$\zeta = \frac{S(1 - S^{-q})}{q} = \frac{S(1 - e^{-q \ln S})}{q}.$$

If the power series for e is used it is easily seen that the limit for $q \rightarrow 0$ is:

$$\zeta = S \ln S$$

$$\text{and } f(\zeta) = S + \int \frac{dS}{\ln S} = S + \ln |\ln S| + \sum_{n=1}^{\infty} \frac{(\ln S)^n}{n \cdot n!} \quad (1.4.6)$$

which will be called the zero plus profile.

Before we continue with negative q values we draw attention to the following mathematical peculiarity:

Let us write (1.3.18) as:

$$q\zeta S^{-1} = 1 - S^{-q}$$

$$\text{or } S^{-q} = 1 - q\zeta S^{-1}. \quad (1.4.7)$$

Now, the following approximation holds for small values of x :

$$1 - x \approx \frac{1}{1 + x}. \quad (1.4.8)$$

It is always possible to make $q\zeta S^{-1}$ sufficiently small by taking a sufficiently low value for ζ , which means that the considerations are restricted to cases of only slight stability or instability. So (1.4.7) can be approximated by:

$$S^{-q} = \frac{1}{1 + q\zeta S^{-1}} \text{ or } S^q = 1 + q\zeta S^{-1}.$$

Hence:

$$\zeta = -\frac{1}{q}(S - S^{1-(q)}). \quad (1.4.9)$$

And this is (1.3.18) again although with the opposite value of q . So we can consider each formula of the Plus group with a positive value of q as an approximation in the sense of (1.4.8) of another formula of the Plus group with a negative value of q and vice versa.

In addition, we can show that solutions for negative values of q can be found immediately from the solutions for positive values of q :

$$\begin{aligned} f(\zeta) &= S + q \int \frac{dS}{S^q - 1} = S - q \int \frac{dS}{1 - S^q} = \\ &= S - q \int \frac{S^{-q}}{S^{-q} - 1} dS = S - qS - q \int \frac{dS}{S^{-q} - 1}. \end{aligned}$$

For $q < 0$ we can write $q = -|q|$. Hence:

$$\begin{aligned} f(\zeta, q < 0) &= S + |q| \int \frac{dS}{S^{|q|} - 1} + |q| S = \\ f(\zeta, q = |q|) &+ |q| S. \end{aligned} \quad (1.4.10)$$

We propose to call the subgroup of the Plus group with $q > 0$ the MOHKEYPS group, because it contains the formulae of KEYPS, Holzman and MO. The individual elements of this group can be indicated by MKq .

Let us now take: $q = -1$, then from (1.4.9):

$$\begin{aligned} \zeta &= S^2 - S \rightarrow S = \frac{1}{2}(1 + \sqrt{1 + 4\zeta}) \\ \text{and: } f(\zeta) &= \sqrt{1 + 4\zeta} + \ln(\sqrt{1 + 4\zeta} - 1) \end{aligned} \quad (1.4.11)$$

This is Su's profile (X).

$$\begin{aligned} q &= -2 \\ \zeta &= \frac{1}{2}(S^3 - S) \text{ or } S^{-2} + 2\zeta S^{-3} = 1 \\ f(\zeta) &= 3S + \ln \left| \frac{S-1}{S+1} \right| \end{aligned} \quad (1.4.12)$$

This is the Rossby-Montgomery profile (IV).

We have already seen that HOLZMAN started from the Rossby-Montgomery equation (1.2.4) and introduced (1.2.6) as an approximation, which yielded the wind profile formula V. This approximation is a special case of the general relation between the members with positive q and the members with negative q of the Plus group. The Su and MO profiles ($q = -1$ and $q = 1$ respectively) are related in a similar way.

1.4.2 *Special cases of the Minus group*

The Minus group is expressed by:

$$\text{and } \left. \begin{aligned} \zeta &= \frac{1}{q}(S^{q-1} - S^{-1}) \\ f(\zeta) &= (q-1)S + q \int \frac{dS}{S^q - 1} \end{aligned} \right\} \quad (1.4.13)$$

Just as in the case of the Plus group, the members with positive q and the members with negative q can be considered as approximations of each other in the sense of (1.4.8).

It can be shown easily, moreover, that:

$$f(\zeta, q < 0) = f(\zeta, q = |q|) - |q| S. \quad (1.4.14)$$

$q = 1$:

$$\left. \begin{aligned} \zeta &= 1 - S^{-1} \text{ or } S = \frac{1}{1 - \zeta} \\ f(\zeta) &= \ln |S - 1| = \ln |\zeta| - \ln |1 - \zeta| \end{aligned} \right\} \quad (1.4.15)$$

This is Businger's second formula (VII), formula (2.8.11) in his thesis.

$q = 2$:

$$\left. \begin{aligned} \zeta &= \frac{1}{2}(S - S^{-1}) \text{ or } S = \zeta + \sqrt{1 + \zeta^2} \\ f(\zeta) &= \zeta + \sqrt{1 + \zeta^2} + \ln |\zeta| - \ln |1 + \sqrt{1 + \zeta^2}| \end{aligned} \right\} \quad (1.4.16)$$

which is the Holzman profile (V) again.

So the Plus and Minus groups both contain the Holzman profile. It is the only group element which transforms into itself when the transformation Tr is applied.

$q = \frac{1}{2}$:

$$\left. \begin{aligned} \zeta &= 2(S^{-\frac{1}{2}} - S^{-1}) \rightarrow S^{\frac{1}{2}} = \frac{1 - \sqrt{1 - 2\zeta}}{\zeta} \\ f(\zeta) &= \frac{2\sqrt{1 - 2\zeta}}{(1 + \sqrt{1 - 2\zeta})^2} + \ln \left| \frac{\sqrt{1 - 2\zeta} - 1}{\sqrt{1 - 2\zeta} + 1} \right| \end{aligned} \right\} \quad (1.4.17)$$

which is Businger's first formula (VI), (2.8.8) in his thesis.

Let us call the subgroup of the Minus group with $q > 0$ the Minus Positive group (Min-Pos).

$q = 0$ results in:

$$\left. \begin{aligned} \zeta &= S^{-1} \ln S \\ \text{and } f(\zeta) &= -S + \ln |\ln S| + \sum_{n=1}^{\infty} \frac{(\ln S)^n}{n \cdot n!} \end{aligned} \right\} \quad (1.4.18)$$

which will be called the zero minus profile.

1.4.3 Tables and figures illustrating the Plus and Minus groups

As far as we know other q -values do not lead to formulae which have been used as wind profile formulae, but for completeness' sake we have calculated the profiles for some additional q -values and all these cases are summarized in parameter form in table 1.4.1.

The $f(\zeta)$ formulae for the Minus group, expressed as functions of S , immediately follow from those for the Plus group by adding $(q - 2)S$, as can be seen by comparing (1.4.13) with (1.4.1).

The cases for which f can be written as a simple explicit function of ζ have been summarized in table 1.4.2, together with the formulae of Goptarev and Swinbank, which will be dealt with in later chapters.

The characteristics of the profile formulae are illustrated in figures 1.4.1 and 1.4.2.

In 1.3.3 it has been shown that the Plus and Minus groups interchange if the transformation Tr is applied. If we introduce: $x = \text{arctg } \zeta$ and $y = \text{arctg } \ln S$, the transformation Tr is equivalent to: $(x, y) \rightarrow (-x, -y)$, which represents a rotation of 180° in an (x, y) diagram.

By using arctg functions we have obtained that the quantities ζ and $\ln S$, which vary over an unlimited range $-\infty \dots +\infty$, are replaced by quantities which vary over a limited range, viz.: $-\frac{1}{2}\pi \dots 0 \dots +\frac{1}{2}\pi$

So a diagram can be constructed in which the complete functions contained in the Plus and Minus groups can be represented. Moreover, when rotated through 180° , the graphs for the MINUS group coincide with those for the Plus group. A number of profile formulae from the Plus group are represented in figure 1.4.1. Areas are also indicated where $1 < q$, $0 < q < 1$ and $q < 0$ respectively. If the figure is rotated through 180° it transforms into figure 1.4.2, in which the Minus group is represented.

1.4.4 Two other groups

Mathematically the general formula (1.3.21) contains many more $S(\zeta)$ functions than the Plus and Minus groups. It is senseless to investigate and determine all of

TABLE 1.4.1

Plus group

ν	$\zeta(S)$	Name	$f(S)$
4	$\frac{1}{4}(S - S^{-3})$	KEYPS	$S + \ln S - 1 - \ln S + 1 - 2 \operatorname{arctg} S$
3	$\frac{1}{3}(S - S^{-2})$	—	$S + \ln S - 1 - \frac{1}{2} \ln(S^2 + S + 1) + \sqrt{3} \operatorname{arctg} \frac{2S + 1}{\sqrt{3}}$
2	$\frac{1}{2}(S - S^{-1})$	Holzman	$S + \ln S - 1 - \ln S + 1 $
$\frac{5}{3}$	$\frac{2}{3}(S - S^{-3})$	—	$S + \ln S^{\frac{2}{3}} - 1 - \frac{1}{2} \ln(S + S^{\frac{2}{3}} + 1) + \sqrt{3} \operatorname{arctg} \frac{2S^{\frac{2}{3}} + 1}{\sqrt{3}}$
1	$S - 1$	MO	$S + \ln S - 1 $
$\frac{1}{2}$	$2(S - S^{\frac{1}{2}})$	—	$S + S^{\frac{1}{2}} + \ln S^{\frac{1}{2}} - 1 $
0	$S \ln S$	zero plus	$S + \ln \ln S + \sum_{n=1}^{\infty} \frac{(\ln S)^n}{n \cdot n!}$
$-\frac{1}{2}$	$2(S^{\frac{3}{2}} - S)$	—	$\frac{3}{2}S + S^{\frac{3}{2}} + \ln S^{\frac{3}{2}} - 1 $
-1	$S^2 - S$	Su	$2S + \ln S - 1 $
$-\frac{3}{2}$	$\frac{2}{3}(S^{\frac{5}{2}} - S)$	—	$\frac{5}{2}S + \ln S^{\frac{5}{2}} - 1 - \frac{1}{2} \ln(S + S^{\frac{5}{2}} + 1) + \sqrt{3} \operatorname{arctg} \frac{2S^{\frac{5}{2}} + 1}{\sqrt{3}}$
-2	$\frac{1}{2}(S^3 - S)$	RM	$3S + \ln S - 1 - \ln S + 1 $
-3	$\frac{1}{3}(S^4 - S)$	—	$4S + \ln S - 1 - \frac{1}{2} \ln(S^2 + S + 1) + \sqrt{3} \operatorname{arctg} \frac{2S + 1}{\sqrt{3}}$
-4	$\frac{1}{4}(S^5 - S)$	—	$5S + \ln S - 1 - \ln S + 1 - 2 \operatorname{arctg} S$

TABLE 1.4.2

Plus group

ν	Name	$S(\zeta)$	$f(\zeta)$
2	Holzman	$\zeta + \sqrt{1 + \zeta^2}$	$\zeta + \ln \zeta + \sqrt{1 + \zeta^2} - \ln 1 + \sqrt{1 + \zeta^2} $
1	MO	$\zeta + 1$	$\zeta + \ln \zeta $
$\frac{1}{2}$	—	$\frac{1}{2}(1 + \zeta + \sqrt{1 + 2\zeta})$	$\frac{1}{2}\zeta + \ln \zeta + \sqrt{1 + 2\zeta} - \ln 1 + \sqrt{1 + 2\zeta} $
-1	Su	$\frac{1}{2}(1 + \sqrt{1 + 4\zeta})$	$\ln \zeta + \sqrt{1 + 4\zeta} - \ln 1 + \sqrt{1 + 4\zeta} $
$\frac{2\zeta}{\ln S}$	Swinbank	$\frac{2\zeta e^{2\zeta}}{e^{2\zeta} - 1}$	$\ln e^{2\zeta} - 1 $

Minus group

\mathcal{V}	$\zeta(S)$	Name	$f(S)$
	$\frac{1}{4}(S^3 - S^{-1})$		$3S + \ln S - 1 - \ln S + 1 - 2 \operatorname{arctg} S$
	$\frac{1}{3}(S^2 - S^{-1})$	—	$2S + \ln S - 1 - \frac{1}{2} \ln(S^2 + S + 1) + \sqrt{3} \operatorname{arctg} \frac{2S + 1}{-\sqrt{3}}$
	$\frac{1}{2}(S - S^{-1})$	Holzman	$S + \ln S - 1 - \ln S + 1 $
	$\frac{2}{3}(S^4 - S^{-1})$	—	$\frac{1}{2}S + \ln S^4 - 1 - \frac{1}{2} \ln(S + S^4 + 1) + \sqrt{3} \operatorname{arctg} \frac{2S^4 + 1}{\sqrt{3}}$
	$1 - S^{-1}$	Businger II	$\ln S - 1 $
	$2(S^{-4} - S^{-1})$	Businger I	$-\frac{1}{2}S + S^4 + \ln S^4 - 1 $
	$S^{-1} \ln S$	zero minus	$-S + \ln \ln S + \sum_{n=1}^{\infty} \frac{(\ln S)^n}{n \cdot n!}$
	$2(S^{-1} - S^{-\frac{3}{2}})$	—	$-S + S^4 + \ln S^4 - 1 $
	$S^{-1} - S^{-2}$	—	$-S + \ln S - 1 $
	$\frac{2}{3}(S^{-1} - S^{-\frac{5}{2}})$	—	$-S + \ln S^4 - 1 - \frac{1}{2} \ln(S + S^4 + 1) + \sqrt{3} \operatorname{arctg} \frac{2S^4 + 1}{\sqrt{3}}$
	$\frac{1}{2}(S^{-1} - S^{-3})$	—	$-S + \ln S - 1 - \ln S + 1 $
	$\frac{1}{3}(S^{-1} - S^{-4})$	—	$-S + \ln S - 1 - \frac{1}{2} \ln(S^2 + S + 1) + \sqrt{3} \operatorname{arctg} \frac{2S + 1}{-\sqrt{3}}$
	$\frac{1}{4}(S^{-1} - S^{-5})$	—	$-S + \ln S - 1 - \ln S + 1 - 2 \operatorname{arctg} S$

Minus group

Name	$S(\zeta)$	$f(\zeta)$
Holzman	$\zeta + \sqrt{1 + \zeta^2}$	$\zeta + \ln \zeta + \sqrt{1 + \zeta^2} - \ln 1 + \sqrt{1 + \zeta^2} $
Businger II	$\frac{1}{1 - \zeta}$	$\ln \zeta - \ln \zeta - 1 $
Businger I	$\frac{2}{\zeta^2}(1 - \zeta - \sqrt{1 - 2\zeta})$	$\frac{2\sqrt{1 - 2\zeta}}{(1 + \sqrt{1 - 2\zeta})^2} + \ln \left \frac{\sqrt{1 - 2\zeta} - 1}{\sqrt{1 - 2\zeta} + 1} \right $
—	$\frac{1}{2\zeta}(1 - \sqrt{1 - 4\zeta})$	$\frac{-2}{(1 + \sqrt{1 - 4\zeta})} + \ln \left \frac{1 - \sqrt{1 - 4\zeta}}{1 + \sqrt{1 - 4\zeta}} \right $
Swin-Trans	$\frac{1}{2\zeta}(e^{2\zeta} - 1)$	$\ln \zeta + \sum_{n=1}^{\infty} \frac{(2\zeta)^n}{n(n+1)!}$

TABLE 1.4.2 (continuation)

Log- and sym-group

$q \neq$	Name	$S(\zeta)$	$f(\zeta)$
0	Goptarev	e^ζ	$\ln \zeta + \sum_{n=1}^{\infty} \frac{\zeta^n}{n \cdot n!}$

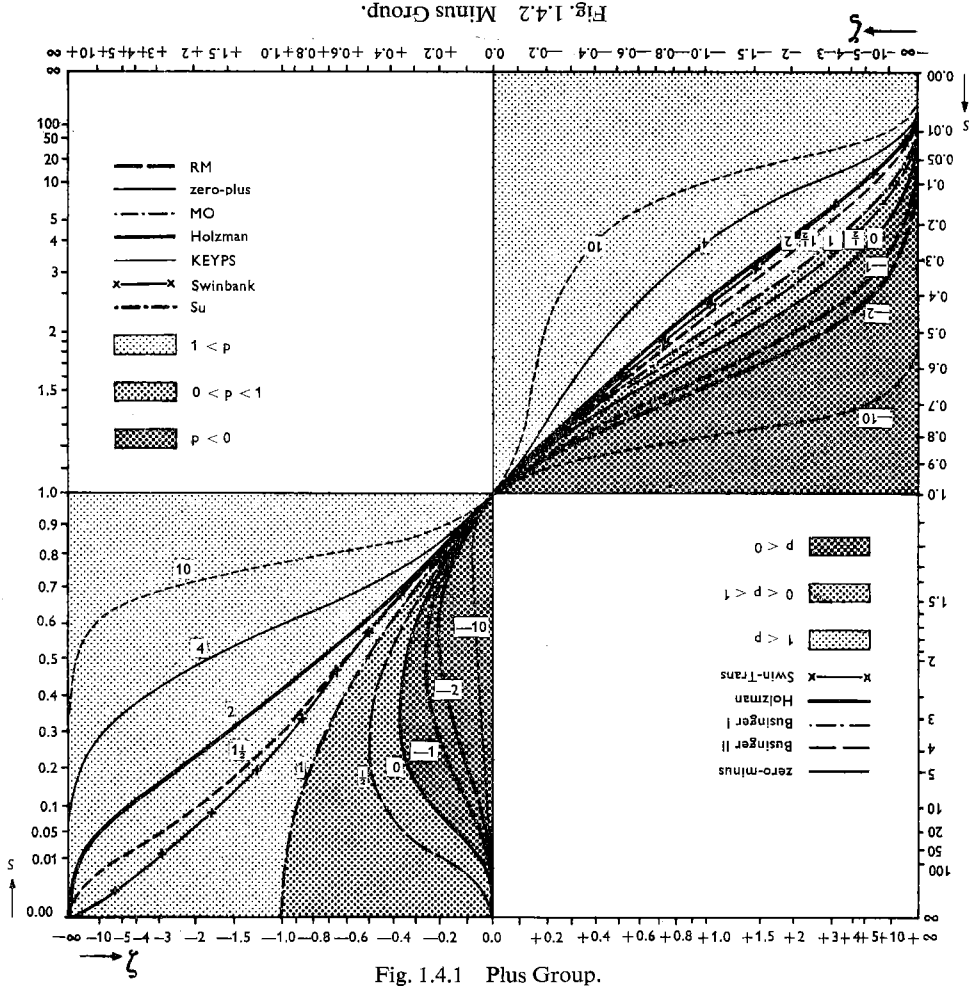


Fig. 1.4.1 and Fig. 1.4.2 Graphical representation of wind profile formulae.

them, because we have no reason to expect that they will all have a physical meaning.

There are only two special groups which are of interest, because they are related to the Plus and Minus groups, viz.:

I $a = b$ and II $a = -b$.

The first relation results in:

$$\left. \begin{aligned} \zeta &= S^a \ln S \\ f(\zeta) &= aS + \int \frac{dS}{\ln S} = aS + \ln |\ln S| + \sum_1^{\infty} \frac{(\ln S)^n}{n n!} \end{aligned} \right\} \quad (1.4.19)$$

as follows from (1.3.23).

Let us call this group the logarithmic group. It contains the zero plus and zero minus profiles for $a = 1$ and -1 respectively and in this way the group is related to the Plus and Minus groups.

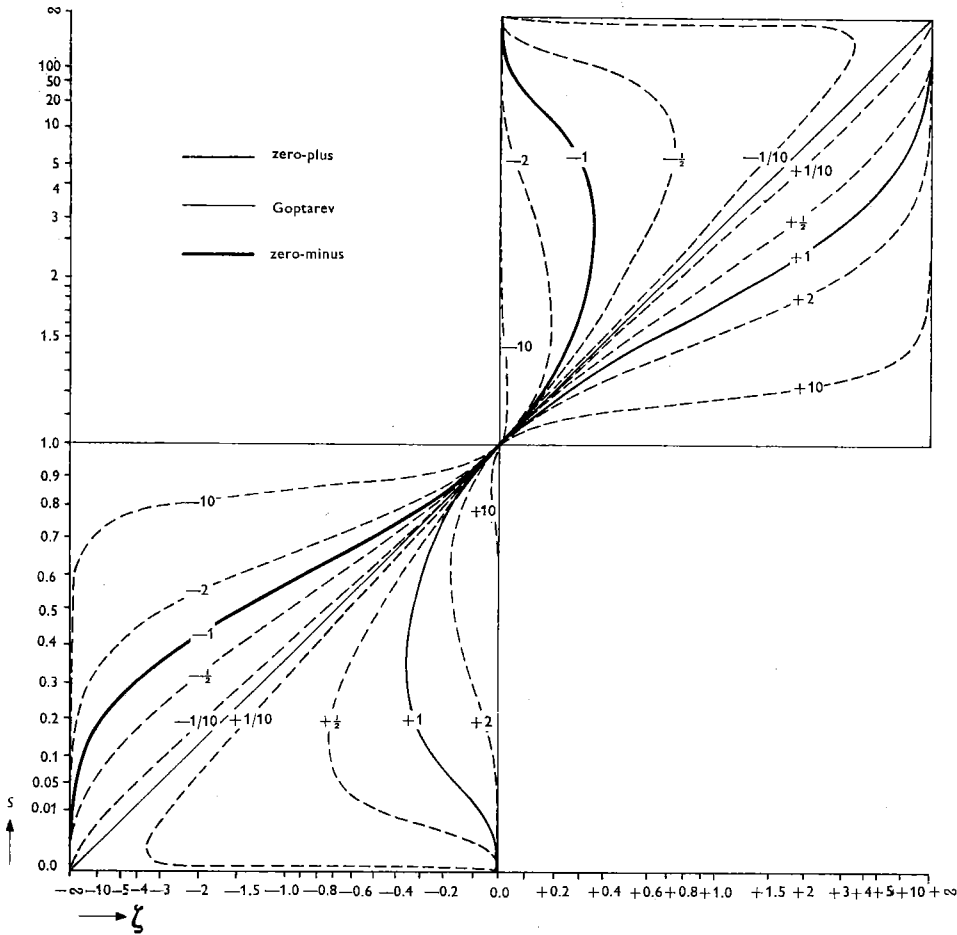


Fig. 1.4.3 Graphical representation of the logarithmic group of wind profile formulae.

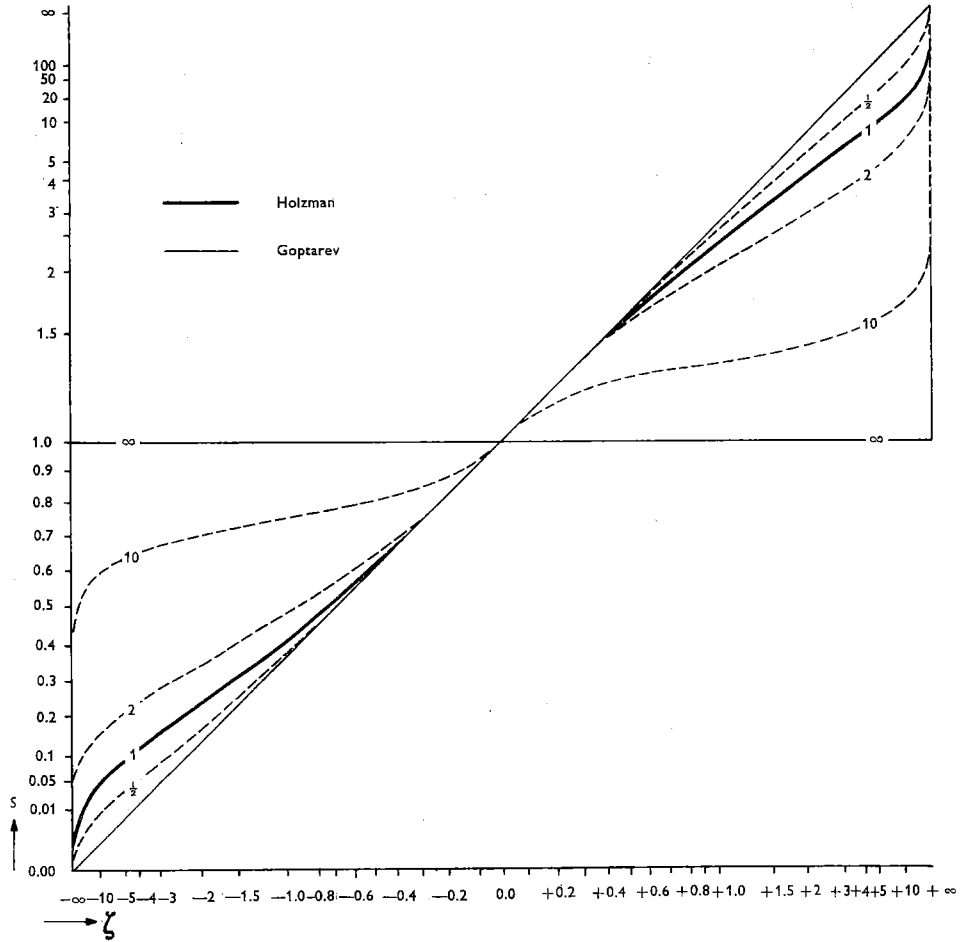


Fig. 1.4.4 Graphical representation of the symmetrical group of wind profile formulae.

TR transforms this group into itself, in such a way that an element with any q changes into an element with opposite q .

The second relation results in:

$$\left. \begin{aligned} \zeta &= \frac{1}{2a} (S^a - S^{-a}) \\ f(\zeta) &= S + 2a \int \frac{dS}{S^{2a} - 1} \end{aligned} \right\} \quad (1.4.20)$$

For $a = 1$ we have the Holzman profile which shows that a relation exists with the Plus and Minus groups.

When the transformation Tr is applied each member of this group transforms into itself.

We suggest that this group be called the symmetrical group.

The logarithmic and the symmetrical groups have in common the element where $a = 0$:

$$\left. \begin{aligned} \zeta &= \ln S \\ f(\zeta) &= \ln |\zeta| + \sum_{n=1}^{\infty} \frac{\zeta^n}{n n!} \end{aligned} \right\} \quad (1.4.21)$$

This formula has been proposed by GOPTAREV to describe the wind profile (XI).

These results are illustrated in figures 1.4.3 and 1.4.4. In figure 1.4.4 only positive parameter values occur, because the formula for a parameter value a is identical to that for $-a$.

1.5 The Swinbank formula

1.5.1 The relation with the Plus group; its equivalent in the Minus group

It has been shown in the foregoing that most wind profile formulae known can be derived from our general formula (1.3.21).

Four formulae from the series we have given in table 1.2.1 have not yet been dealt with, the power profile, the Deacon profile, the Pandolfo formula and the Swinbank formula. The power profile and the Deacon profile cannot be written in the general form (1.3.2), so that we cannot expect them to be related to our general system; the Pandolfo formula is a combination of the MO profile and an equivalent of the Priestley temperature profile and hence cannot be included in the system.

The Swinbank profile can be expressed in the form (1.3.2), however, and SWINBANK derived his formula starting from (1.2.18), so that it seems probable that this formula is related to our system.

If $c\zeta = a_{sz}/L$ is introduced into Swinbank's profile formula XII, we can write according to (1.3.2):

$$f(\zeta) = \ln |e^{c\zeta} - 1| \quad (1.5.1)$$

so that:

$$S = \zeta \frac{c e^{c\zeta}}{e^{c\zeta} - 1}$$

For $\zeta = 0$ we find $S = 1$, as is to be expected.

We now require, just as in our complete system, that $\left(\frac{dS}{d\zeta}\right)_{\zeta=0} = 1$. It then follows that c has to be taken as equal to 2.

So we have:

$$S = \frac{2\zeta e^{2\zeta}}{e^{2\zeta} - 1},$$

which equation can be transformed into:

$$e^{2\zeta} - 2\zeta e^{2\zeta} S^{-1} = 1, \quad (1.5.2)$$

which can also be written as:

$$S^{2\zeta/\ln S} - 2\zeta S^{2\zeta/\ln S - 1} = 1. \quad (1.5.3)$$

Comparing this relation with (1.3.13) we see that (1.5.3) can be considered as a Plus formula with varying q (varying in the same way as $2\zeta/\ln S$). The factor q in the second term must not be changed into $2\zeta/\ln S$ because this q is in fact a constant, c , which is fixed by the requirement $(dS/d\zeta)_{\zeta=0} = 1$. As $(2\zeta/\ln S)_{\zeta=0} = 2$ this requirement is fulfilled in the Swinbank formula too.

The numerical values of $2\zeta/\ln S$ for a number of ζ values are given in the following table:

TABLE 1.5.1 Values of $2\zeta/\ln S$ for the Swinbank profile

ζ	$-\infty$	-4	-3	-2	-1	0	1	2	3	4	$+\infty$
$2\zeta/\ln S$	1.00	1.35	1.40	1.54	1.72	2.00	2.38	2.85	3.34	3.85	∞

We have also drawn the graph of the Swinbank profile in figure 1.4.1.

So we find that the Swinbank profile is closely related to the Plus group and numerically in particular to the Holzman profile. This relation can be further elucidated by the following reasoning:

If we write the Holzman profile as:

$$S - 2\zeta = S^{-1} \text{ or } \ln |S - 2\zeta| = -\ln S$$

and the Swinbank profile as:

$$S - 2\zeta = \exp(\ln S - 2\zeta) \text{ or } \ln |S - 2\zeta| = \ln S - 2\zeta,$$

we see that three quantities occur in these relations, i.e.:

I: $\ln |S - 2\zeta|$, II: $\ln S - 2\zeta$ and III: $-\ln S$.

Equating I to II results in the Swinbank profile.

Equating I to III results in the Holzman profile.

Equating II to III results in the Goptarev profile.

Because the transformation TR changes the Plus group into the Minus group, the Swinbank profile, which is closely related to the Plus group, must be transformed by TR into a profile formula which is related in a similar way to the Minus group.

The result of the transformation reads:

$$S = \frac{e^{2\zeta} - 1}{2\zeta}$$

and from (1.3.3):

$$f(\zeta) = \ln |\zeta| + \sum_{n=1}^{\infty} \frac{(2\zeta)^n}{n(n+1)!}. \quad (1.5.4)$$

Let us call this profile the Swin-Trans (Swinbank Transformation) profile.

Analogous to the foregoing reasoning concerning the Swinbank, Holzman and Goptarev profiles, we now have:

$$I^*: \ln |S^{-1} + 2\zeta|, \quad II^*: 2\zeta - \ln S \text{ and} \quad III^*: \ln S.$$

Equating I* to II* results in the Swin-Trans profile.

Equating I* to III* results in the Holzman profile.

Equating II* to III* results in the Goptarev profile.

1.5.2 *A by-path: Generalization of the Swinbank profile.*

As has already been mentioned in the review of the derivation of formula XII, Swinbank introduces a quantity X with the dimension of length by requiring

$$\frac{du}{dX} = \frac{u_*}{kX} \quad (1.2.26) \text{ to be a generalization of } \frac{\hat{du}}{dz} = \frac{\hat{u}_*}{kz}.$$

Applying this to (1.3.2) we obtain:

$$\frac{u_*}{k} \frac{df(\zeta)}{dX} = \frac{u_*}{kX} \text{ or } df(\zeta) = d \ln X$$

Hence:

$$X = A e^{f(\zeta)}. \quad (1.5.5)$$

It is evident that $\hat{X} = z$ must hold good. Since for small values of ζ the function $f(\zeta)$ can be approximated by $\ln |\zeta|$, as follows from (1.3.15), formula (1.5.5) must change into $z = A e^{\ln |\zeta|}$ or $A = z e^{-\ln |\zeta|}$ for small values of ζ . So we finally have:

$$X = z e^{f(\zeta) - \ln |\zeta|} \quad (1.5.6)$$

It would now be logical to introduce a non-dimensional quantity ξ by defining:

$$\xi \equiv \frac{d}{z} X = e^{f(\zeta) - \ln|\zeta|} \quad (1.5.7)$$

for which $\hat{\xi} = 1$ holds good.

We can now generalize (1.3.10) into:

$$\varepsilon = \frac{K_M^{q-1} u_*^{4-q}}{k^q z^q \xi^m} \quad (1.5.8)$$

where m can take any positive value.

Substituting (1.5.8) into (1.2.18) and using the symbols S and ζ we find, analogous to the generalization of the derivation of the KEYPS profile in 1.3.1:

$$\xi^m S^q - (m + q) \zeta \xi^m S^{q-1} = 1 \quad (1.5.9)$$

where the requirement $\left(\frac{dS}{d\zeta}\right)_{\xi=0} = 1$ is again fulfilled.

The equation (1.5.9) contains the Plus group (if $m = 0$) and of course the Swinbank profile (if $m = q = 1$). Taking $m = q$ we may consider the resulting equation:

$$(\xi S)^q - 2q \zeta \xi (\xi S)^{q-1} = 1 \quad (1.5.10)$$

as the differential equation for a group of generalized Swinbank profiles.

The solution in parameter form can easily be found if $\omega \equiv \xi S$ is introduced.

We have:

$$\zeta \xi = \zeta e^{f(\zeta) - \ln|\zeta|} = (\text{sign } \zeta) e^{f(\zeta)}$$

and

$$\omega = \xi S = \xi \zeta \frac{df(\zeta)}{d\zeta} = \xi \zeta \frac{d \ln |\xi \zeta|}{d\zeta} = \frac{d(\xi \zeta)}{d\zeta},$$

so that from (1.5.10) we get:

$$\zeta \xi = \frac{\omega^q - 1}{2q\omega^{q-1}} \quad (1.5.11)$$

or

$$f(\zeta) = \ln \frac{\omega^q - 1}{2q\omega^{q-1}} \quad (1.5.12)$$

and from (1.5.11) by differentiation:

$$\frac{d(\zeta \xi)}{d\omega} = \frac{1}{2q} - \frac{1-q}{2q} \omega^{-q},$$

thus:

$$\frac{d\zeta}{d\omega} = \frac{\frac{d(\zeta \xi)}{d\omega}}{\frac{d(\zeta \xi)}{d\zeta}} = \frac{\frac{1}{2q} - \frac{1-q}{2q} \omega^{-q}}{\omega} = \frac{1}{2q} \omega^{-1} - \frac{1-q}{2q} \omega^{-1-q}$$

and hence:

$$\zeta = \frac{1}{2q} \ln \omega + \frac{1-q}{2q^2} \omega^{-q} + \text{constant.}$$

Since $\zeta = 0$, where $\omega = 1$, the constant has to be $\frac{q-1}{2q^2}$ so that:

$$\zeta = \frac{1}{2q} \ln \omega + \frac{1-q}{2q^2} (\omega^{-q} - 1). \quad (1.5.13)$$

The formulae (1.5.12) and (1.5.13) together form the parameter solution for the generalized Swinbank profile. For $q = 1$ we immediately get:

$$\omega = e^{2\zeta} \text{ and } f(\zeta) = \ln \left| \frac{e^{2\zeta} - 1}{2} \right|,$$

which is Swinbank's original formula.

1.6 The wind speed difference ratio as a function of stability

It is usual in papers on wind profiles to estimate values of S and z/L from the observations and to plot these values in an $(S, z/L)$ diagram, which is a transformation of our figure 1.4.1. The theoretical curves corresponding to the various wind profile formulae are then compared with the results of observations in order to judge which theoretical formula is to be preferred.

There is one serious objection to this method.

Both S and z/L contain the quantity u_* , which has to be determined from measurements of the deviations u' and w' of both the horizontal and the vertical wind components. The inaccuracy in the estimates of u_* results in a systematic deviation of the plotting positions of the observations from the "true position" in the $(S, z/L)$ diagram. SWINBANK (1966) already paid attention to this fact in his discussion of his wind profile formula. The systematic deviation consist of a shift of the plotting positions of the observations. In the stable part of the diagram the shift is in the direction of the theoretical curve; in the unstable part the shift is in the opposite direction. This will be demonstrated in Chapter 2.

It is always difficult to judge the goodness of fit of a curve by eye, and even more

so if there is a systematic deviation as in the case of the $(S, z/L)$ diagram. On the other hand, it is also rather difficult to assess by means of a statistical test in this case.

It is much more satisfactory to use the wind speed difference ratio defined by:

$$V = \frac{u(z_3) - u(z_2)}{u(z_3) - u(z_1)} = \frac{f(\zeta_3) - f(\zeta_2)}{f(\zeta_3) - f(\zeta_1)}. \quad (1.6.1)$$

If we take an arbitrary value for z_1 and fixed values for the ratios z_2/z_1 and z_3/z_1 , V is only a function of z/L . A choice with practical advantages is: $z_2/z_1 = 2$ and $z_3/z_1 = 4$. These values will be used in the following.

V can be determined from wind speed measurements and z/L from flux measurements. So here we have two quantities, V and z/L , the measuring errors of which are independent of each other.

If we determine the value of ζ from the V -value with the aid of the theoretical curves in the (V, ζ) diagram, denoted by ζ_{th} , we can construct a $(\zeta_{th}, z/L)$ diagram in which these ζ_{th} -values are plotted against z/L -values as determined from flux measurements. In this $(\zeta_{th}, z/L)$ diagram we have to examine whether the best linear regression passes through the origin or not. Even though the scatter may have become greater, it is easier to judge a linear relation than a curved one as in the case of the $(S, z/L)$ diagram. Besides, if we should succeed in collecting larger numbers of observations, this would increase the reliability of the relationship in the $(\zeta_{th}, z/L)$ diagram, whereas assessment of the relationship in the $(S, z/L)$ diagram would still be hampered by the systematic deviations referred to above.

The character of the $V(\zeta)$ functions will now be investigated.

As a consequence of $\hat{S} = 1$, with the additional requirement $\left(\frac{dS}{d\zeta}\right)_{\zeta=0} = 1$, all (V, ζ) curves pass through one point with the same slope. In the case of the values we have selected, $z_2/z_1 = 2$ and $z_3/z_1 = 4$, this point is $(V = \frac{1}{2}, \zeta = 0)$, as can be easily demonstrated:

Taking account of (1.3.15) we find:

$$V(\zeta) = \frac{f(4\zeta) - f(2\zeta)}{f(4\zeta) - f(\zeta)} = \frac{\ln 2 + 2\zeta + 0(\zeta^2)}{\ln 4 + 3\zeta + 0(\zeta^2)} \quad \zeta \rightarrow 0 \quad \frac{1}{2} \quad (1.6.2)$$

and

$$\begin{aligned} \frac{dV(\zeta)}{d\zeta} &= \frac{(2 + 0(\zeta))(\ln 4 + 0(\zeta)) - (3 + 0(\zeta))(\ln 2 + 0(\zeta))}{(\ln 4 + 0(\zeta))^2} = \\ &= \frac{2\ln 4 - 3\ln 2 + 0(\zeta)}{\ln^2 4 - 0(\zeta)} \quad \zeta \rightarrow 0 \quad \frac{1}{4\ln 2} \approx 0.36. \end{aligned} \quad (1.6.3)$$

To see how $V(\zeta)$ behaves for high absolute values of ζ , we will now determine the limits of $V(\zeta)$ for $\zeta \rightarrow +\infty$ and $-\infty$ respectively. By using (1.3.3), we can write:

$$V = \frac{f(4\zeta) - f(2\zeta)}{f(4\zeta) - f(\zeta)} = \frac{\int_{2\zeta}^{4\zeta} (S/\zeta) d\zeta}{\int_{\zeta}^{4\zeta} (S/\zeta) d\zeta}. \quad (1.6.4)$$

The ζ interval $-\infty \dots 0, \dots +\infty$ has to correspond with the S interval $0 \dots, 1, \dots +\infty$, if we are to find a wind profile formula which holds good in the complete ζ interval.

From the general equation (1.3.21) we can find the asymptotic relations $S(\zeta)$ for $\zeta \rightarrow +\infty$ or $-\infty$. These will be substituted into (1.6.4).

It is sufficient if we consider all possible combinations of $a \leq b$, because a and b can be interchanged without changing (1.3.21). The following combinations should be investigated:

$$\begin{aligned} a < b < 0; \quad a = b < 0; \quad a < b = 0; \quad a = b = 0 \\ a < 0 < b; \quad a = 0 < b; \quad 0 < a = b; \quad 0 < a < b \end{aligned}$$

The asymptotic relation between S and ζ for all combinations is given in table 1.6.1.

TABLE 1.6.1 Asymptotic relations $\zeta(S)$

	$S \rightarrow +\infty$	$S \rightarrow 0$
$a < b < 0$	$\zeta \approx \frac{1}{b-a} S^b \rightarrow 0$	$\zeta \approx \frac{1}{a-b} S^a \rightarrow -\infty$
$a = b < 0$	$\zeta \approx S^a \ln S \rightarrow 0$	$\zeta \approx S^a \ln S \rightarrow -\infty$
$a < b = 0$	$\zeta \approx \frac{1}{a} (S^a - 1) \rightarrow -\frac{1}{a}$	$\zeta \approx \frac{1}{a} (S^a - 1) \rightarrow -\infty$
$a = b = 0$	$\zeta \approx \ln S \rightarrow +\infty$	$\zeta \approx \ln S \rightarrow -\infty$
$a < 0 < b$	$\zeta \approx \frac{1}{b-a} S^b \rightarrow +\infty$	$\zeta \approx \frac{1}{a-b} S^a \rightarrow -\infty$
$a = 0 < b$	$\zeta \approx \frac{1}{b} (S^b - 1) \rightarrow +\infty$	$\zeta \approx \frac{1}{b} (S^b - 1) \rightarrow -\frac{1}{b}$
$0 < a = b$	$\zeta \approx S^a \ln S \rightarrow +\infty$	$\zeta \approx S^a \ln S \rightarrow 0$
$0 < a < b$	$\zeta \approx \frac{1}{b-a} S^b \rightarrow +\infty$	$\zeta \approx \frac{1}{a-b} S^a \rightarrow 0$

We see from the above that only in the cases $a = b = 0$ and $a < 0 < b$ does the complete S interval $0 \dots +\infty$ correspond to the complete ζ interval $-\infty \dots +\infty$.

The values of $V(\zeta)$ for $\zeta \rightarrow +\infty$ and $-\infty$ can now be found easily for the various groups. The result is summed up in table 1.6.2.

TABLE 1.6.2 V -values for $\zeta = +\infty$ and $-\infty$

q	Plus group		Minus group	
	$V(-\infty)$	$V(+\infty)$	$V(-\infty)$	$V(+\infty)$
$+\infty$	$+\frac{1}{2}$	$+\frac{2}{3}$	$+\frac{1}{3}$	$+\frac{1}{2}$
$+2$	$+\frac{1}{3}$	$+\frac{2}{3}$	$+\frac{1}{3}$	$+\frac{2}{3}$
$+1 + \delta$	0	$+\frac{2}{3}$	$+\frac{1}{3}$	$+1$
$+1$	—	$+\frac{2}{3}$	$+\frac{1}{3}$	—
0	—	$+\frac{2}{3}$	$+\frac{1}{3}$	—
—	—	$+\frac{1}{2}$	$+\frac{1}{2}$	—
	Swinbank		Swin-Trans	
	0	$+\frac{2}{3}$	$+\frac{1}{3}$	$+1$
	Logarithmic group		Symmetrical group	
a	$V(-\infty)$	$V(+\infty)$	$V(-\infty)$	$V(+\infty)$
$+\infty$	—	$+\frac{1}{2}$	$+\frac{1}{2}$	$+\frac{1}{2}$
$+1$	—	$+\frac{2}{3}$	$+\frac{1}{3}$	$+\frac{2}{3}$
0	0	$+1$	0	$+1$
-1	$+\frac{1}{3}$	—	$+\frac{1}{3}$	$+\frac{2}{3}$
$-\infty$	$+\frac{1}{2}$	—	$+\frac{1}{2}$	$+\frac{1}{2}$

The formulae of the Plus group where $q < 1$ do not have real V -values in the very stable region and the formulae in the Minus group where $q < 1$ do not have real V values in the very unstable region. These results are illustrated schematically in figure 1.6.1, while fig. 1.6.2. gives the V function for a number of profile formulae, viz.: MO, Holzman, MK₃, KEYPS, MK_{4/3}, RM, Su, Businger II, Swinbank, Swin-Trans, Goptarev and Pandolfo.

What can be said about the form of the actual wind profile in the extreme cases of stable and unstable situations?

In stable cases the most extreme possibility is that there is no turbulent exchange so that the flow is laminar; in this case K_M represents molecular viscosity and is

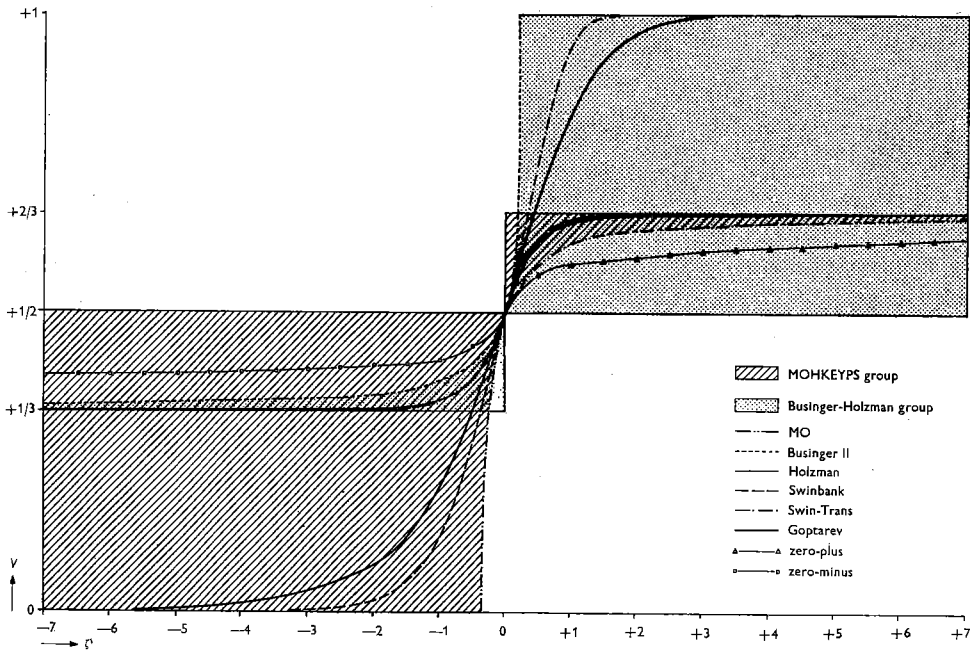


Fig. 1.6.1 Wind speed difference ratio — height, stability parameter regions for different wind profile groups.

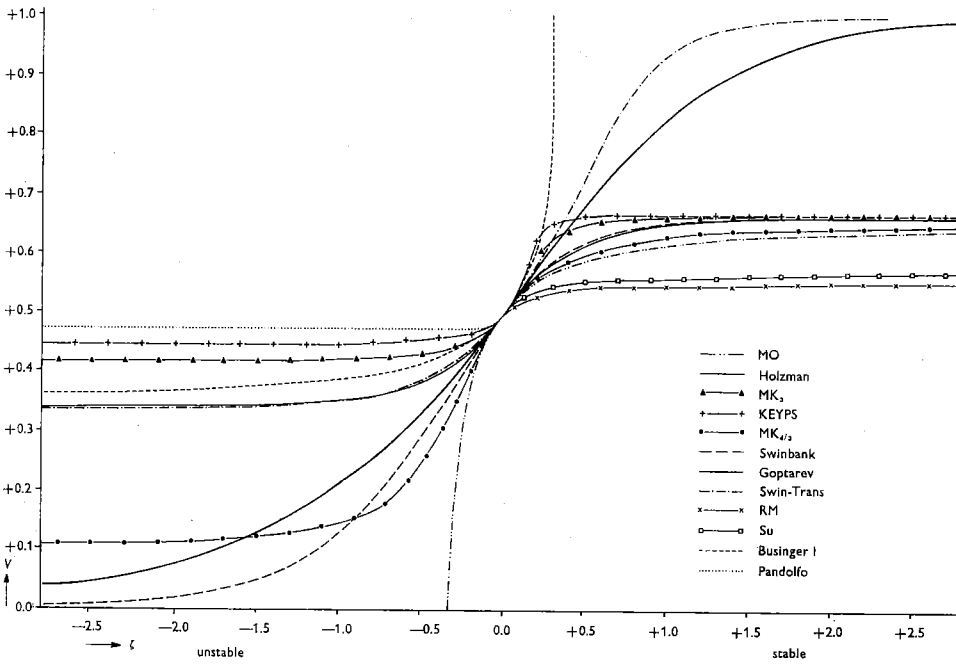


Fig. 1.6.2 Wind speed difference ratio as a function of ζ for different wind profile formulae.

independent of z , so that, according to (1.1.1), du/dz must be constant. Hence u must be in the form of $Az + B$ and therefore:

$$V = \frac{A \cdot 4z - A \cdot 2z}{A \cdot 4z - A \cdot z} = + \frac{2}{3}.$$

All formulae of the MOHKEYPS group and the related Swinbank formula are consistent with this result.

In extremely unstable situations it is not easy to say what the form of the profile will be.

MONIN and OBUKHOV consider the extreme case of purely thermal turbulence with u (and u_*) = 0. Since there the only characteristic quantities are the heat flux H , the buoyancy parameter g/T and the height z , it follows from dimensional analysis that the temperature profile can be represented by: $T(z) = C_1 + C_2 z^{-1/3}$ and from the assumed similarity of temperature and wind profile:

$$u(z) = C_3 + C_4 z^{-1/3}.$$

Hence:

$$V(z) = \frac{4^{-1/3} - 2^{-1/3}}{4^{-1/3} - 1} \approx 0.442.$$

This is in agreement with the KEYPS formula. But V -values calculated from observational data are sometimes lower than 0.442, and this may therefore indicate that the KEYPS formula is not applicable, at least in very stable cases.

We suggest a different line of reasoning; K_M is often written as $\Delta u \cdot \lambda$. This expression was used in the derivation of the KEYPS profile. Δu is a velocity difference, characteristic of the rotation speed of the eddies, and λ is a length which is characteristic of the size of the eddies. Now it seems reasonable to assume that both Δu and λ increase linearly with height so that the maximum variation of K_M can be considered to be proportional to the square of height. According to (1.1.1) this would result in:

$$u(z) = A_1 + A_2 z^{-1}$$

and therefore:

$$V = \frac{4^{-1} - 2^{-1}}{4^{-1} - 1^{-1}} = + \frac{1}{3}.$$

This is in agreement with a statement by Ito (1966) that laboratory results of Malkus and Townsend show that the following approximation applies in the case of free convection:

$$f(\zeta) \sim \zeta^{-1}$$

The formulae of the Min-Pos group and the Swin-Trans profile are consistent

with this result. The only profile function which is consistent with both limits, i.e. $+ \frac{2}{3}$ for $\zeta \rightarrow +\infty$ and $+ \frac{1}{3}$ for $\zeta \rightarrow -\infty$, is the Holzman profile.

1.7 General comments on the theoretical results

As far as we can see, the various derivations of diabatic wind profile formulae as published in meteorological literature to date have only a very limited physical basis, viz., a balance equation in a simplified form with an unknown general expression ε for the total energy dissipation. Dimensional analysis alone is not sufficient to find an analytical form for ε . Some hypotheses (often of a purely mathematical nature) must be introduced and this has been done by different authors in different ways, being almost without exception a matter of trial and error. What is more, the terms of the turbulent balance equation can be formulated in different dimensions, which results in several possible forms for the profile formulae. Finally there is the numerical constant α , the value of which has to be found empirically.

A physical or partly physical reasoning, as used by different authors, suggests that the profile formulae obtained gives a better approximation of the true profile formula than a purely mathematical generalization of the logarithmic profile. The large differences between the well-known formulae (like KEYPS, Swinbank etc.) prove that this need not be the case at all.

It is clear from the figures 1.4.1 . . . 1.4.4 that a large number of "potential" wind profile formulae exist, which differ only very little from one another, and it is impossible to distinguish between them with the present instrumental accuracy of wind observations. On the other hand, we believe that, if sufficient observations were available, it would be possible to select a formula which describes the wind profile adequately over quite a large range of stability values.

It will not be possible to form a complete physical theory of wind profiles until the problem of wind structure (wind spectra depending on stability) is satisfactorily solved. A first attempt in this direction was made by Businger in his 1959 treatise.

2. APPLICATIONS OF PROFILE FORMULAE TO NUMERICAL RESULTS OF OBSERVATIONS

2.0 Introduction

Two groups of observations are needed for complete testing of wind profile formulae, in the first place wind speed observations from at least three heights and secondly observations of momentum and heat flux. The measurements in these two groups have to be independent of each other with respect to measuring errors.

The only observations of this kind available to us at the moment are the results of the "Great Plains Turbulence Field Program" carried out at O'Neill, Nebraska (in 1953) as published by LETTAU and DAVIDSON (1957). Many authors have already used these observations.

We must emphasize that due to the inaccuracy of the available observations the following results of the applications cannot be considered to have general validity. We would rather regard these applications as an example of how to apply the theoretical results to observations; and of course we do not mean to suggest that this would be the only way.

Measurements of the mean cross-products $\overline{u'w'}$ and $\overline{T'w'}$ have been used to determine values of the friction velocity u_* and the heat flux H . These observations were made by the Massachusetts Institute of Technology at heights of 1.5, 3 and 6 m. Simultaneous measurements of the mean wind speed made by a research group from Johns Hopkins University at heights 1.6, 3.2 and 6.4 m. were taken to form the second group.

With the u_* , H and T values, the Monin-Obukhov length L was calculated for each of the three levels taking $k = 0.4$. Because L is assumed to be independent of height, the mean value of the three $1/L$ values was used as an estimate of the true value of $1/L$.

The wind speed difference ratio

$$V = \frac{u_{6.4} - u_{3.2}}{u_{6.4} - u_{1.6}}$$

has been calculated from each triplet of mean wind speed measurements.

In figure 2.1.0 the values of V are plotted as a function of z/L , where $z = 160$ cm. There are 44 points altogether. Unfortunately there is a group of seven observations with very large V -values, (for $z/L = 0$, caused by $\overline{w'T'} = 0$, $H = 0$, $L = \infty$), which are situated completely outside the group of the other observations. There must have been something wrong with these measurements but we have not been able to find out the cause of the discrepancy. Of course we have been forced to leave these observations out of consideration because a homogeneous group of observations is needed.

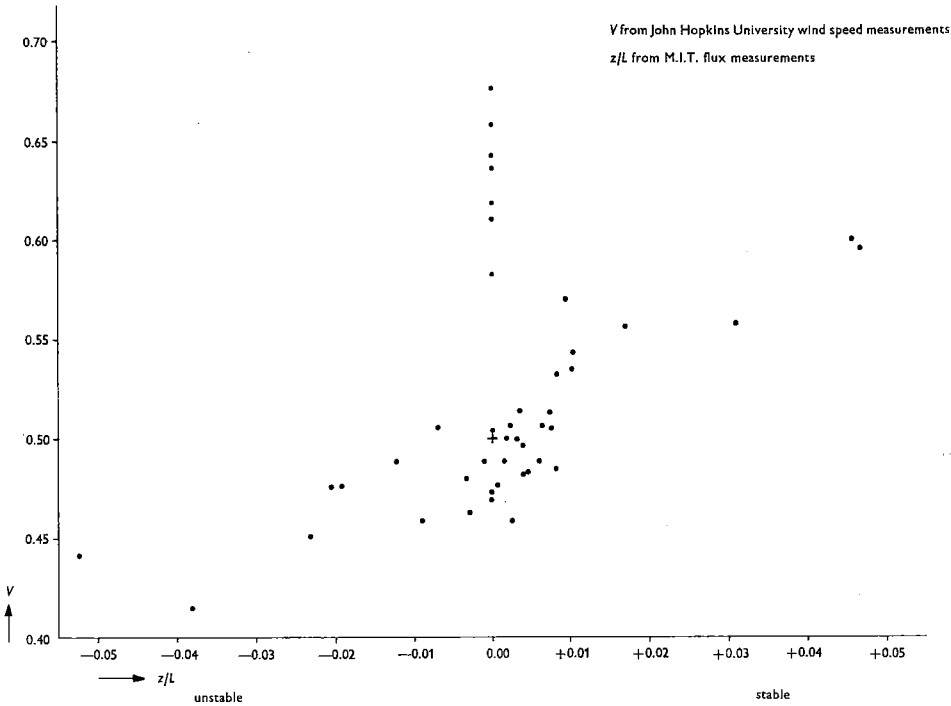


Fig. 2.1.0 Wind speed difference ratio and values of z/L from "Great Plains Turbulence Field Program" data.

2.1 Objections to the $(S, z/L)$ diagram

The remaining 37 observations will first be used to show the disadvantages which are inherent in the $(S, z/L)$ diagram when it is used to investigate which wind profile formula agrees best with the observations.

Figure 2.1.1 is the $(V, z/L)$ representation of the observations again. Figure 2.1.2 is the result of a randomization process. The V -values have been randomized with the use of random numbers and so they no longer bear any relation to the z/L -values. Randomization was done as follows: there are 37 pairs $(V, z/L)_i; i = 1, \dots, 37$. One V -value from the 37 is drawn at random and joined to $(z/L)_1$. Next a second V is drawn at random from the remaining 36 V -values and joined to $(z/L)_2$, etc. These new $(V, z/L)$ pairs were plotted in figure 2.1.2.

We now proceed to the $(S, z/L)$ diagrams. Values of S for two different levels have been calculated for each of the 37 sets of observations in the randomized case. This was done in the following way: for du/dz we took $(0.03125)(u_{6.4} - u_{3.2})$ and $(0.0625)(u_{3.2} - u_{1.6})$ respectively with $z = 4.52 (= \sqrt{6.4 \times 3.2})$ and 2.26

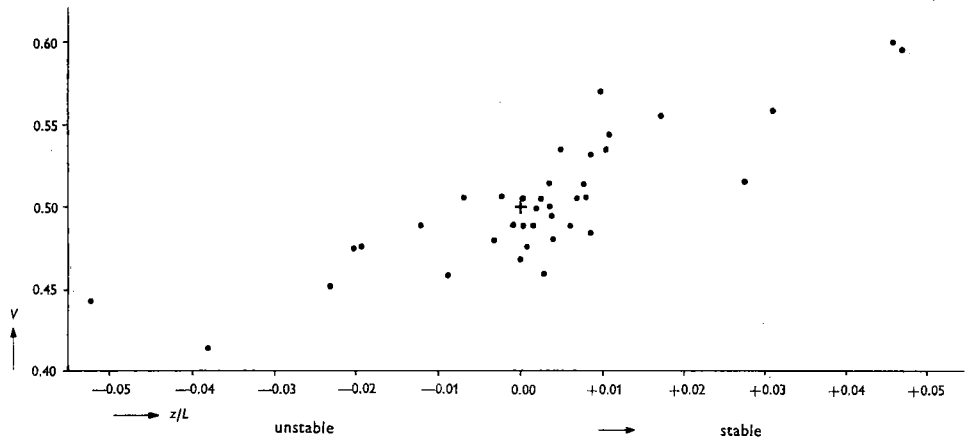


Fig. 2.1.1 Wind speed difference ratio V versus z/L (for $z = 160$ cm).

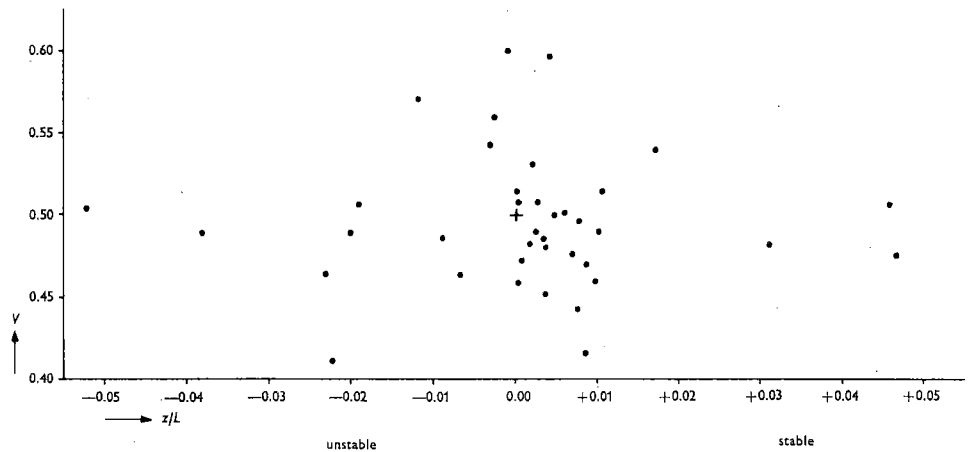


Fig. 2.1.2 Wind speed difference ratio V versus z/L , data from Fig. 2.1.1 after randomization.

($= \sqrt{3.2 \times 1.6}$). These values were multiplied by kz/u_* . In the first calculation we coupled the values of u_* and du/dz as they were observed together. In the second calculation we combined u_* -values with the randomized du/dz estimates (in accordance with the randomization of the V -values). Figures 2.1.3 and 2.1.4 (each with $2 \times 37 = 74$ points, with either $z = 2.26$ or $z = 4.52$) show the results. In figure 2.1.3 the characteristic shape of the $(S, z/L)$ diagrams can be recognized. In figure 2.1.4 there is much more scatter than in figure 2.1.3, but a relation between S and z/L similar to that of figure 2.1.3 is clear. An increase in S with increasing z/L on the stable side of the diagram can be observed together with the fact that on the unstable side the S values are much smaller than on the stable side. The difference between figure 2.1.3 and figure 2.1.4 is that in figure 2.1.3 a decrease in S with decreasing z/L is present,

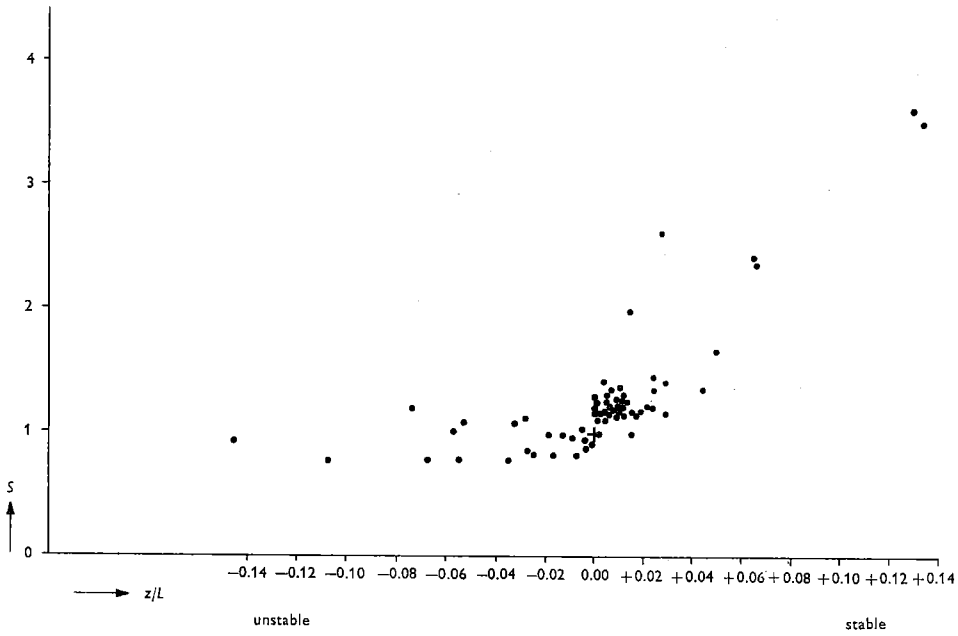


Fig. 2.1.3 Non-dimensional windshear S against height, stability ratio z/L .

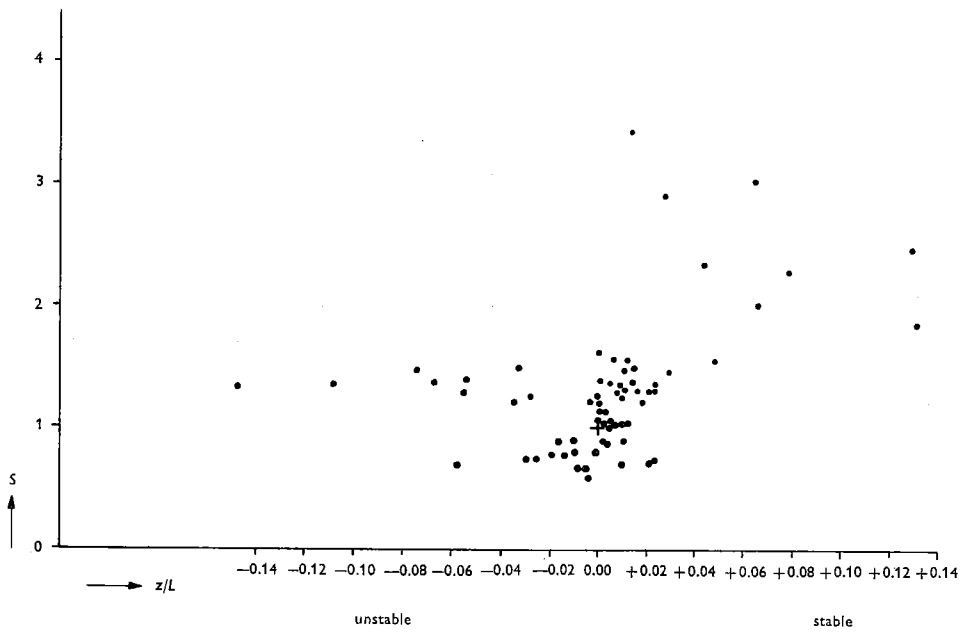


Fig. 2.1.4 Non-dimensional windshear S against height, stability parameter z/L after randomization.

just as is to be expected from theory, but in the “randomized” picture a slight increase in S with decreasing z/L could be seen.

There is bound to be an increase in S with increasing z/L because u_* occurs in the denominator in both S and z/L . So in the first instance we should expect similar increases in S on the stable and on the unstable side. But because generally in stable situations the vertical wind speed fluctuations (w') are small, whereas in unstable situations w' is much larger, this difference between the stable and unstable sides of the diagram can be explained by a difference in u_* values.

It will be clear from the foregoing that measuring inaccuracies in u_* result in a systematic deviation of the plotting positions of the observations from the true positions in the $(S, z/L)$ diagram. The deviations on the stable side roughly follow the slope of the $(S, z/L)$ curve and on the unstable side they are opposed to the slope of the curve.

2.2 Application of some of the wind profile formulae to O'Neill data (Great Plains Turbulence Field Program)

2.2.0 Introduction

As already mentioned in the foregoing section, unfortunately the observations of the “Great Plains Turbulence Field Program” are insufficiently accurate, so that we cannot expect to arrive at a conclusive statement as to the applicability of the various profile formulae. The flux measurements, in particular, are inaccurate owing to the inadequacy of the spectral range.

It does not seem worthwhile therefore, to apply detailed statistical tests. We think, however, that the material is good enough to show how the different formulae could be tested in future, as soon as better material becomes available.

2.2.1 The $(\zeta, z/L)$ diagram

The application of the formulae to the observation results was made as follows:

The ζ -value corresponding to each of the calculated V -values (37 cases) was read off from the theoretical (V, ζ) curves of figure 1.6.2, for each of the following six profile formulae:

KEYPS; MK₃; MO; Holzman; Swinbank; Goptarev.

The ζ -values obtained in this way and the corresponding measured z/L -values were plotted in diagrams (figures 2.2.1 . . . 2.2.6).

A formula as true as the L -hypothesis would yield a linear relation $\zeta = \alpha z/L$ over the whole range of stability. So a correlation coefficient between ζ and z/L , or a regression line ζ on z/L , can yield information on how well the different formulae approximate to this ideal.

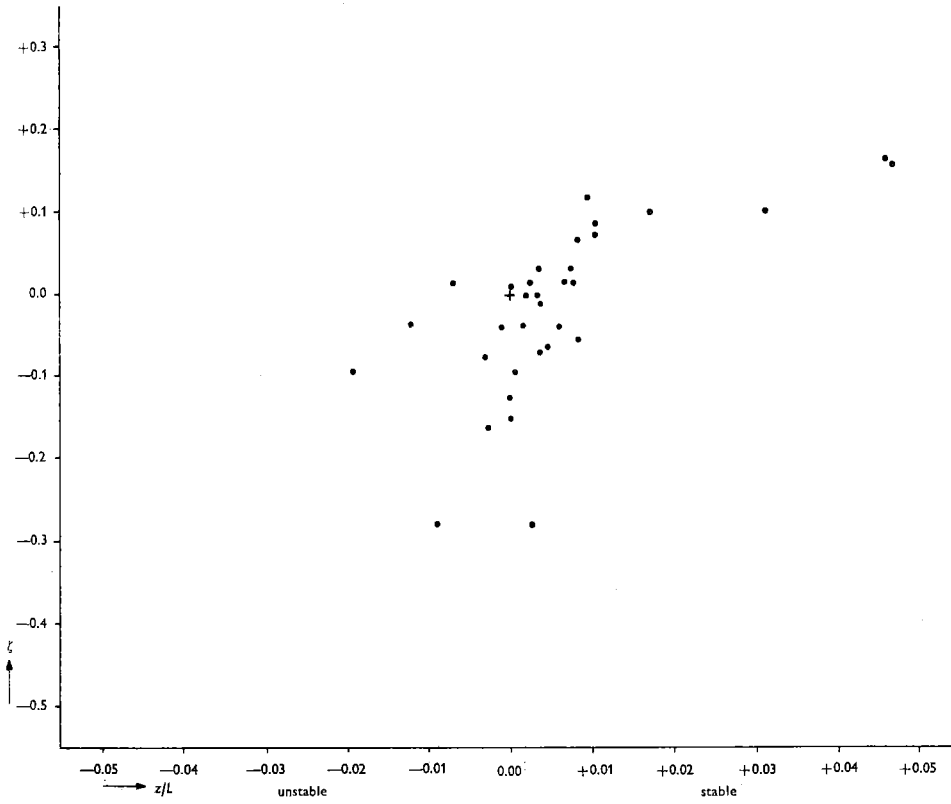


Fig. 2.2.1 Height, stability parameter ζ determined from the wind speed difference ratio according to the KEYPS profile formula against z/L . (for $z = 160$ cm)

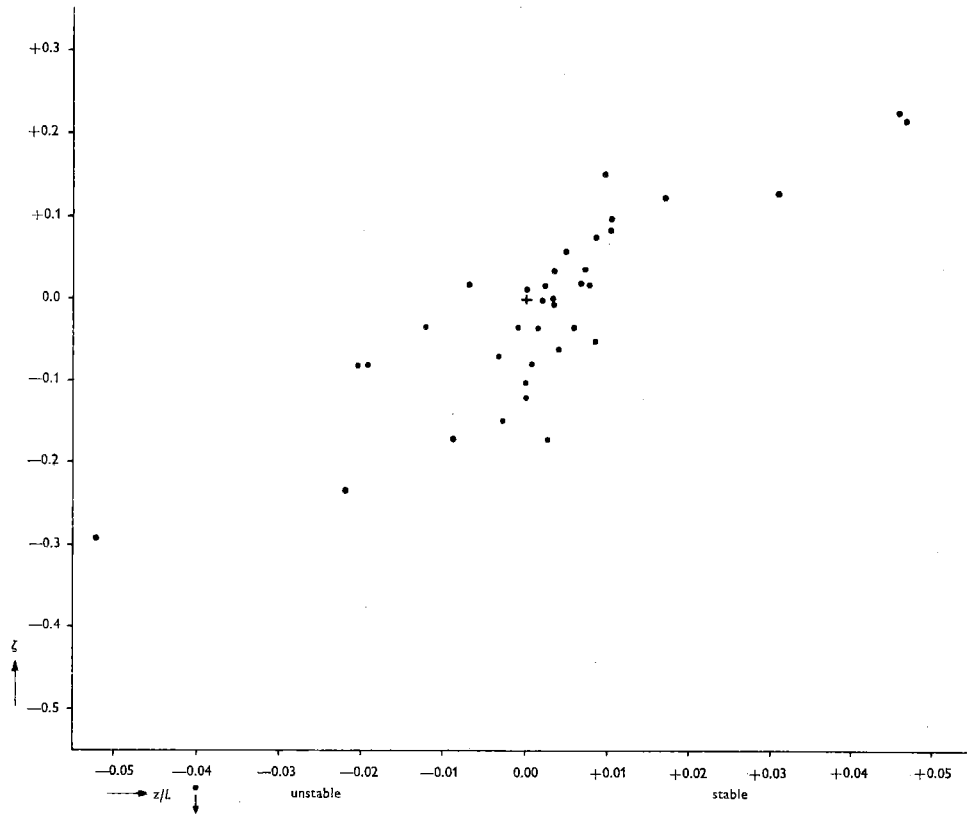


Fig. 2.2.2 Height, stability parameter ζ determined from the wind speed difference ratio according to the MK_3 profile formula against z/L (for $z = 160$ cm).

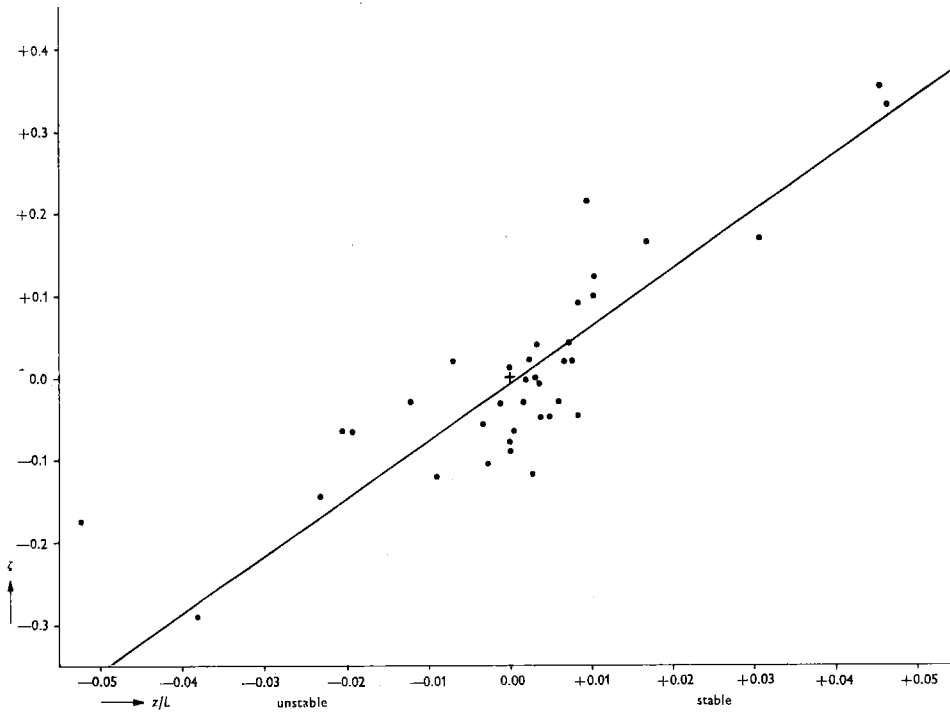


Fig. 2.2.3 Height, stability parameter ζ determined from the wind speed difference ratio according to the Holzman profile formula against z/L (for $z = 160$ cm).

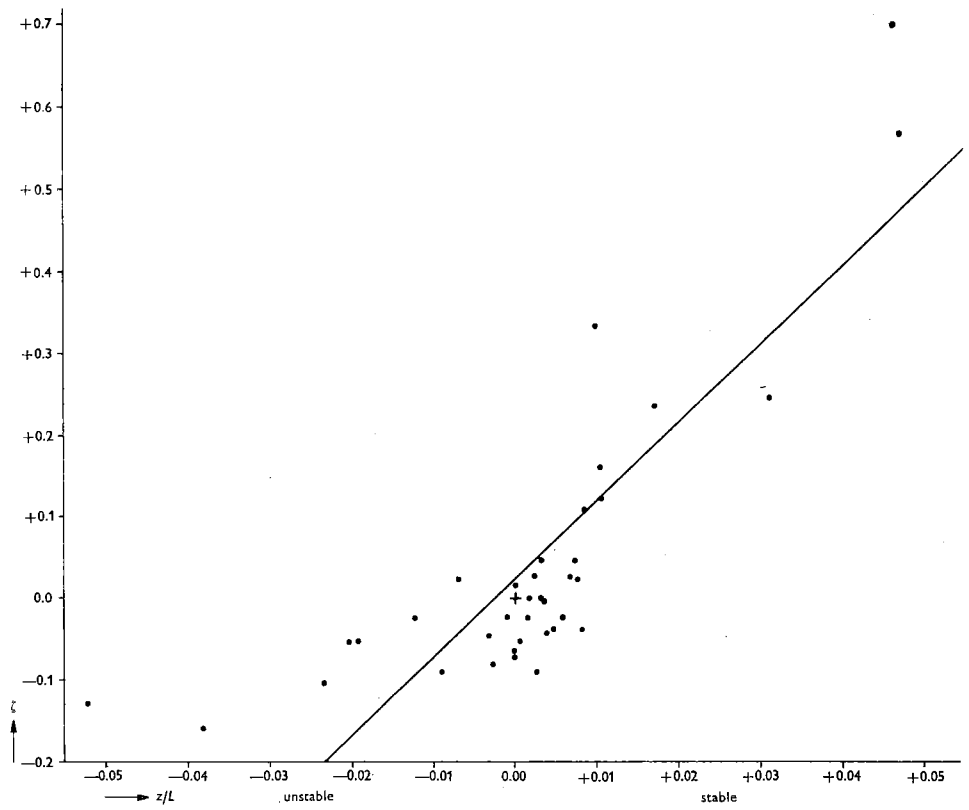


Fig. 2.2.4 Height, stability parameter ζ determined from the wind speed difference ratio according to the *MO* profile formula against z/L (for $z = 160$ cm).

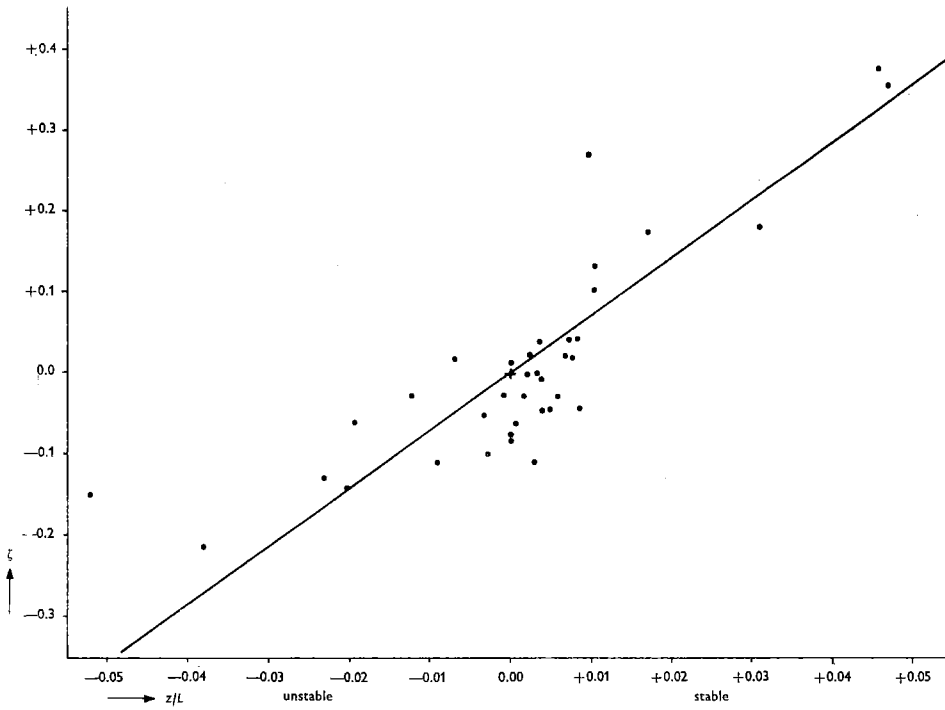


Fig. 2.2.5 Height, stability parameter ζ determined from the wind speed difference ratio according to the Swinbank profile formula against z/L (for $z = 160$ cm).

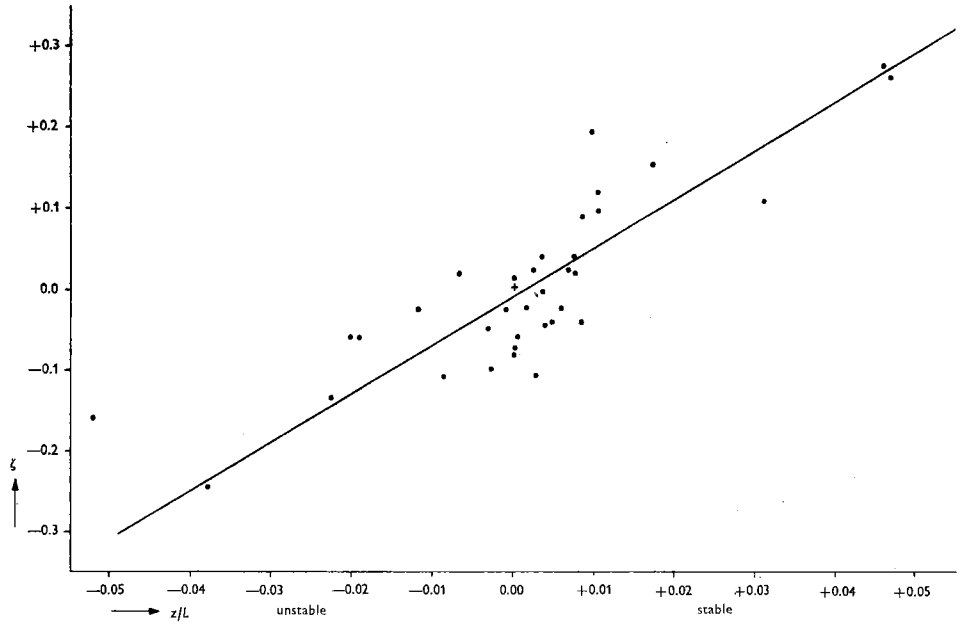


Fig. 2.2.6 Height, stability parameter ζ determined from the wind speed difference ratio according to the Goptarev profile formula against z/L (for $z = 160$ cm).

Without wishing to lay too much emphasis on the statistical importance, we determined the correlation coefficients for five of the six cases. This could not be done in the case of KEYPS, because one of the V -values is lower than 0.442 (the lower limit of KEYPS' (V, ζ) curve for $\zeta \rightarrow -\infty$) and therefore no real ζ exist in this case.

The values of the correlation coefficients r are:

Formula	r
MK ₃	0.559
Holzman	0.855
MO	0.798
Swinbank	0.829
Goptarev	0.848

The value of r for MK₃ is so much lower than the other r -values that it seems unlikely that this formula (and hence the KEYPS formula and all other Plus formulae where $q > 3$) can be used for practical purposes as a formula valid for a large stability range.

The results for the other formulae do not differ substantially. We have calculated regression lines for these formulae representing the variation of the true value of ζ with the true value of z/L .

Because the measurements of the two variables (ζ and z/L) contain a rather large margin of error, we decided not to use the common regression line of ζ on z/L , which is based upon errorless z/L -values, but to use a method described by LINDLEY (1947) (Appendix II).

Rough estimates of the standard deviations of both variables have been obtained in the following way:

The standard deviation $s_{z/L}$ of the measuring error of each z/L , which was determined from 3 observations, was found to be $z s_{1/L}$, where $s_{1/L}$ represents the sampling standard deviation of the three values of $1/L$. With $z = 160$ cm. we have:

$$s_{z/L} = 160 \left\{ \frac{1}{2} \sum_1^3 \left(\frac{1}{L} - \overline{\frac{1}{L}} \right)^2 \right\}^{\frac{1}{2}}.$$

To find the measuring error standard deviation of each ζ we have based ourselves upon the accuracy of the Johns Hopkins measurements of the u values as given by LETTAU and DAVIDSON (1957 vol I, p. 132) viz. 3 cm/s. We do not know exactly how this figure has been arrived at. We read "a comparability of the velocity as measured by the modified three-cup SCS anemometer at any level of the order of 0.5 per cent or 3 cm/s". But let us assume that this indicates a 2σ range so that the standard deviation

TABLE 2.2.1

z/L	$s_{z/L}$	V	s_v	KEYPS		MK ₃	
				ζ_1	s_{ζ_1}	ζ_2	s_{ζ_2}
+ 0.0075	0.0007	0.506	0.011	+ 0.015	0.028	+ 0.016	0.030
+ 0.0034	0.0019	0.514	0.013	+ 0.032	0.037	+ 0.035	0.030
- 0.0028	0.0014	0.463	0.012	- 0.212	0.248	- 0.148	0.062
- 0.0011	0.0006	0.489	0.013	- 0.039	0.061	- 0.035	0.045
+ 0.0308	0.0058	0.558	0.016	+ 0.103	0.020	+ 0.128	0.033
+ 0.0466	0.0026	0.596	0.011	+ 0.160	0.019	+ 0.217	0.030
+ 0.0456	0.0231	0.600	0.012	+ 0.167	0.020	+ 0.227	0.034
+ 0.0095	0.0095	0.570	0.016	+ 0.120	0.022	+ 0.153	0.036
- 0.0123	0.0033	0.489	0.021	- 0.037	0.092	- 0.035	0.074
- 0.0194	0.0010	0.477	0.017	- 0.093	0.119	- 0.080	0.074
- 0.0523	0.0188	0.443	0.019	- ∞	-	- 0.290	0.523
- 0.0382	0.0026	0.415	0.019	- ∞	-	- 2.500	-
- 0.0234	0.0037	0.451	0.020	- 0.560	-	- 0.220	0.226
+ 0.0047	0.0024	0.483	0.023	- 0.062	0.064	- 0.058	0.050
	0.0000	0.472	0.009	- 0.125	0.071	- 0.103	0.042
+ 0.0038	0.0006	0.482	0.011	- 0.067	0.035	- 0.061	0.043
+ 0.0026	0.0014	0.459	0.011	- 0.278	0.429	- 0.170	0.060
+ 0.0019	0.0010	0.500	0.010	0.000	0.030	0.000	0.029
+ 0.0015	0.0008	0.489	0.010	- 0.038	0.042	- 0.035	0.037
+ 0.0084	0.0011	0.532	0.013	+ 0.068	0.023	+ 0.076	0.028
	0.0000	0.504	0.014	+ 0.009	0.029	+ 0.011	0.030
+ 0.0005	0.0005	0.477	0.012	- 0.093	0.075	- 0.080	0.052
+ 0.0066	0.0017	0.507	0.014	+ 0.016	0.033	+ 0.018	0.035
+ 0.0073	0.0025	0.514	0.013	+ 0.031	0.028	+ 0.035	0.031
+ 0.0058	0.0003	0.489	0.014	- 0.038	0.051	- 0.035	0.045
+ 0.0084	0.0014	0.485	0.014	- 0.054	0.065	- 0.050	0.052
+ 0.0023	0.0022	0.507	0.012	+ 0.016	0.030	+ 0.018	0.031
	0.0000	0.469	0.013	- 0.150	0.190	- 0.118	0.062
- 0.0090	0.0024	0.459	0.012	- 0.278	0.429	- 0.170	0.065
- 0.0204	0.0080	0.477	0.012	- 0.093	0.075	- 0.080	0.052
- 0.0070	0.0027	0.506	0.011	+ 0.015	0.022	+ 0.016	0.024
- 0.0034	0.0005	0.480	0.010	- 0.075	0.054	- 0.068	0.040
+ 0.0032	0.0017	0.500	0.012	0.000	0.035	0.000	0.034
+ 0.0035	0.0018	0.497	0.012	- 0.010	0.038	- 0.008	0.036
+ 0.0103	0.0010	0.543	0.014	+ 0.086	0.020	+ 0.098	0.028
+ 0.0101	0.0051	0.535	0.010	+ 0.073	0.016	+ 0.082	0.020
+ 0.0170	0.0085	0.556	0.014	+ 0.102	0.018	+ 0.125	0.029

TABLE 2.2.1 (continuation)

HA		MO		Swinbank		Goptarev	
ζ_3	s_{ζ_3}	ζ_4	s_{ζ_4}	ζ_5	s_{ζ_5}	ζ_6	s_{ζ_6}
+ 0.020	0.032	+ 0.023	0.032	+ 0.020	0.031	+ 0.018	0.030
+ 0.041	0.036	+ 0.047	0.042	+ 0.043	0.038	+ 0.037	0.033
- 0.135	0.036	- 0.080	0.022	- 0.097	0.030	- 0.100	0.033
- 0.030	0.038	- 0.024	0.032	- 0.027	0.036	- 0.028	0.035
+ 0.172	0.055	+ 0.247	0.104	+ 0.183	0.062	+ 0.156	0.045
+ 0.331	0.060	+ 0.567	0.181	+ 0.356	0.062	+ 0.261	0.030
+ 0.355	0.072	+ 0.700	0.190	+ 0.380	0.069	+ 0.274	0.032
+ 0.215	0.062	+ 0.330	0.139	+ 0.272	0.071	+ 0.191	0.046
- 0.029	0.060	- 0.024	0.056	- 0.027	0.058	- 0.028	0.056
- 0.065	0.051	- 0.053	0.039	- 0.060	0.046	- 0.061	0.048
- 0.174	0.070	- 0.128	0.031	- 0.148	0.046	- 0.160	0.058
- 0.290	0.108	- 0.158	0.020	- 0.213	0.040	- 0.245	0.059
- 0.144	0.069	- 0.104	0.035	- 0.127	0.050	- 0.135	0.059
- 0.047	0.039	- 0.039	0.032	- 0.042	0.036	- 0.044	0.036
- 0.079	0.028	- 0.065	0.020	- 0.074	0.024	- 0.075	0.025
- 0.049	0.032	- 0.042	0.026	- 0.045	0.029	- 0.046	0.030
- 0.119	0.034	- 0.090	0.020	- 0.108	0.028	- 0.110	0.031
0.000	0.028	0.000	0.030	0.000	0.028	0.000	0.026
- 0.030	0.030	- 0.024	0.024	- 0.027	0.027	- 0.028	0.028
+ 0.092	0.038	+ 0.110	0.052	+ 0.095	0.040	+ 0.086	0.035
+ 0.014	0.032	+ 0.017	0.032	+ 0.015	0.032	+ 0.012	0.030
- 0.065	0.035	- 0.053	0.028	- 0.060	0.033	- 0.061	0.034
+ 0.021	0.036	+ 0.026	0.039	+ 0.023	0.038	+ 0.020	0.034
+ 0.042	0.036	+ 0.047	0.042	+ 0.044	0.038	+ 0.037	0.034
- 0.030	0.040	- 0.024	0.032	- 0.026	0.036	- 0.027	0.035
- 0.047	0.040	- 0.039	0.032	- 0.042	0.036	- 0.044	0.036
+ 0.021	0.034	+ 0.026	0.035	+ 0.023	0.032	+ 0.020	0.031
- 0.089	0.039	- 0.071	0.028	- 0.081	0.035	- 0.083	0.037
- 0.119	0.035	- 0.090	0.020	- 0.108	0.029	- 0.110	0.031
- 0.065	0.058	- 0.053	0.014	- 0.060	0.029	- 0.061	0.038
+ 0.020	0.021	+ 0.023	0.027	+ 0.020	0.025	+ 0.018	0.023
- 0.055	0.030	- 0.046	0.023	- 0.050	0.028	- 0.052	0.028
0.000	0.033	0.000	0.034	0.000	0.033	0.000	0.032
- 0.006	0.036	- 0.004	0.036	- 0.005	0.035	- 0.005	0.034
+ 0.124	0.034	+ 0.160	0.072	+ 0.130	0.047	+ 0.116	0.038
+ 0.100	0.029	+ 0.122	0.044	+ 0.105	0.031	+ 0.094	0.028
+ 0.166	0.048	+ 0.235	0.088	+ 0.176	0.052	+ 0.152	0.039

must be 0.015 m/s. The standard deviation of V can then be calculated easily (Appendix I).

A rough estimate of the measuring error standard deviation s_ζ of each ζ was then found graphically with the aid of figure 1.6.2.

Table 2.2.1 gives a complete list of the z/L , V and ζ -values with the standard deviations $s_{z/L}$, s_V and s_ζ , for the six profile formulae. In three cases for KEYPS and in one case for MK₃ no value of s_ζ is given. In these cases the calculated V -values are very close to the limit (for $\zeta = -\infty$) of the respective theoretical profiles.

The $s_{z/L}$ and s_ζ -values have been "pooled" to overall mean values of the standard deviations $\bar{s}_{z/L}$ and \bar{s}_ζ , for the Holzman, MO, Swinbank and Goptarev profiles only, according to:

$$\bar{s}_{z/L} = \sqrt{\frac{1}{37} \sum s_{z/L}^2} \text{ and } \bar{s}_\zeta = \sqrt{\frac{1}{37} \sum s_\zeta^2}$$

from which resulted:

$\bar{s}_{z/L} = 0.0059$ and $\bar{s}_{\zeta_3} = 0.047$; $\bar{s}_{\zeta_4} = 0.065$; $\bar{s}_{\zeta_5} = 0.042$ and $\bar{s}_{\zeta_6} = 0.038$, where the indices 3, . . . , 6 indicate Holzman, MO, Swinbank and Goptarev respectively.

The regression lines $\zeta = \alpha_r z/L + \beta_r$ are now determined for the four formulae (Appendix II).

The regression lines are drawn in figures 2.2.3, 2.2.4, 2.2.5 and 2.2.6, while the values of α_r and β_r are summarized in table 2.2.2.

TABLE 2.2.2 *Regression coefficients for profile formulae*

	Holzman	MO	Swinbank	Goptarev
α_r	6.91	9.53	7.08	5.99
β_r	-0.007	+0.026	+0.002	-0.009

The regression lines for the Holzman, Swinbank and Goptarev profiles almost pass through the origin. The regression line for the MO profile deviates more from the origin; the picture also suggests a non-linear relation for MO.

But, as we have already mentioned, we do not want to lay too much emphasis on the statistical results, because of the inaccuracy of the observations. All we are trying to do is to indicate that with more extensive material it must be possible to select a limited number of profile formulae that will serve for practical purposes.

In the foregoing, α is assumed to be constant in each formula under different stability conditions; we should not, however exclude, the possibility that different values of α or even different formulae have to be applied for the stable and unstable cases.

2.2.2 Probability distribution of V -values as a rough method of selection

We have seen that there are cases for which a real value of ζ cannot be determined because V is smaller than the limiting value of the theoretical V -function for $\zeta \rightarrow -\infty$.

It is obvious that theoretical formulae which yield a V -limit-value such that V -values below this limit are actually obtained by measurement cannot be considered to be completely correct.

If we are to investigate this, using the V -values obtained from the O'Neill data, we must not forget that each of the V -values contains a certain degree of error. What we need is the "true" value of V , denoted by the symbol V^* . Of course it is not possible to determine this "true" value in each individual case. The only thing we can do is try to estimate the distribution function of V^* , and then determine the fraction of the distribution which indicates the number of values below the theoretical limits. If this fraction is too large, the theoretical formula yields too many cases in which no real ζ can be found and hence must be rejected. Of course the decision on whether the fraction is too large is a subjective one. In our opinion the limit should be 1%.

Let us now write:

$$V_i = V_i^* + \varepsilon_i$$

where V_i is the measured value of V , V_i^* the unknown true value and ε_i the unknown measuring error.

We want to know the probability distribution of V^* , a stochastic variable, of which V_i^* is an individual realization.

The probability distribution of V can be estimated from the sample. The probability distribution of ε_i is assumed to be a normal one, with $E\varepsilon_i = 0$ ¹⁾ and variance $\sigma^2_{\varepsilon_i}$. The values of the estimates s_{ε_i} of the standard deviation σ_{ε_i} of ε_i have already been used in the previous section and are given in table 2.2.1.

Let us now suppose that σ_{ε_i} is constant ($\sigma_{\varepsilon_i} = \sigma_\varepsilon$ for every i); that ε_i is independent of V_i^* ($E(\varepsilon_i \cdot V_i^*) = 0$) and that V is normally distributed. The problem is then quite simple. We have a case where V is normally distributed with $EV = EV^*$ and

$$\sigma_V^2 = \sigma_{V^*}^2 + \sigma_\varepsilon^2. \quad (2.2.1)$$

The sample mean value of V happens to be exactly 0.500 and the standard deviation is 0.040. For testing the hypothesis that the group of 37 V -values is a random sample from a normal population, the χ^2 test of goodness of fit is applied (Appendix III). The result is that the hypothesis need not be rejected. An obvious but rough check on normality can be made by using normal probability paper. If the population is normal, a graph of the sample cumulative percentage frequencies on this paper will approximate a straight line. See figure 2.2.7, in which the points lie almost along a

1) E stands for expectation.

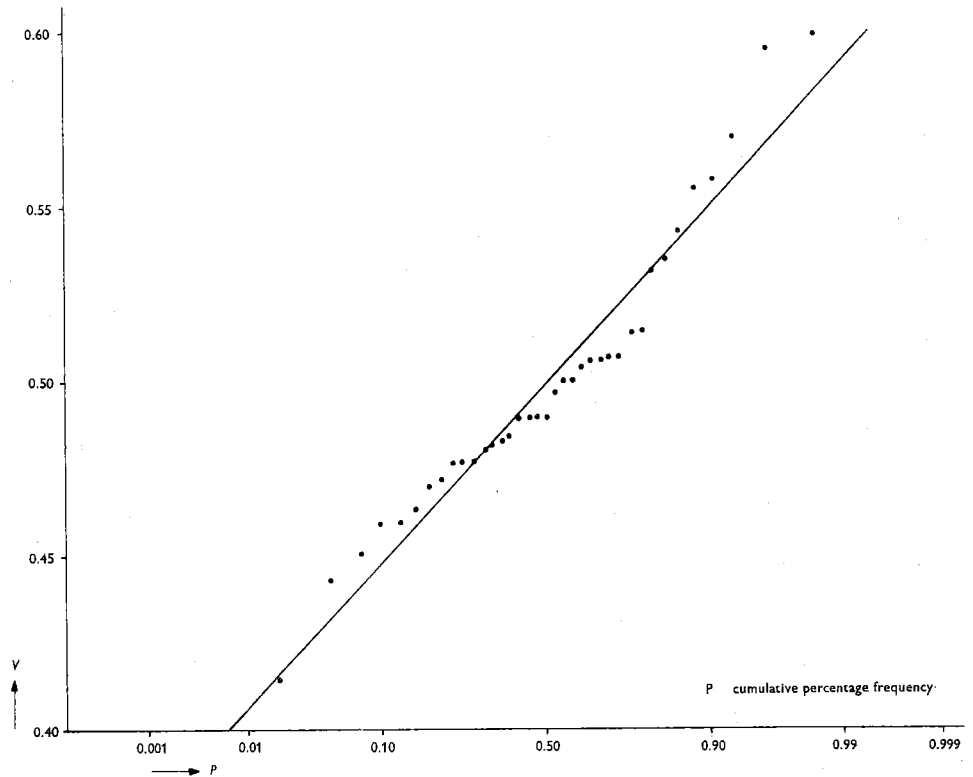


Fig. 2.2.7 Frequency distribution of the wind speed difference ratio based on "Great Plains Turbulence Field Program" data.

straight line. The positions of the points in this figure have been obtained by first arranging the V 's in order of increasing value $V_1 \leq V_2 \leq \dots \leq V_i \leq \dots \leq V_{37}$ and then plotting them against $\frac{i-0.3}{37+0.4}$. This is an estimate of the cumulative frequency (see BENARD and BOS-LEVENBACH, 1953).

It is not possible to test statistically the condition that $\sigma_{e_i} = \sigma_e = \text{constant}$, because V^* and σ_e are unknown, but visually it seems very likely that s_e and V are independent of each other. The values of s_e have been plotted against V in figure 2.2.8 and we think that this figure justifies the assumption of independence without testing. It can then be assumed that s_e and V^* are also independent of each other.

As a universal value of s_e we have taken:

$$\sqrt{\frac{1}{37} \sum_1^{37} (s_{e_i}^2)} = 0.014.$$

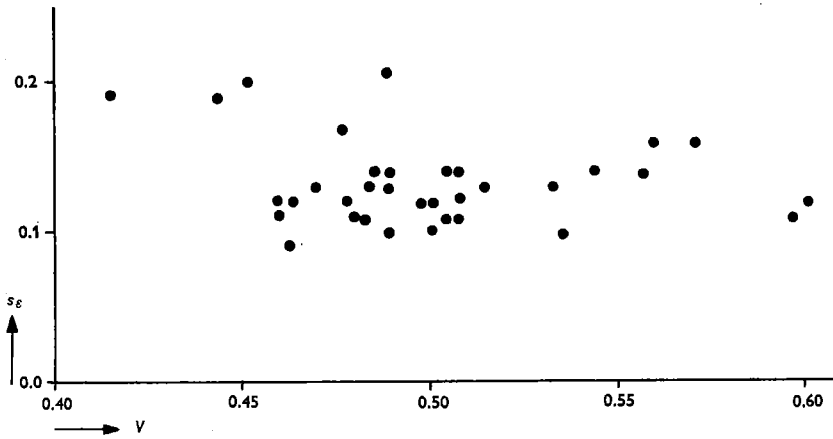


Fig. 2.2.8 Standard deviation of the measuring error of the wind speed difference ratio against the wind speed difference ratio itself.

From formula 2.2.1 we find:

$$s_{V^*}^2 = s_V^2 - s_\epsilon^2 = (0.040)^2 - (0.014)^2 \approx 0.0014 \text{ so that } s_{V^*} \approx 0.038.$$

In determining the fraction Q_1 of V^* -values below the theoretical limits we have to take into account that the estimate $s_V \approx 0.038$ was obtained from a sample of only 37 observations. So Q_1 itself cannot be determined exactly and we can only give a confidence interval ($Q_{1,l}, Q_{1,u}$) (see LEVERT, 1959). We shall take a 95% confidence interval.

The results are as follows:

Profile	V limit	$Q_{1,l}$	$Q_{1,u}$
KEYPS	0.442	2.3%	15.9%
MK ₃	0.414	0.2%	5.5%
Holzman	0.333	0.00%	0.06%

Now we can conclude that the number of V -values that can occur below the KEYPS limit is so large ($> 1\%$) that the formula cannot be considered as correct.

The MK_3 formula seems to be doubtful in this sense. The Q -value for the Holzman profile is so small that the formula is completely acceptable.

It is clear that all Plus formulae with $q > 4$ must also be excluded.

In the above we have paid attention only to the lower limit of the V -values (cor-

responding to extremely unstable situations). We can determine confidence intervals for the upper limits in the same way in respect of the fraction Q_2 of V^* -values above the upper limit. For all formulae of the MOHKEYPS group this upper limit is $+\frac{2}{3}$ and the Q_2 interval is $0.00 \dots 0.06\%$. So there is no reason to exclude any formula in this group. This can be the case only for Plus formulae with $q < 0$.

Finally we may remark that analogous results obtain for the Minus group. Formulae in the Min-Pos group with $q \geq 4$ must be excluded because V^* -values above the upper V -limit may occur, but no formulae of the Min-Pos group have to be excluded because V^* -values occur below the lower V -limit. This can occur only for Minus formulae with $q < 0$.

2.3 Application of some of the wind profile formulae to wind speed observations from Project Prairie Grass

2.3.0 Introduction

In 1956 a Field Program in Diffusion called Project Prairie Grass was carried out at O'Neill, Nebraska. Results were published in 1958 and edited by M. L. BARAD.

TABLE 2.3.1

Series	N	Range of $(\theta_4 - \theta_{\frac{1}{2}}) / u_1^2$		u_{16}	u_8	u_4	u_2	u_1	$u_{\frac{1}{2}}$	$u_{\frac{1}{4}}$	
I	4	1.9	...	2.5	405	316	243	175	115	90	70
II	4	1.0	...	1.4	478	381	287	222	152	119	85
III	7	0.59	...	0.87	534	394	282	215	160	135	98
IV	5	0.42	...	0.49	405	322	256	206	168	140	105
V	4	0.19	...	0.29	552	440	352	286	235	202	162
VI	12	0.10	...	0.17	572	455	378	317	273	229	185
VII	11	0.058	...	0.094	641	532	450	388	335	288	236
VIII	10	0.034	...	0.050	686	569	501	435	383	331	274
IX	13	0.019	...	0.031	795	691	612	531	470	408	334
X	13	0.000	...	0.016	898	794	708	621	545	476	393
XI	9	-0.016	...	0.000	861	770	703	618	546	478	401
XII	9	-0.031	...	-0.019	904	831	754	675	602	523	427
XIII	16	-0.053	...	-0.032	1022	948	854	760	681	589	494
XIV	21	-0.097	...	-0.057	841	783	710	636	568	502	422
XV	16	-0.16	...	-0.10	586	548	515	464	420	372	316
XVI	16	-0.30	...	-0.18	470	444	416	382	346	298	258
XVII	13	-0.48	...	-0.33	368	350	328	306	278	252	211

Wind and temperature data from this project have already been used by KONDO (1962). The same observations will be used here.

Observations were made at heights of $\frac{1}{4}$, $\frac{1}{2}$, 1, 2, 4, 8 and 16 m. KONDO arranged the observations in 17 groups according to the value of $(\theta_4 - \theta_1) / u_1^2$, which was used as a stability measure, positive values corresponding with stable and negative values with unstable situations. The symbol θ represents potential temperature and u wind speed. The indices indicate the height in m.

Table 2.3.1 contains a summary of these data, copied from table 1 of KONDO.

The numbers of observations in the various groups vary between 4 and 21 and the wind speed values have been averaged over this number of observations.

2.3.1 General results

The application of the wind profile formulae to the observations can be made in two different ways.

By the first method, V -values can be calculated for each of the 17 groups, for wind speeds of different combinations of three heights. Values of ζ can then be determined with the aid of the (V, ζ) diagram (figure 1.6.2). These ζ values have to be divided by the relevant z and then yield α/L values of α/L . The α/L -values obtained in this way have to be averaged.

The second method is by fitting the profile formulae to the experimental data by means of the method of least squares. This is very difficult for most formulae, because the equations from which the parameters have to be determined are not linear in the parameters (see YULE and KENDALL, 1965, Chapter 15). In these cases the only way is to calculate the sum of the square deviations for fixed values of the stability parameter ζ . By giving different values to ζ a series of square sums is obtained of which the smallest indicates the relevant value of ζ .

The values of α/L , z_0 and u_* can be obtained by either method, but we prefer the second. The reason is that, owing to measuring errors, V -values below the lower or above the upper limit of the theoretical V -function of some profile formulae can occur.

The first method will be applied nevertheless, but restricted to the calculation of the V -values, because the results are interesting in themselves and can also be used to obtain a conclusion concerning the Deacon profile.

2.3.2 The wind speed difference ratios

We have seen in chapter 1 that the Deacon profile (see table 1.2.1, III and 1.5) cannot be incorporated into the general system because it is not possible to write formula III in the form (1.3.2), for this would imply that ζ could be written as a function of β and z , and ζ_0 as the same function of β and z_0 . This is only possible if we allow that ζ is a function of z_0 too, but such an assumption contradicts the design of the theory.

Nevertheless, it is possible to use the wind speed difference ratio for the Deacon profile.

If the definition of V (with $z_3 = 4z$; $z_2 = 2z$ and $z_1 = z$) is applied to formula III we obtain:

$$V = \frac{4^{1-\beta} - 2^{1-\beta}}{4^{1-\beta} - 1} = \frac{1 - 2^{\beta-1}}{1 - 4^{\beta-1}} \quad (2.3.1)$$

Therefore, according to the Deacon formula, V is independent of height. On the other hand, according to all the formulae of our general system (1.3.23), V is a function of ζ and since we assumed that L is independent of height, ζ is proportional to z , which means that V has to vary with z , viz.: increasing in stable situations and decreasing in unstable ones.

It follows then, that if a number of V -values are available for different heights, we can decide between the Deacon profile and the other formulae by testing whether V depends on z or not. We are now trying to make this decision.

In table 2.3.2 the values of V are shown for the 17 groups and for the 5 successive triples of wind speed values, viz. for $z_3 = 4z$, $z_2 = 2z$ and $z_1 = z$, where $z = \frac{1}{4}, \frac{1}{2}, 1, 2$ and 4 respectively. The five V -values are indicated by $V_{\frac{1}{4}}, V_{\frac{1}{2}}, V_1, V_2$ and V_4 .

TABLE 2.3.2 *Wind speed difference ratios*

Series	V_4	V_2	V_1	$V_{\frac{1}{2}}$	$V_{\frac{1}{4}}$	$V_{\frac{1}{4}, \frac{1}{2}}$
I	0.560	0.518	0.529	0.705	0.556	0.630
II	0.509	0.590	0.492	0.678	0.490	0.584
III	0.557	0.625	0.549	0.686	0.402	0.544
IV	0.557	0.569	0.565	0.572	0.442	0.507
V	0.560	0.570	0.572	0.608	0.450	0.529
VI	0.602	0.558	0.581	0.500	0.500	0.500
VII	0.572	0.568	0.538	0.530	0.475	0.502
VIII	0.630	0.508	0.558	0.500	0.472	0.486
IX	0.578	0.495	0.532	0.492	0.452	0.472
X	0.549	0.495	0.531	0.522	0.451	0.486
XI	0.576	0.440	0.540	0.515	0.470	0.492
XII	0.487	0.492	0.521	0.478	0.451	0.465
XIII	0.439	0.500	0.502	0.460	0.491	0.476
XIV	0.442	0.495	0.520	0.506	0.451	0.478
XV	0.532	0.392	0.535	0.488	0.461	0.474
XVI	0.480	0.450	0.486	0.428	0.543	0.486
XVII	0.450	0.500	0.440	0.519	0.454	0.487

Each test that can be used to investigate whether V is independent of height or not requires that all 5 V -values are independent of each other. Unfortunately they are not, because they have u -values in common. So V_4 and V_2 both have two u -values, viz. u_4 and u_8 in common etc., and V_4 and V_1 both have one u -value in common viz. u_4 etc. To overcome this difficulty we can compare either V_4 with the mean $V_{\frac{1}{2}, \frac{1}{2}}$ of $V_{\frac{1}{2}}$ and $V_{\frac{1}{2}}$, or $V_{\frac{1}{2}}$ with the mean of V_4 and V_2 . We prefer the first alternative, because the inaccuracy of the $V_{\frac{1}{2}}$ and $V_{\frac{1}{2}}$ -values is larger than those of the V_4 and V_2 -values. Now the mean of two variables has a smaller standard deviation than the original variables themselves. So the quantities V_4 and $V_{\frac{1}{2}, \frac{1}{2}}$ have standard deviations which differ less than those of the quantities $V_{2,4}$ and $V_{\frac{1}{2}}$.

Let us now test the null hypothesis that V is independent of height. The alternative hypotheses differ for the stable and unstable cases. In stable situations $V > \frac{1}{2}$ and V increases with increasing ζ (which is > 0); this means with increasing z , because α/L is assumed to be constant. So the hypothesis $V_4 = V_{\frac{1}{2}, \frac{1}{2}}$ is to be tested against $V_4 > V_{\frac{1}{2}, \frac{1}{2}}$.

If the true values of V were independent of height there would be a probability $\frac{1}{2}$ that $V_4 > V_{\frac{1}{2}, \frac{1}{2}}$ because of the presence of measuring errors. The number of cases with $V_4 > V_{\frac{1}{2}, \frac{1}{2}}$ in a sample of N pairs would then be distributed according to a binomial probability distribution. In the actual sample of 11 stable cases I . . . XI, there are 9 cases $V_4 > V_{\frac{1}{2}, \frac{1}{2}}$. The probability of finding 9 or more cases $V_4 > V_{\frac{1}{2}, \frac{1}{2}}$ is 0.033 according to the binomial distribution (Appendix IV). This is below the 5% level of significance, so we can reject the hypothesis that V is independent of height for stable situations.

In unstable situations V increases with increasing ζ , but because of $\zeta < 0$, this means that V decreases with increasing z , so we now have to test $V_4 = V_{\frac{1}{2}, \frac{1}{2}}$ against the alternative $V_4 < V_{\frac{1}{2}, \frac{1}{2}}$. Now there are 4 cases out of 6 with $V_4 < V_{\frac{1}{2}, \frac{1}{2}}$. Of course this is not significant, the probability of getting 4 or more cases being 0.34. For the unstable group the hypothesis that V is independent of height cannot be rejected, therefore, but of course this negative statement does not mean that $V_4 < V_{\frac{1}{2}, \frac{1}{2}}$ cannot be true.

2.3.3 *Least squares estimates of the parameters of different wind profile formulae*

Although certain objections have been raised to some of the formulae (KEYPS: no V -values possible below 0.442; Deacon: V is constant), it might still prove worthwhile to fit a number of formulae to the observations of table 2.3.1 by the method of least squares. We have done so for the following formulae: KEYPS, Holzman, MO, Swinbank, Goptarev, Deacon and the power profile. The power profile has been added in order to compare this simple formula, which will be dealt with in Chapter 3, with the more complex ones.

Direct application of the method of least squares (Appendix V) is only possible in the case of MO and the power profile (the latter if written in the logarithmic form: $\ln u = \ln A + p \cdot \ln z$). For it is only in these cases that the least squares normal equations, from which the values of the parameters are to be estimated, are linear in these parameters.

For the other formulae a rough estimate of the range of α/L values has been made by plotting the u values against $\ln z$ and judging the curvature by eye. For each of a number of α/L values increasing by steps of 0.01, and lying within this roughly estimated range, seven values ζ can be determined for the seven heights. The seven values $f(\zeta)$ can then be found from graphs of $f(\zeta)$ as a function of ζ . These seven $f(\zeta)$ -values correspond to the seven u -values of table 2.3.1. The parameters u_*/k and $f(\zeta_0)$ for each series and each step value of α/L can then be calculated by the method of least squares. The seven theoretical values $\tilde{u} = \frac{\tilde{u}_*}{k} * (f(\zeta) - \widetilde{f(\zeta_0)})$ and the sum of the square deviations $W = \sum_1^7 (u - \tilde{u})^2$ have been determined from the least squares parameter values $\tilde{u}_*/k, \widetilde{f(\zeta_0)}$.

So each individual α/L yields a sum W and each series of α/L -values yields a series of W -values. The minimum value of these W -values fixes a value of α/L which gives the most reliable values of u_*/k and $f(\zeta_0)$ and therefore of ζ_0 , and finally of z_0 itself. The results are summarized in table 2.3.3.

TABLE 2.3.3

Series	Formula	$\alpha/L(m^{-1})$	$(cm \cdot s^{-1})$		s (cm)	$1/L(m^{-1})$
			u_*/k (cm)	z_0 (cm)		
I.	KEYPS	+ 0.05	62	11.2	14.7	
	Holzman	+ 0.10	57	10.0	13.4	+ 0.017
	MO	+ 0.26	43	5.6	13.9	
	Swinbank	+ 0.11	56	9.5	13.2	+ 0.022
	Goptarev	+ 0.08	60	10.7	14.1	+ 0.017
	Deacon	(+ 0.35)	15	1.7	7.2	
	Power			$p = 0.44$	$A = 125$	10.4
II.	KEYPS	+ 0.06	70	9.0	13.2	
	Holzman	+ 0.10	66	8.5	11.9	+ 0.017
	MO	+ 0.26	65	8.1	10.7	
	Swinbank	+ 0.10	67	8.5	11.6	+ 0.020
	Goptarev	+ 0.08	69	9.0	12.9	+ 0.017
	Deacon	(+ 0.31)	22	2.1	5.8	
	Power			$p = 0.42$	$A = 157$	12.5

Series	Formula	$\alpha/L(m^{-1})$	$(cm \cdot s^{-1})$		s (cm)	$1/L(m^{-1})$
			u_*/k (cm)	z_o (cm)		
III.	KEYPS	+ 0.09	60	5.7	12.7	
	Holzman	+ 0.18	53	6.3	10.6	+ 0.023
	MO	+ 0.58	31	1.0	20.4	
	Swinbank	+ 0.29	38	1.7	18.4	+ 0.057
	Goptarev	+ 0.12	60	6.0	14.0	+ 0.025
	Deacon	(+ 0.67)	- 60	complex	24.0	
	Power			$p = 0.37$	$A = 166$	33.6
IV.	KEYPS	+ 0.06	52	3.6	5.8	
	Holzman	+ 0.10	48	3.0	4.6	+ 0.018
	MO	+ 0.17	44	2.6	3.6	
	Swinbank	+ 0.11	48	3.0	4.7	+ 0.022
	Goptarev	+ 0.09	48	4.5	5.5	+ 0.019
	Deacon	(+ 0.34)	- 7	complex	3.1	
	Power			$p = 0.32$	$A = 167$	3.0
V.	KEYPS	+ 0.06	65	2.4	9.4	
	Holzman	+ 0.12	60	2.1	7.0	+ 0.020
	MO	+ 0.20	54	1.4	5.7	
	Swinbank	+ 0.12	61	2.5	7.2	+ 0.024
	Goptarev	+ 0.09	64	2.3	8.0	+ 0.019
	Deacon	(+ 0.38)	- 22	complex	3.0	
	Power			$p = 0.20$	$A = 240$	7.9
VI.	KEYPS	+ 0.06	64	1.4	3.5	
	Holzman	+ 0.11	60	1.2	2.1	+ 0.019
	MO	+ 0.18	56	0.9	1.8	
	Swinbank	+ 0.12	59	1.2	2.1	+ 0.024
	Goptarev	+ 0.09	62	1.3	3.0	+ 0.019
	Deacon	(+ 0.35)	- 28	complex	6.2	
	Power			$p = 0.26$	$A = 269$	8.5
VII.	KEYPS	+ 0.05	73	1.0	3.7	
	Holzman	+ 0.08	69	0.9	2.6	+ 0.014
	MO	+ 0.13	66	0.7	1.9	
	Swinbank	+ 0.09	69	0.8	2.3	+ 0.018
	Goptarev	+ 0.07	72	1.0	2.9	+ 0.014
	Deacon	(+ 0.27)	- 14	complex	5.7	
	Power			$p = 0.23$	$A = 331$	5.9

Series	Formula	$a/L(m^{-1})$	$(cm \cdot s^{-1})$		s (cm)	$1/L(m^{-1})$
			u_*/k (cm)	z_0 (cm)		
VIII.	KEYPS	+ 0.05	74	0.60	2.4	
	Holzman	+ 0.08	72	0.55	3.4	+ 0.013
	MO	+ 0.10	70	0.49	4.6	
	Swinbank	+ 0.08	72	0.44	3.9	+ 0.016
	Goptarev	+ 0.07	72	0.53	2.7	+ 0.014
	Deacon	(+ 0.22)	— 3	complex	8.9	
	Power			$p = 0.21$	$A = 375$	9.0
IX.	KEYPS	+ 0.03	94	0.67	3.7	
	Holzman	+ 0.05	92	0.66	4.0	+ 0.008
	MO	+ 0.06	91	0.62	3.9	
	Swinbank	+ 0.05	91	0.60	3.7	+ 0.010
	Goptarev	+ 0.04	93	0.66	4.2	+ 0.008
	Deacon	(+ 0.12)	43	0.09	6.0	
	Power			$p = 0.20$	$A = 535$	9.0
X.	KEYPS	+ 0.02	108	0.67	3.5	
	Holzman	+ 0.02	109	0.70	3.6	+ 0.004
	MO	+ 0.04	107	0.33	3.3	
	Swinbank	+ 0.03	108	0.67	3.3	+ 0.006
	Goptarev	+ 0.03	107	0.60	3.7	+ 0.006
	Deacon	(+ 0.10)	56	0.12	4.2	
	Power			$p = 0.10$	$A = 535$	12.5
XI.	KEYPS	+ 0.01	106	0.58	3.9	
	Holzman	+ 0.02	102	0.52	3.1	+ 0.004
	MO	+ 0.02	104	0.51	4.2	
	Swinbank	+ 0.02	102	0.50	4.3	+ 0.004
	Goptarev	+ 0.01	106	0.61	4.3	+ 0.002
	Deacon	(+ 0.03)	91	0.43	4.2	
	Power			$p = 0.18$	$A = 535$	15.6
XII.	KEYPS	— 0.02	120	0.69	4.7	
	Holzman	— 0.02	119	0.70	4.8	— 0.002
	MO	— 0.01	116	0.57	5.4	
	Swinbank	— 0.01	116	0.60	5.0	— 0.002
	Goptarev	— 0.01	116	0.57	5.6	— 0.002
	Deacon	(— 0.05)	147	0.25	4.0	
	Power			$p = 0.18$	$A = 580$	23.8

Series	Formula	$a/L(m^{-1})$	$(cm \cdot s^{-1})$		s (cm)	$1/L(m^{-1})$
			u_*/k (cm)	z_o (cm)		
XIII.	KEYPS	-0.01	131	0.58	4.5	
	Holzman	-0.02	134	0.67	4.7	-0.004
	MO	-0.01	131	0.56	5.3	
	Swinbank	-0.01	132	0.15	4.4	-0.002
	Goptarev	-0.02	135	0.63	6.0	-0.004
	Deacon	(-0.02)	143	0.85	4.4	
	Power			$p = 0.17$	$A = 659$	24.3
XIV.	KEYPS	-0.02	106	0.45	3.8	
	Holzman	-0.02	106	0.50	3.8	-0.002
	MO	-0.01	105	0.43	4.0	
	Swinbank	-0.01	105	0.45	3.8	-0.002
	Goptarev	-0.02	107	0.48	4.4	-0.004
	Deacon	(-0.03)	121	0.94	3.8	
	Power			$p = 0.16$	$A = 555$	18.9
XV.	KEYPS	-0.06	74	0.34	2.5	
	Holzman	-0.04	73	0.32	2.9	-0.007
	MO	-0.03	72	0.30	3.4	
	Swinbank	-0.04	73	0.31	3.2	-0.008
	Goptarev	-0.04	74	0.32	2.9	-0.008
	Deacon	(-0.11)	116	0.94	2.4	
	Power			$p = 0.15$	$A = 408$	15.4
XVI.	KEYPS	-0.15	67	0.50	1.9	
	Holzman	-0.06	62	0.39	2.5	-0.011
	MO	-0.04	60	0.34	3.1	
	Swinbank	-0.06	62	0.38	2.6	-0.012
	Goptarev	-0.06	61	0.35	2.8	-0.012
	Deacon	(-0.17)	115	1.54	2.2	
	Power			$p = 0.14$	$A = 332$	15.1
XVII.	KEYPS	-0.12	47	0.24	3.1	
	Holzman	-0.08	47	0.25	3.1	-0.014
	MO	-0.04	42	0.14	4.3	
	Swinbank	-0.06	45	0.19	3.4	-0.012
	Goptarev	-0.09	48	0.27	3.4	-0.019
	Deacon	(-0.20)	97	1.20	1.7	
	Power			$p = 0.13$	$A = 269$	11.2

Explanation of symbols:

α/L = the stability parameter ($1 - \beta$ for Deacon)

$\frac{u_*}{k}$ = friction velocity divided by k .

z_o = roughness parameter.

s = standard deviation of the difference $u - \tilde{u}$, from $s^2 = W/6$.

$1/L$ = reciprocal Monin-Obukhov length (only for Holzman, Swinbank and Goptarev)

The $1/L$ values are derived from α/L by using the values for α from table 2.2.2, MO being left out of consideration, because α cannot be considered as a reliable value in that case.

The results of table 2.3.3 will be discussed in more detail in the following paragraphs.

2.3.4 The standard deviation values

We have constructed figure 2.3.1 to facilitate study of the results.

The most remarkable feature is that the s -values of the power profile for unstable situations (series XII . . . XVII) are very high, while the s -values for the other formulae are much lower and almost consistent. In the stable group (series I . . . XI) the s -values of the various formulae show a general tendency to increase with increasing stability from I to XI, but the differences between them vary and no formula gives a picture which clearly deviates from the others.

We have used the method of m -rankings, the so-called Friedman test (Appendix VI) in order to judge the reality of the differences between the formulae. The agreement in the rank order of a number of series of observations can be tested by this method.

The stable and unstable groups were considered separately in applying the test. The theory behind the test applies to the present case as follows:

If one or more formulae fit the observations better than the others, their s -values will be smaller. If within each series rank-numbers in order of size are given to the s -values for the different formulae, the "better" formulae will obtain the lower rank numbers and there will be agreement between the rank-order sequences of the different series. If the formulae are equally good there will be no agreement between the rank-orders. This can be tested statistically.

For the stable group (series I . . . XI) the test shows significant agreement between the separate rankings of the series (see Appendix VI, table VI.1). On closer examination it seems, however, that this is mainly due to the power profile, the s -values of which are on the whole larger than those of the other formulae. If the s -values of the other six formulae are considered separately, the agreement between the rank-orders is no longer significant.

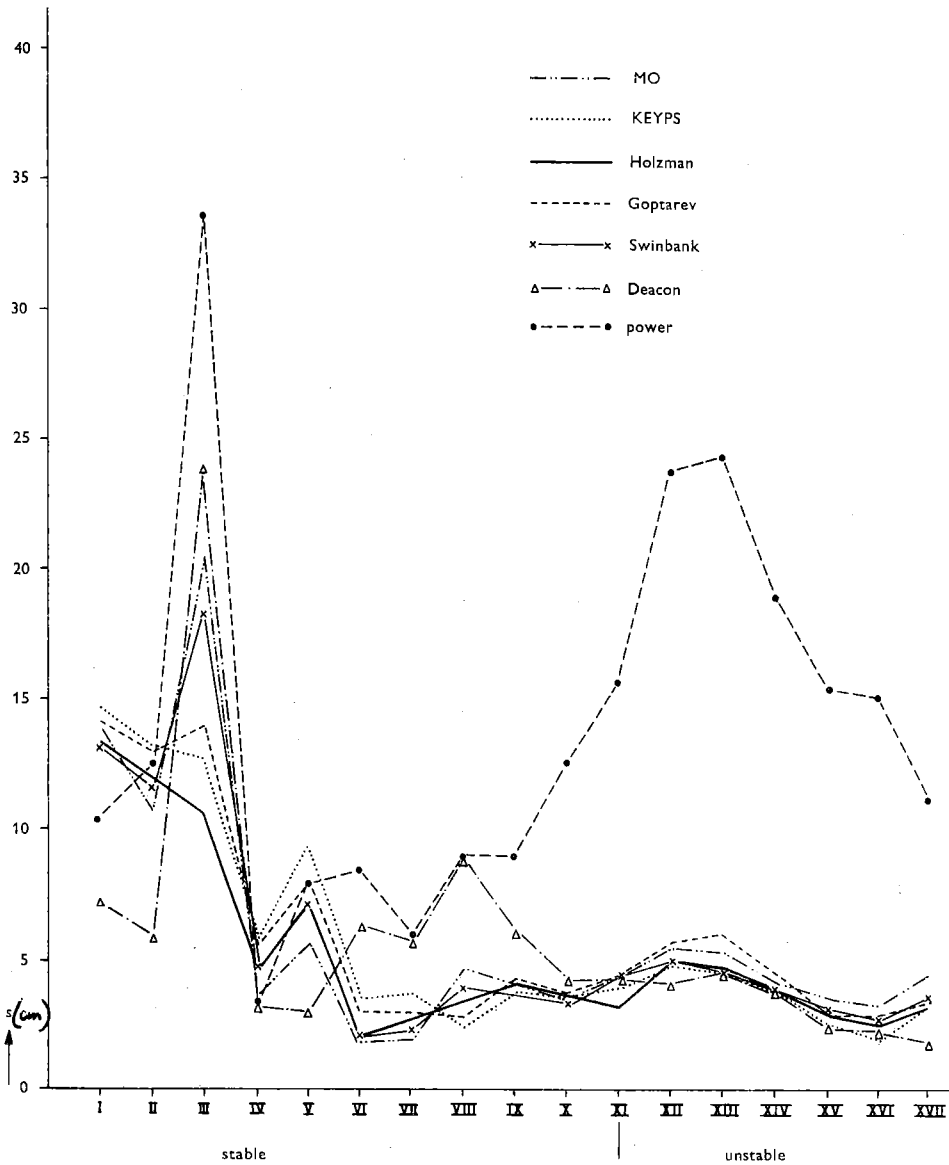


Fig. 2.3.1 Standard deviations of the difference between observations and theoretical profile formulae.

For the unstable group the power profile can be left out of consideration at once. Nevertheless agreement between the rank-orders remains significant. The MO profile yields larger s -values than the others, with the Goptarev profile in second place.

That the power profile formula fits less accurately than the other formulae was to be expected because the power formula contains only two parameters whereas the others contain three, and as a rule a closer fitting is obtained with three parameters than with two.

Furthermore, the curvature of the graph of the power functions ($u = Az^p$) in a $(u, \ln z)$ diagram is always the same because the second derivative $d^2u/d(\ln z)^2 = Ap^2z^p$ is positive for all p . By contrast, for the other functions the curvature in stable cases is opposite to that in unstable cases and as far as we know this fact is borne out by the observations.

The fact that the MO profile in unstable situations seems to be less in accordance with the observations than the other formulae can be considered to conform to figure 1.6.2, which shows that the V -function for the MO profile in stable cases has a curvature opposite to the curvature of the other formulae.

On the whole we can conclude from figure 2.3.1 that the formulae fit less well to the observations as stability increases.

Finally, the O'Neill observations that have been used here do not enable any clear distinction to be made between a number of profile formulae viz.: KEYPS, Holzman, Swinbank, Goptarev and Deacon. There is some indication that MO is less good in unstable situations but the numerical values of the standard deviations differ so little for the different formulae that there is no question of a serious discrepancy. Only the power profile seems to be inferior to the other formulae, at least during unstable stratification.

2.3.5 *The stability parameter values*

The α/L -values given in table 2.3.3 are, on the whole, in agreement with what can be expected from figure 1.6.2. In the stable situations (series I . . . XI, $\alpha/L > 0$) the MO stability values (α/L) are the highest, followed by Holzman and Swinbank with nearly equal values, Goptarev and finally KEYPS. The Deacon values are not α/L but $1 - \beta$ -values and hence are omitted here; they have been placed in brackets in the table.

It is striking that the α/L values for series III are much higher than those for series I and II. It seems therefore, that these series are not arranged quite correctly in order of increasing stability, which means that $(\theta_4 - \theta_2)/u_1^2$ is not a correct stability parameter. Series III may show the strongest stability and according to the value of α/L it does. This could be in agreement with what we see in figure 2.3.1 where the s -values for series III are on the whole higher than those of series I and II. If series III is considered to represent the most stable case the decrease of s -values with increasing instability is even more obvious.

2.3.6 The friction velocity values

The friction velocity values must be positive according to the definition $u_* = \sqrt{(-\overline{u'w'})}$, where u' and w' are the fluctuations of wind speed in the x and the z direction respectively where the x -axis lies in the direction of the mean wind vector. The product of u' and w' must be negative on the average, because only the case of the wind speed increasing with height is being considered.

In table 2.3.3 the u_* values are positive in most cases. Only in the series III... VIII are the u_* values negative for the Deacon profile. There are great differences between the u_* values of Deacon and those of the other formulae in the series I, II, IX, ... XVII, while the u_* values obtained from the other formulae do not differ very much from each other.

Let us now investigate how it is that negative u_* values can occur in the Deacon formulae.

The Deacon formula reads:

$$u = \frac{u_*}{kB} \left\{ (z/z_0)^B - 1 \right\} \text{ with } B = 1 - \beta.$$

B is negative in unstable situations and positive in stable ones.

For the three levels $z_3 = 4z$; $z_2 = 2z$ and $z_1 = z$ we have:

$$\frac{u_3 - u_2}{u_2 - u_1} = \frac{(4z)^B - (2z)^B}{(2z)^B - (z)^B} = 2^B. \quad (2.3.1)$$

Also:

$$\frac{u_2}{u_1} = \frac{(2z)^B - z_0^B}{z^B - z_0^B} = \frac{2^B - (z_0/z)^B}{1 - (z_0/z)^B}. \quad (2.3.2)$$

z/z_0 can be solved from these equations:

$$\frac{z}{z_0} = \left\{ \frac{(u_2 - u_1)^2}{u_2^2 - u_1 u_3} \right\}^{1/B}. \quad (2.3.3)$$

Finally, u_* can be found from:

$$u_* = k \frac{u_1 \cdot B}{(z/z_0)^B - 1}. \quad (2.3.4)$$

So we have three equations (2.3.1), (2.3.3) and (2.3.4) in the three unknown parameters B , z_0 and u_* with given wind speed values u_1 , u_2 and u_3 and the height z .

Since we are only considering "normal" cases, where wind speed increases with height, we have:

$$0 < u_1 < u_2 < u_3. \quad (2.3.5)$$

The different ranges of values that can be obtained by the parameters, depending

on the values of u_1 , u_2 and u_3 and taking account of the fact that according to (2.3.1) and (2.3.5) B must always be real, are given in table 2.3.4.

TABLE 2.3.4 Behaviour of the parameter values of the Deacon profile

	unstable	neutral	stable
$B = 1 - \beta:$	< 0	0	> 0
	↓		↓
(2.3.1) → $u_3 - u_2 < u_2 - u_1$ or $u_1 - 2u_2 < -u_3$ or $u_1^2 - 2u_1u_2 < -u_1u_3$			$u_3 - u_2 > u_2 - u_1$ $-u_3 < -2u_2 + u_1$ $-u_1u_3 < -2u_1u_2 + u_1^2$
	↓		↓
$0 < (u_2 - u_1)^2 < u_2^2 - u_1u_3$			$u_2^2 - u_1u_3 < (u_2 - u_1)^2$
	↓		↓
(2.3.3) → $0 < (z/z_0)^B < 1$		$u_2^2 - u_1u_3 > 0$ $(z/z_0)^B > 1$	$u_2^2 - u_1u_3 < 0$ $(z/z_0)^B < 0$
	↓		↓
z/z_0 real and > 1		z/z_0 real and < 1	z_0 complex; z_0 real negative only if B odd.
		$0 < z_0 < z$	
(2.3.4) → u_* real and > 0		u_* real and > 0	$u_* < 0$
		$u_3 - u_2 = u_2 - u_1$	$u_2^2 = u_1u_3$

The result is that in unstable situations the Deacon formula gives real positive values for the parameters u_* and z_0 . In stable situations u_* and z_0 are only real and positive if $u_2^2 > u_1u_3$. If $u_2^2 < u_1u_3$ the parameter z_0 is complex or real negative and u_* is real negative.

Figure 2.3.2 illustrates these results. Table 2.3.4 suggests taking the co-ordinates x and y as proportional to $u_2 - u_1$ and $u_3 - u_2$ respectively ($x = c(u_2 - u_1)$, $y = c(u_3 - u_2)$), for in that case the adiabatic stratification is given by $x = y$. The boundary between real and complex values of z_0 is given by the curve $y = x + x^2$ if c is taken as $1/u_1$.

Both real and complex values can occur in the stable area. If values for the differences $a = u_3 - u_2$ and $b = u_2 - u_1$ are given (so that the stability value is fixed) the transition from a real z_0 value to a complex value occurs as soon as the wind speed u_1 becomes lower than $b^2/(a - b)$.

So in certain regions the Deacon profile is contrary to nature. In this connection it is interesting to refer to Klug's paper of 1963, where he states that the Deacon

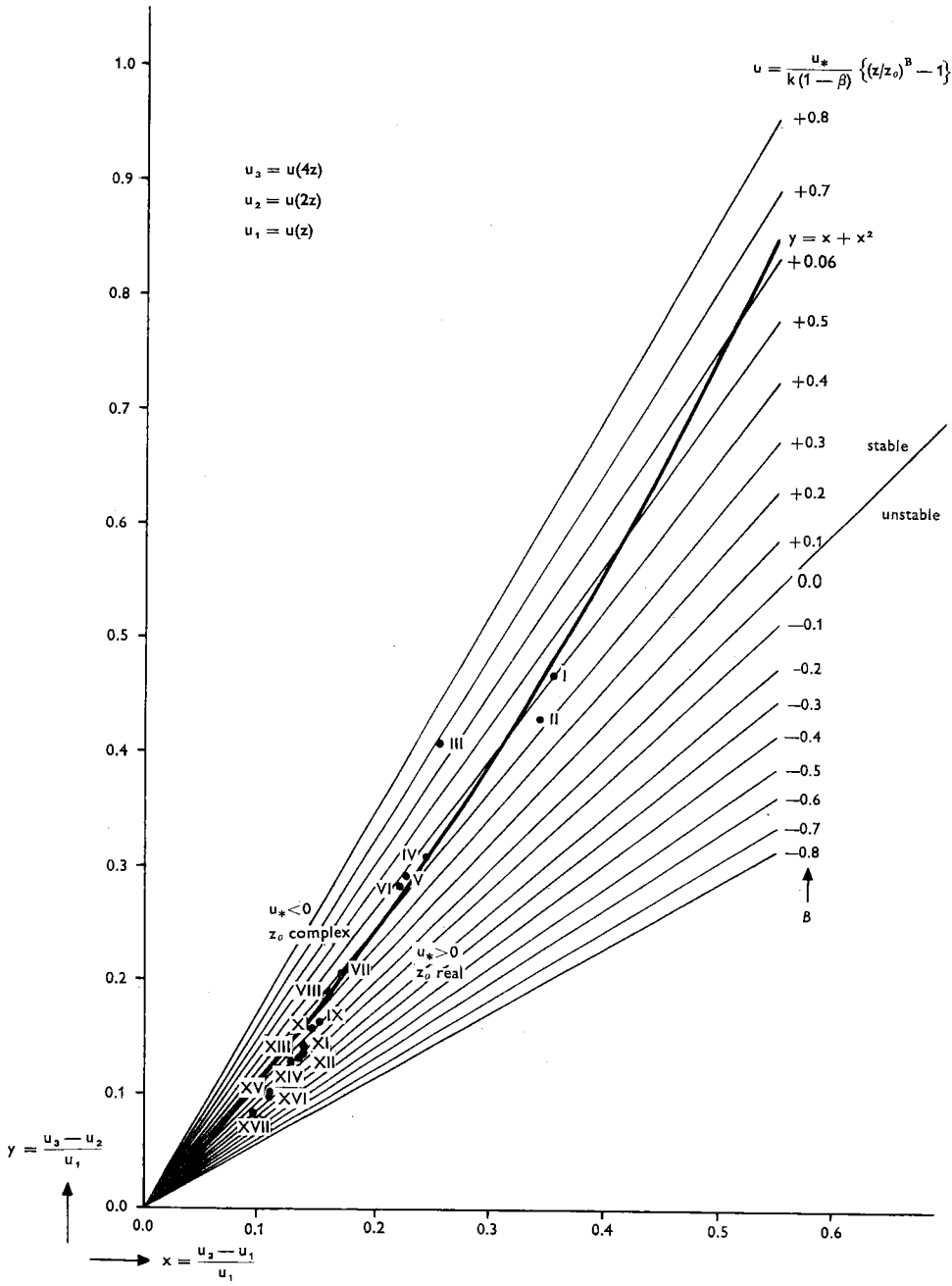


Fig. 2.3.2 Deacon wind profile. Regions of real and complex z_0 respectively positive and negative u_* values.

parameter is a function of the Richardson flux number Rf . As Rf depends on du/dz among other things, the parameter β cannot be a true constant and it is therefore unlikely that Deacon's statement: $du/dz \sim z^\beta$ gives a true description of a natural phenomenon. This reasoning might be objected to on the grounds that KLUG's statement that β is connected with Rf is derived from the KEYPS formula, so that KLUG's conclusion depends on the validity of the KEYPS formula. Our conclusion that Deacon's profile cannot describe nature completely is derived from the formula itself.

In some papers (for instance LAKE, 1952) it is customary to introduce a so-called zero level displacement d , by replacing z by $z + d$, so that d is a further unknown parameter. In the case of the Deacon formula this does not affect our objection, because negative u_* and complex z_0 values can exist even after the introduction of d . The proof is omitted here for the sake of brevity.

2.3.7 *The roughness parameter values*

It is striking that in table 2.3.3 z_0 is not constant. Some large z_0 values occur, particularly in stable cases (series I . . . XI). For z_0 to be a function of stability would be in contradiction to the hypothesis from which the formulae were derived.

But let us compare z_0 with the wind speed itself; if for instance we plot z_0 as a function of u_1 we obtain figure 2.3.3 (for the stable group) and figure 2.3.4 (for the unstable cases). In the stable group we see that z_0 decreases with increasing u_1 up to 3 or 4 m/s. In the unstable group z_0 increases almost imperceptibly with increasing u_1 .

The statistical significance is obvious in the stable group. The rank correlation test (Appendix VII) applied to the mean values of the five z_0 values (ignoring Deacon) yields significance on the 0.001 level. In the unstable cases the 5% level is just reached.

As an explanation for the occurrence of larger z_0 values for low wind speed we can imagine that a surface which is not completely rigid changes its roughness character under the influence of the wind speed itself; and then it would be logical to expect that increasing wind speed would cause decreasing roughness due to bending of grass-blades etc. We can also imagine that at a certain value of the wind speed the maximum effect is reached and that further increase of wind speed makes no difference.

In the first instance we should expect the same effect for both stable and unstable situations. Now figure 2.3.4 seems to contradict this; but as the statistical result is just on the 5% level of significance, it seems that not too much emphasis should be laid on it.

There is no evidence that the supposed effect of wind speed on z_0 is the same in stable and unstable situations.

Finally it must be borne in mind that z_0 is considered to be related in some way to surface roughness but it is not necessarily a direct measure of roughness. After all,

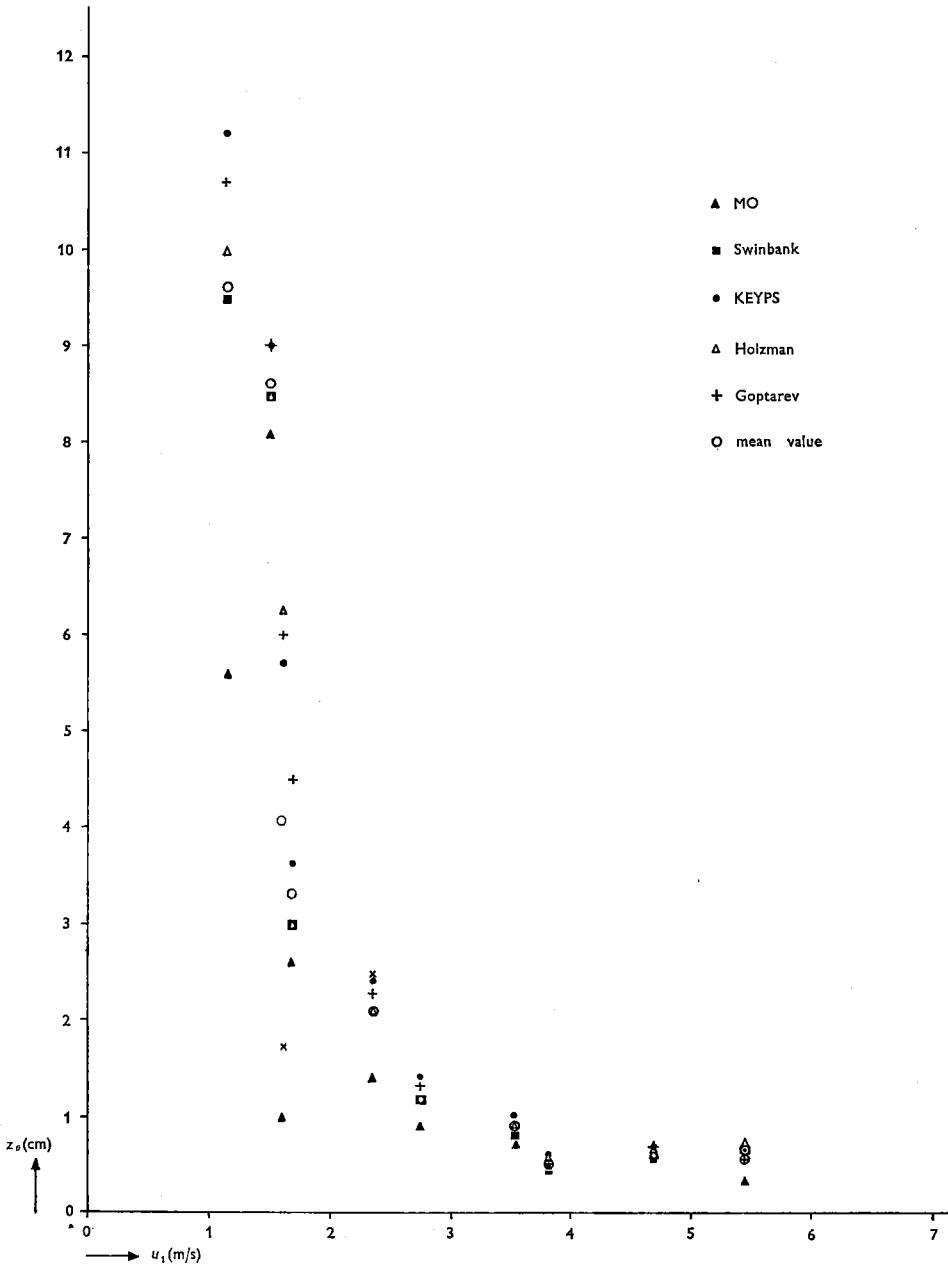


Fig. 2.3.3 Roughness parameter z_0 as a function of wind speed at 1 m height (u_1) for stable cases.

z_0 is introduced into the theory simply as the height at which the wind speed becomes zero, and there is no reason why this should be the same under all circumstances.

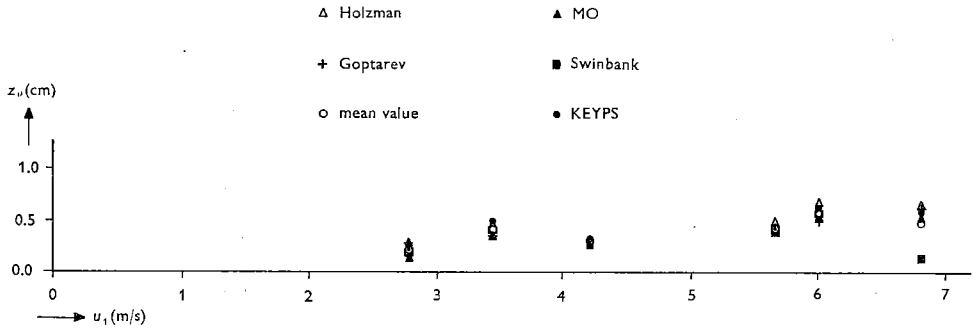


Fig. 2.3.4 Roughness parameter z_o as a function of wind speed at 1 m height (u_1) for unstable cases.

At the end of chapter 3 we shall propose another explanation of the variation of z_o .

KONDO, in his 1962 paper, from which we took the O'Neill data, used these data to investigate whether the KEYPS profile can be used to describe the increase of wind speed with height and he states that under very stable conditions it only holds good in very shallow layers.

His reasoning was as follows:

In the first place he calculated z_o values for near neutral situations and found $z_o = 0.65$ cm for the M.I.T. observations. This value was used for all cases. Theoretical curves from the YAMAMOTO (1959) diagram were now fitted to the observations. The YAMAMOTO diagram gives ku/u_* as a function of z/z_o with ζ_o as a parameter for the KEYPS profile. KONDO then put together all observations into one "universal" profile. His method can be generalized as follows:

$$\frac{ku}{u_*} = f(\zeta) - f(\zeta_o)$$

and

$$\frac{d}{d\zeta} \frac{ku}{u_*} = f'(\zeta)$$

so:

$$\frac{ku}{u_*} = \int_{\zeta_o}^{\zeta} f'(\zeta) d\zeta.$$

Now a value ζ^* is selected between ζ_o and the value of ζ for the lowest level of observation. Now we can write:

$$\frac{ku}{u_*} = \int_{\zeta_o}^{\zeta^*} f'(\zeta) d\zeta + \int_{\zeta^*}^{\zeta} f'(\zeta) d\zeta.$$

For small values of ζ (ζ^* is assumed to belong to the range of small values) we have as an approximation:

$$f(\zeta) \approx \ln |\zeta|$$

hence

$$\frac{ku}{u_*} - \ln \frac{\zeta^*}{\zeta_0} \approx f(\zeta) - f(\zeta^*).$$

So if ζ^* is fixed, $\frac{ku}{u_*} - \ln \frac{\zeta^*}{\zeta_0}$ is a universal function of ζ .

Kondo took $\zeta^* = -0.01$ for unstable and $\zeta^* = +0.01$ for stable stratification. (In fact KONDO used opposite signs because he defined $\zeta = -az/L$, whereas in our study $\zeta = +az/L$).

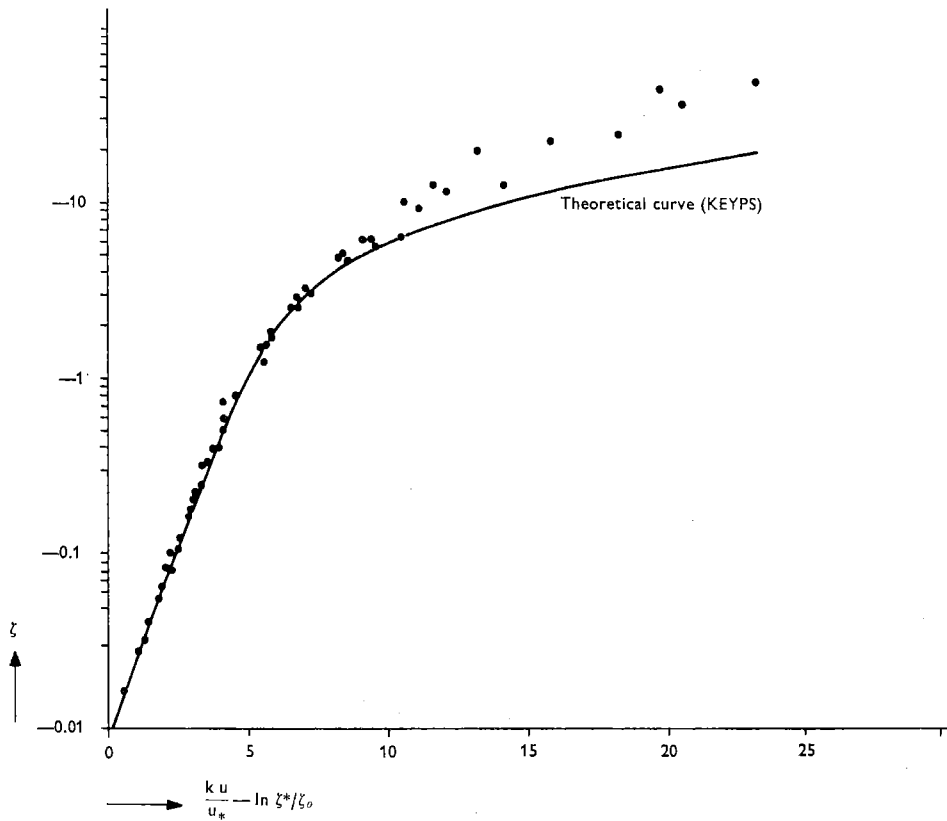


Fig. 2.3.5 Reproduction of fig. 5B from Kondo (1962). Fitting of a universal wind profile according to the KEYPS formula to observation data from the "Great Plains Turbulence Field Program".

In his figures 5A and 5B he shows the observation results together with the universal theoretical curve. In the unstable case (his figure 5A) the observations coincide almost exactly with the curve. In the stable case however (his figure 5B) there are large deviat-

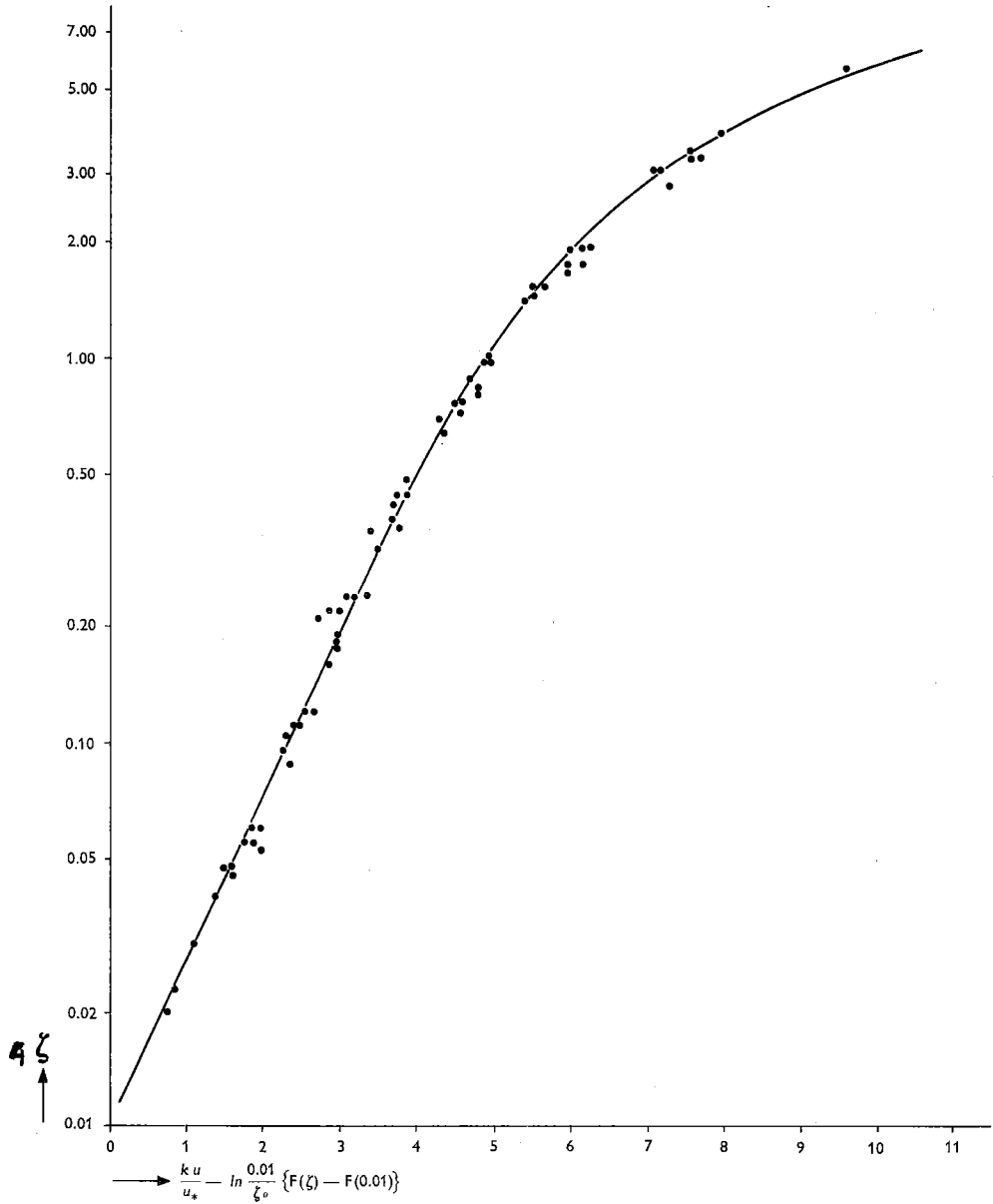


Fig. 2.3.6 Fitting of a universal wind profile according to the KEYPS formula to observations from the "Great Plains Turbulence Field Program".

ions for higher ζ values. In figure 2.3.5 we reproduce the O'Neill data from KONDO's figure 5B. (KONDO also used other data viz.: RIDER's 1954 data and Japanese data obtained at Sendai).

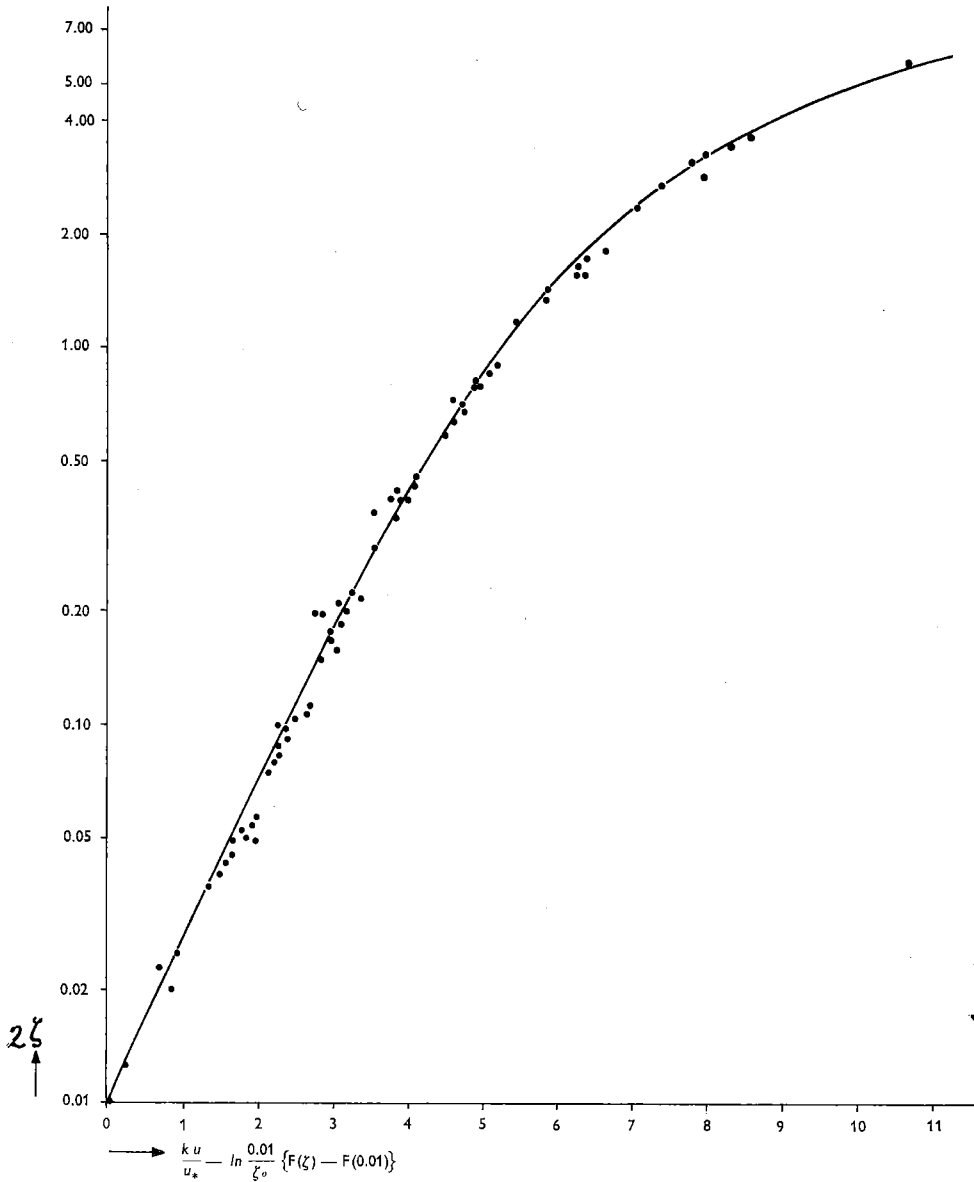


Fig. 2.3.7 Fitting of a universal wind profile according to the Holzman formula to observations from the "Great Plains Turbulence Field Program".

If we now apply KONDO's method to the same observations but use the z_o values from table 2.3.3, a figure can be constructed (figure 2.3.6) which is analogous to figure 2.3.5, but where in very stable situations the deviations between the observations and the theoretical curve are not present. Obviously the deviations which KONDO found can be explained by the fact that he takes one constant value for z_o and we have seen in figure 2.3.3 that for very stable situations (in which cases the u_1 values are very small) the z_o values are much larger than 0.65 cm, the value KONDO used.

The close agreement between the observations and the KEYPS profile which can be found by letting z_o vary, does not imply that KEYPS gives a correct description of the wind profile, for this agreement only results from the fact that the curve has been fitted rather well to the observations. Similar results can be obtained by using other theoretical curves, for instance the Holzman profile (figure 2.3.7). So we can conclude that the foregoing method is not suitable for discriminating between the various profile formulae.

In connexion with our results we mention a conclusion of BARRY (1966): ... "to limit the freedom by fixing z_o (and k) is arbitrary and may disguise the existence of fundamental mechanisms."

3. THE VALUE OF THE POWER PROFILE EXPONENT AS A FUNCTION OF STABILITY

3.0 Introduction

We noted in 2.3.4 that the curvature of the power profile curve in unstable situations does not agree with the curvature suggested by observations when plotted in a $(u, \ln z)$ diagram and with the curvature of the wind profiles found from the general system. We must therefore expect the value of p (the power profile exponent in $u = Az^p$) to depend on height, so that strictly speaking the power profile is not suited to describe the vertical wind profile completely. Nevertheless the power profile is often used because of its simplicity, and under certain conditions this is permissible, for instance if a fixed atmospheric layer is being considered, for which the value of p is known from observations, or if wind speeds higher than about 8 m/s are being used. We shall show that the value of p does not vary much in the latter case.

The values of the power profile exponent for the 17 series of observations of M.I.T. have been inserted in table 2.3.3. They vary from about 0.4 for the very stable cases (series I . . . III) to about 0.1 for unstable conditions (series XVII).

A relation between the power profile exponent p and stability has often been mentioned in meteorological literature. A rather rough relation is given by FROST (1947), who uses only the temperature difference at two heights as a measure of stability.

Extensive results of measurements of p -values are published by the Brookhaven National Laboratory (SINGER and NAGLE, 1962). The publications contain graphs of p as a function of wind speed, gustiness, temperature difference (between 150 and 37 feet), the averaging time and solar time.

J. SAÏSSAC (1960) determined values of the power profile exponent p from wind speed observations at 12 and 33 m. (Observatoire de Magny les Hameaux). His figure 2 is reproduced here as figure 3.0.1. The p -values are given as functions of the potential temperature lapse rate γ ($^{\circ}\text{C}/100$ m) for different mean wind speed groups (2 . . . 3 m/s etc.).

SHIOTANI published fairly extensive results concerning power profile exponent values in the journal of the Meteorological Society of Japan, in 1962. He relates p to $\Delta\theta/u^2$, where $\Delta\theta$ is the potential temperature difference between two specified heights and u is the wind speed at a suitable height. SHIOTANI determined p from a $(\log u, \log z)$ graph for the heights of 8.9, 18.4, 30.8 and 48.2 m. $\Delta\theta$ was determined from temperatures at heights of 12.2 and 24.5 m. and for u the wind speed at 18.4 m was used. His result was that p increases from about 0.10 to 0.25 for $\Delta\theta/u^2$ (in 10^{-3} $^{\circ}\text{C s}^2/\text{m}^2$) increasing from -5.0 to 0 and from 0.25 to 0.60 for $\Delta\theta/u^2$ increasing from 0 to 5.0 .

KLUG (1963) relates the power profile exponent to the Richardson flux number Rf or the Monin-Obukhov parameter z/L . For the MO profile this results in:

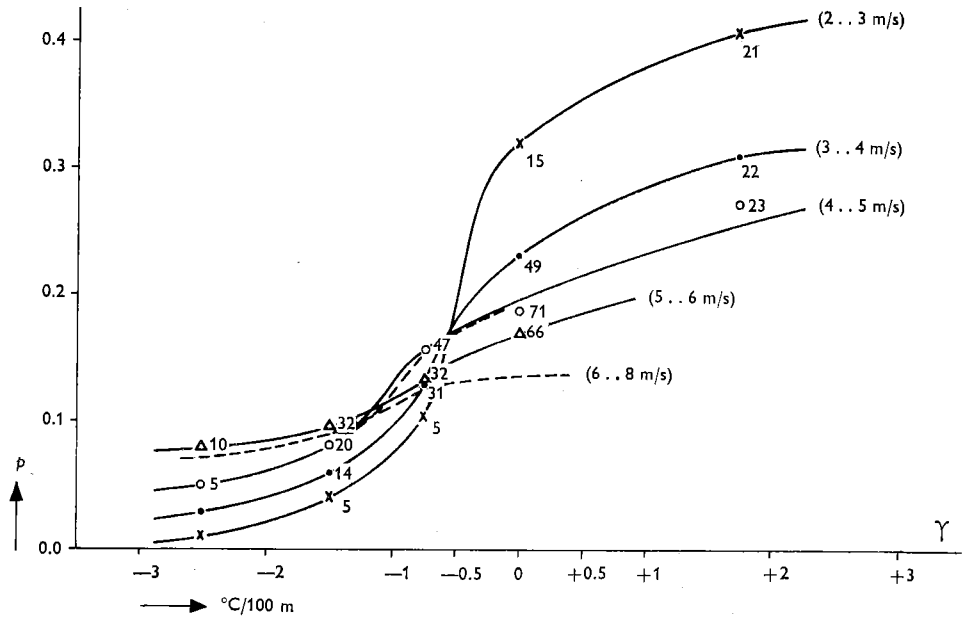


Fig. 3.0.1 Reproduction of fig. 2 from Saïssac (1960). Power profile exponent as a function of temperature lapse rate.

$$p = \frac{1 + \alpha z/L}{\ln(z/z_0) + \alpha z/L}$$

PANOFSKY, BLACKADAR and McVEHILL (1960) determined p -values from the KEYPS formula as a function of $1/L$ and z_0 and constructed a graph for the $1/L$ range $-0.1 \dots +0.1$ (m^{-1}) and the z_0 range $0.2 \dots 80$ (cm), while p varies from 0.05 to 0.60.

In the next section we shall describe a similar investigation using observations made in the Netherlands.

3.1 Values of the power profile exponent from wind speed measurements at Lopik

A virtually complete series of observations of wind speed and temperature at different heights at Lopik (in the centre of the Netherlands) is available for the year 1959.

The wind speed observations at heights of 10 and 30 m were recorded at one of the masts of the World Broadcasting Station; the temperature at a height of 1.5 m was recorded at a distance of about 50 m from the "old" television tower and the temperature at 53.5 m was recorded by means of an instrument mounted on the television tower itself.

Because the wind speed observations are not very accurate it was decided to average

the wind speeds over 4 hours and then to use only 4 night hours viz.: 1, 2, 3 and 4 hour and 4 day-time hours viz.: 12, 13, 14 and 15 hour. This restriction was intended to eliminate periods in which stability varies strongly owing to the diurnal variation.

The power profile exponent is calculated according to:

$$p = \frac{\ln u_{30} - \ln u_{10}}{\ln 3} \quad (3.1.1)$$

and the temperature lapse rate γ , expressed in degrees Celsius per 100 m, according to:

$$\gamma = \frac{100}{52} (T_{53.5} - T_{1.5}). \quad (3.1.2)$$

The mean values $\bar{u} = \frac{1}{2}(u_{30} + u_{10})$ were also determined.

The available data were divided into seven groups based on \bar{u} , expressed in m/s, as follows:

2.0 ... 2.9 (48); 3.0 ... 3.9 (62); 4.0 ... 4.9 (42); 5.0 ... 5.9 (32); 6.0 ... 6.9 (15); 7.0 ... 8.9 (7); 9.0 (7) (the figures in brackets indicate the number of data available).

The night and day observations will be dealt with separately.

3.2 The night hours observations

3.2.1 Graphical representation of the observations

Each \bar{u} group was divided into a number of sub-groups, each containing 7 to 11 observation pairs (p, γ). The mean values of p and γ for these sub-groups were determined and plotted in figure 3.2.1. The number of observations in each sub-group is indicated at the plotting position. The number of observations in each \bar{u} group is indicated in brackets.

The increase of the mean value of p with increasing mean value of γ for a given \bar{u} group is quite clear. The level of p -values can also be seen to decrease with increasing \bar{u} . For \bar{u} -values of about 8 m/sec the p -value reaches the level of the p -values of day-time. Anticipating the results of part 3.3, we have therefore inserted in the graph an estimate of the relation between the day-time p -value and γ . The p -level is indeed very near to the value 1/7 found in hydrodynamics.

Qualitatively the picture agrees rather well with Saïssac's results (see figure 3.0.1).

3.2.2 The theoretical variation of the power profile exponent as derived from the Holzman profile

As we have seen in the introduction to this chapter, the p -value can be expressed in terms of a diabatic wind profile (see KLUG 1963 and PANOFSKY, BLACKADAR and MC-VEHILL 1960).

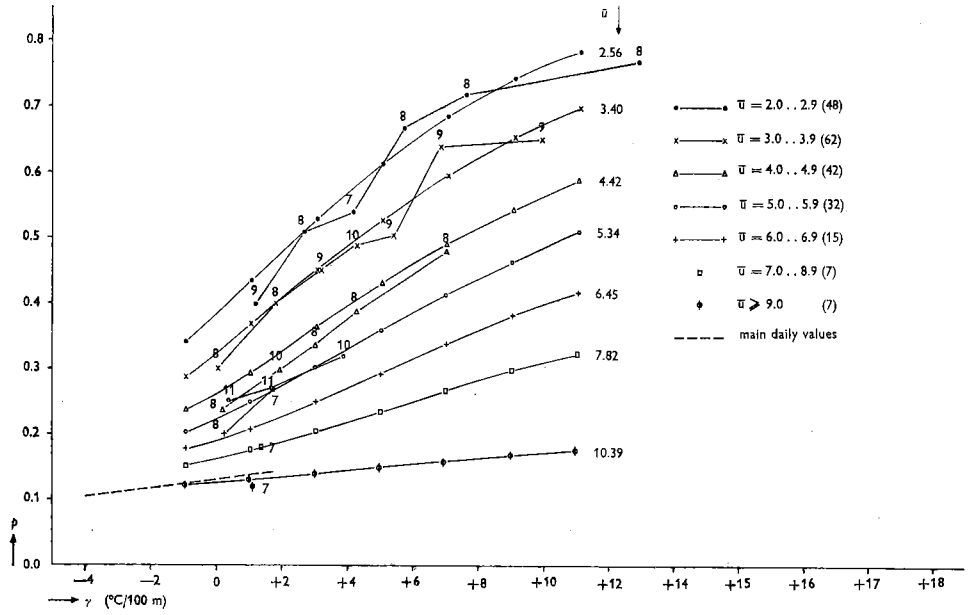


Fig. 3.2.1 Power profile exponent p as a function of temperature lapse rate and mean wind speed (empirical).

Fig. 3.2.4 Power profile exponent p as a function of temperature lapse rate and mean wind speed (theoretical).

If we start from the general profile formula:

$$u = \frac{u_*}{k} \{f(\zeta) - f(\zeta_0)\} \tag{3.2.1}$$

on the one hand and the power profile:

$$u = Az^p \tag{3.2.2}$$

on the other, we have from (3.2.1), using (1.3.1):

$$\frac{du}{dz} = \frac{\alpha}{cL} \frac{u_*}{k} \frac{df(\zeta)}{d\zeta} = \frac{\zeta}{z} \frac{u_*}{k} f'(\zeta)$$

and from (3.2.2):

$$p = \frac{d \ln u}{d \ln z} = \frac{z}{u} \frac{du}{dz}$$

Whence:

$$p = \frac{z}{u} \frac{du}{dz} = \frac{\zeta}{u} \frac{u_*}{k} f'(\zeta) = \frac{f(\zeta)}{f(\zeta) - f(\zeta_0)} \tag{3.2.3}$$

Thus p can be considered as a function of ζ with ζ_0 as parameter. But because

ζ and ζ_o both contain the Monin-Obukhov length, we prefer to use $\zeta/\zeta_o = z/z_o$ as a parameter.

It is proved in this way that theoretically p is a function of z and consequently is not constant with height.

Since, as we saw in Chapter 2, the Holzman profile proves to be a useful diabatic profile formula (although not the only one) we have applied this formula to (3.2.3).

Substituting the Holzman formula for $f(\zeta)$ (see formula (1.4.3)) it follows:

$$f'(\zeta) = \frac{1}{\zeta} + 1 + \frac{\zeta}{1 + \sqrt{1 + \zeta^2}}$$

so that:

$$p = \frac{1 + \zeta + \frac{\zeta}{1 + \sqrt{1 + \zeta^2}}}{f(\zeta) - f(\zeta_o)} \quad (3.2.4)$$

The power profile exponent p as a function of ζ is given in figure 3.2.2 for

$$\zeta/\zeta_o = 10, 20, 50, 100, 200, 500, 1000, 2000 \text{ and } 4000,$$

which parameters are denoted by $i = 1, 2, \dots, 9$ for the sake of brevity.

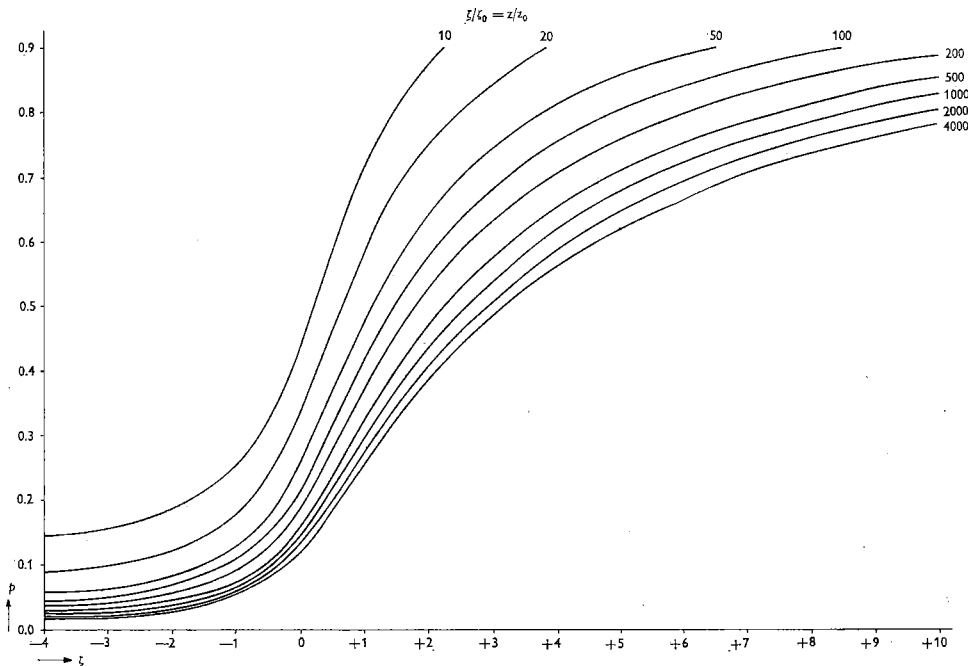


Fig. 3.2.2 Power profile exponent p as a function of stability derived from the Holzman profile formula.

To be able to find the variation of p completely from theory we have to fit the theoretical curves derived from figure 3.2.2 to the empirical curves of figure 3.2.1, which can only be done if ζ and γ are related. Let us suppose that this relation, if it exists at all, is a linear one. Then it must be of the form:

$$\zeta = a(1 + \gamma) \quad (3.2.5)$$

because $\gamma = -1$ must obtain for the adiabatic case ($\zeta = 0$).

A straightforward solution would result from substitution of (3.2.5) into (3.2.4), followed by the application of the least squares method to the numerical (p, γ) data. This would yield the least squares values of a and of z/z_0 for the different \bar{u} groups. However, this is mathematically a very complicated procedure.

For this reason a combination of a graphical and a least squares method has been chosen, which is explained in Appendix VIII.

The results are summarized in table 3.2.1, where estimates are given of z/z_0 and a . These estimates are rather inaccurate. In particular the 95% confidence interval for the "true" values of z/z_0 is very wide. Estimates of the limits of this interval are given for z/z_0 as L (lower) and U (upper) in table 3.2.1. We stress the fact that the distribution of z/z_0 for given \bar{u} is not symmetrical so that the standard deviation alone does not convey the right impression of the reliability interval of z/z_0 . The 95% confidence interval of the true value of a for given \bar{u} can well be constructed with the estimated standard deviation s_a , by means of $a \pm 2s_a$.

TABLE 3.2.1

n	\bar{u}	L_{z/z_0}	z/z_0	U_{z/z_0}	$\widetilde{z/z_0}$	a	s_a	\tilde{a}
48	2.56	< 10	15	> 4000	20	-0.160	0.035	-0.195
62	3.40	20	37	300	38	-0.185	0.021	-0.185
42	4.42	75	140	350	78	-0.183	0.018	-0.164
32	5.34	64	110	210	166	-0.115	0.024	-0.145
15	6.45	220	1300	> 4000	383	-0.345	0.086	-0.125
7	7.82	160	1100	> 4000	1070	-0.100	0.067	-0.100
7	10.39	270	1700	> 4000	7360	+0.050	0.056	-0.050

In spite of the rather large confidence intervals for z/z_0 the increase of z/z_0 with increasing \bar{u} is certainly statistically significant. Application of Kendall's rank correlation test (see Appendix VII) results in the rejection of the null hypothesis that z/z_0 is independent of \bar{u} on the 5% level of significance.

Since we want to smooth the irregular values, the question now arises in what way z/z_0 depends on \bar{u} . A linear dependency does not seem plausible. More likely is a linear dependency of $\ln z/z_0$ on \bar{u} (see figure 3.2.3), so we shall fit a straight line:

$\ln \zeta/\zeta_o = \ln z/z_o = c\bar{u} + d$. Because the least squares regression line intersects all the confidence intervals, the hypothesis that z/z_o depends on \bar{u} in this way seems to be an acceptable one.

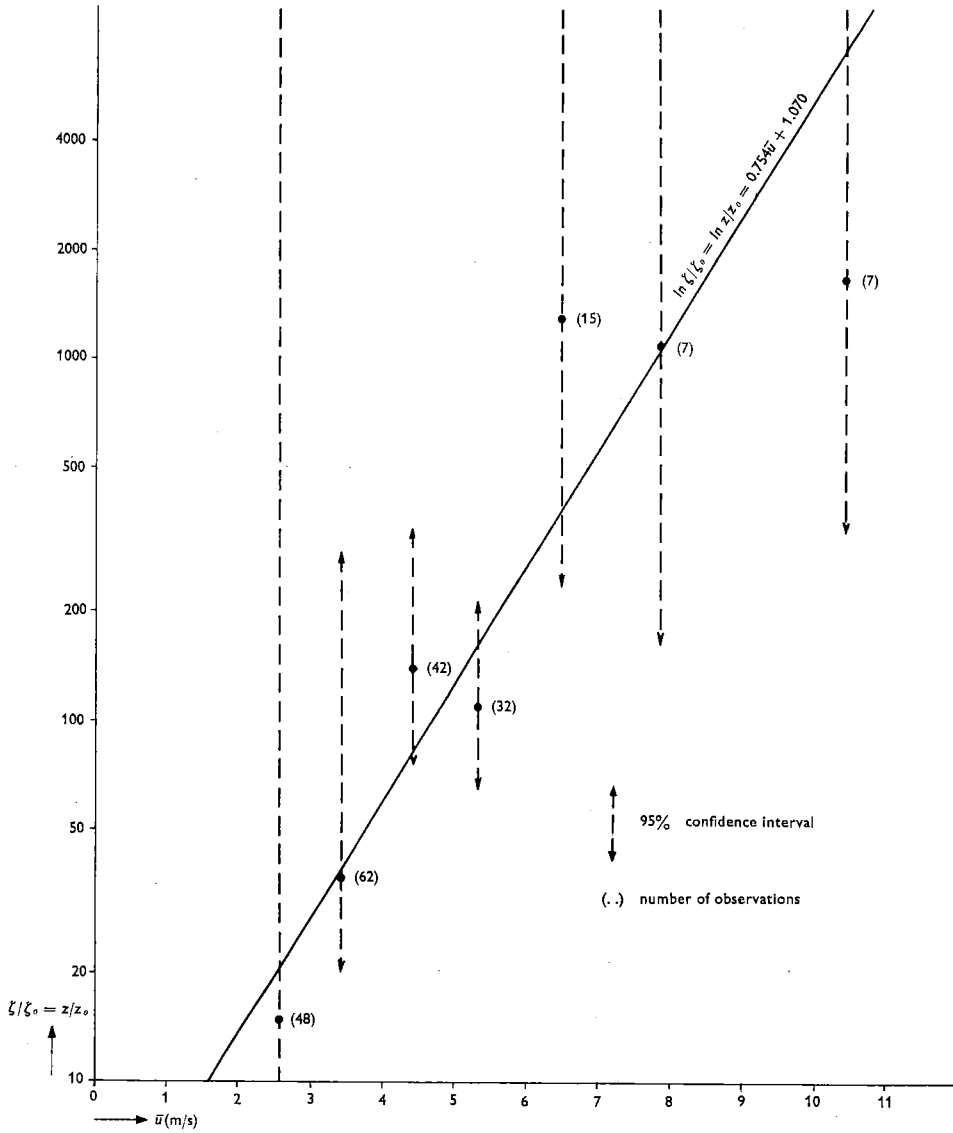


Fig. 3.2.3 Auxiliary diagram for fitting theoretical variation of the power profile exponent p to observed values. Parameter $\zeta/\zeta_o (= z/z_o)$ as a function of mean wind speed.

The smoothed values $\widetilde{z/z_o}$ read from the least squares regression line have been inserted in table 3.2.1.

It is not so easy to find a relevant relation for the variation of a with \bar{u} . We have tried different assumptions (linear, reciprocal etc.) but all have to be rejected on the 5% level of significance if the χ^2 test is applied. An explanation for this might be the fact that one of the a -values, viz. the value -0.345 belonging to the \bar{u} group 6.45, deviates strongly from the other values. Unfortunately we could not attribute this to an error in the observations.

We decided to draw a graphical freehand relation, of which the smoothed a -values (\tilde{a}) are given in table 3.2.1.

The theoretical curves $p(\gamma)$ against γ for different \bar{u} values (figure 3.2.4 red, p. 90) can be constructed by using the smoothed values \tilde{a} and $\widetilde{z/z_o}$ ($= \widetilde{\xi/\xi_o}$) of table 3.2.1, either with the help of (3.2.4) and (3.2.5) or with figure 3.2.2.

Comparing figure 3.2.4 with figure 3.2.1 shows a "good" agreement.

3.3 The day-time observations

The observations made during day-time vary much less than the night-time values. The values of the power profile exponent are rarely larger than 0.20. The corresponding values of ΔT ($= T_{53.5} - T_{1.5}$) are also limited. The scatter, however, is so large that we do not believe that the deviation from a linear relation between p and γ , which should exist if any one of the theoretical profile formulae obtains, can be recognized. We have therefore simply determined the seven linear regression lines (for the seven

\bar{u} groups) for p as a function of Γ ($= \frac{d\theta}{dz}$):

$$p = c\Gamma + d.$$

The standard deviations of c and d , s_c and s_d respectively, have also been calculated. Table 3.3.1 shows the results.

In figure 3.3.1 and figure 3.3.2 we have plotted the values of c and d against \bar{u} together with the confidence interval $c \pm 2s_c$ and $d \pm 2s_d$. It is evident that the values of d are independent of \bar{u} . The values of c suggest an increase with increasing \bar{u} , but the inaccuracies of the c estimates are so great that a statistical test did not lead to rejection of the null hypothesis that c is independent of \bar{u} . Nevertheless, judging on purely visual evidence, it seems that the hypothesis that c and \bar{u} are linearly related may be true. The least squares relation $c = -0.0164 + 0.00132 \bar{u}$ proves to give a better fit to the c values than a constant value -0.00904 (the mean of all c values). The theoretical diabatic formulae, moreover, indicate that there may be an increase of c with \bar{u} analogous to that in the case of the night values.

TABLE 3.3.1 Regression coefficients for the relation between p and Γ for different \bar{u} groups.

\bar{u}	n	c	s_c	d	s_d
2.49	32	0.0128	0.0038	0.1186	0.0063
3.49	35	0.0141	0.0048	0.1245	0.0070
4.46	31	0.0078	0.0031	0.1188	0.0045
5.38	39	0.0115	0.0030	0.1247	0.0045
6.47	35	0.0041	0.0026	0.1195	0.0036
7.47	23	0.0083	0.0032	0.1284	0.0050
9.44	38	0.0046	0.0019	0.1220	0.0038

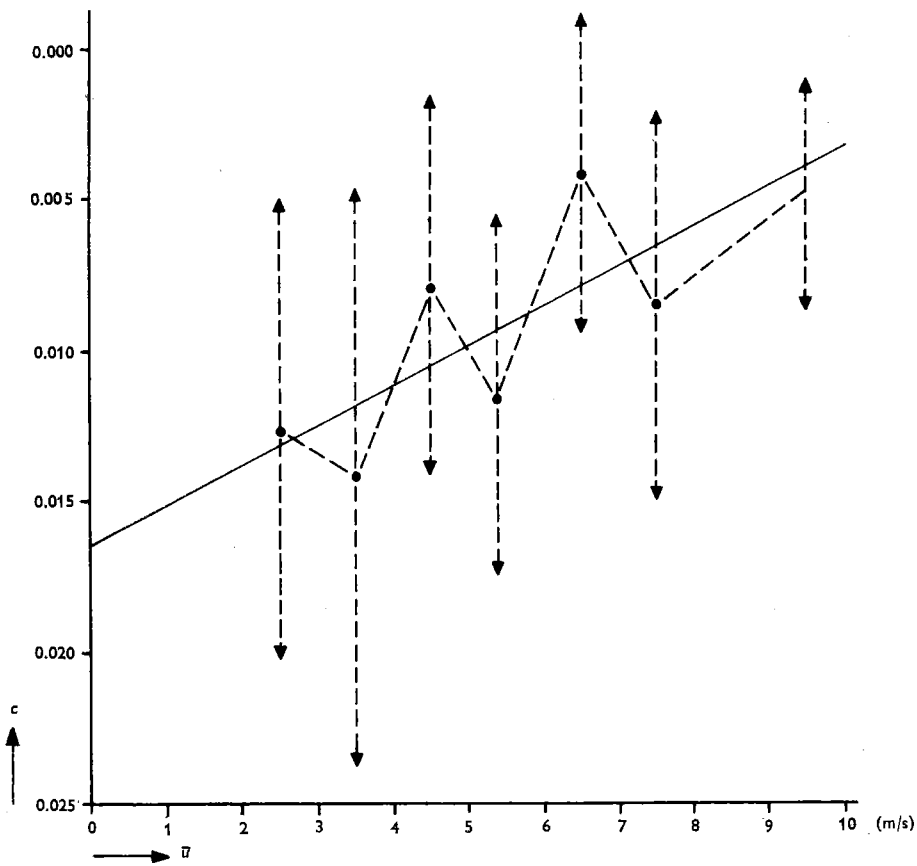


Fig. 3.3.1 Relation between the regression coefficient c of the power profile exponent as a function of the potential temperature lapse rate ($p = c\Gamma + d$) and the mean wind speed \bar{u} .

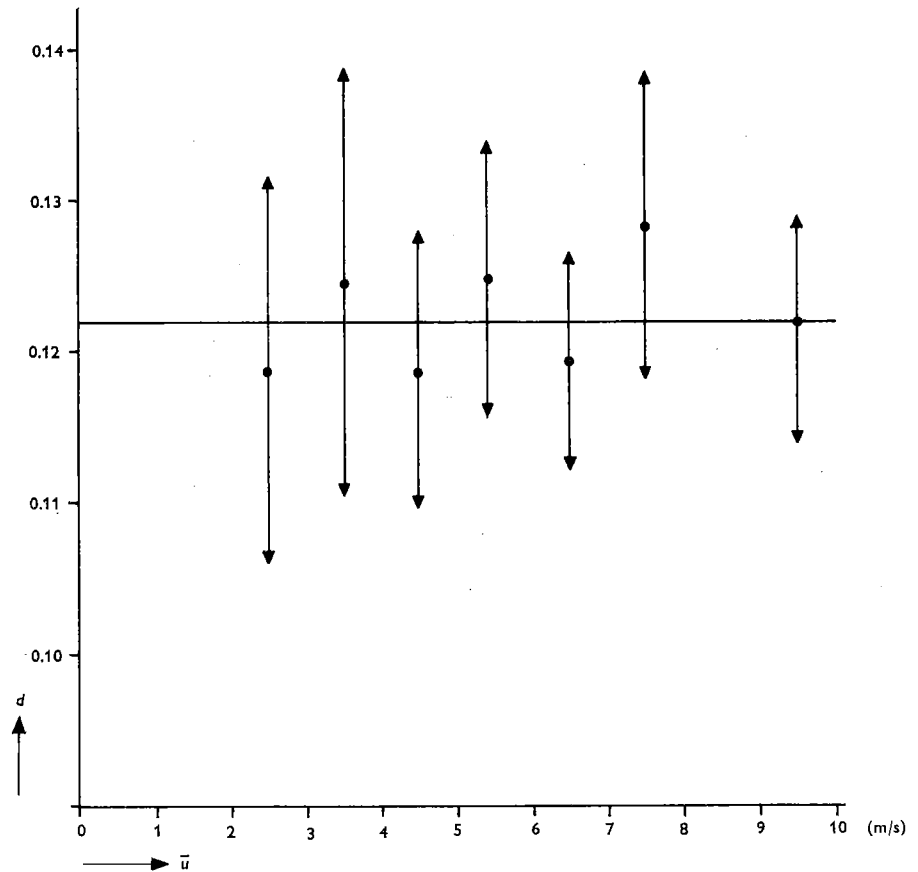


Fig. 3.3.2 Relation between the regression coefficient d of the power profile exponent as a function of the potential temperature lapse rate ($p = cT + d$) and the mean wind speed \bar{u} .

3.4 The variation of z_o as derived from the variation of p

We have found a difference between the night and day values concerning the power profile exponent as a function of temperature lapse rate. In night situations (which usually relate to stable stratification) we find an increase of p if the degree of stability increases. An increase of p with decreasing \bar{u} is found in neutral situations, if we start from a diabatic theoretical profile formula like, for instance, the Holzman formula. This can only be explained by supposing that z_o increases as \bar{u} decreases.

This conclusion is in agreement with what we found in Chapter 2 on the basis of an analysis of the O'Neill data.

In the mainly unstable day-time cases there is some slight indication of an increase of p with increasing temperature lapse rate, but this increase proved to be not statisti-

cally significant; besides, the neutral cases do not show an increase of p with decreasing \bar{u} , and this may be considered as an indication that no increase of z_0 is present here, which again is in agreement with the conclusions of Chapter 2.

The different behaviour of z_0 as a function of \bar{u} in stable and in unstable situations has been found in this way for two completely independent groups of observations, and hence it can hardly be imputed to measuring inaccuracies.

In 2.3.7, when considering the different behaviour of z_0 in stable and unstable cases we mentioned, on the one hand that, since the statistical result is just on the 5% level of significance, the different behaviour might not be real; but that, on the other hand, the same behaviour in stable and in unstable cases is not a priori a necessity.

We are now in need of a better explanation for the different behaviour and a reasonable one may be the following:

We would remind readers of the definition of aerodynamically smooth and rough surfaces (e.g. SUTTON 1953, p. 77). If the surface roughness elements (called protuberances by SUTTON) are submerged in a viscous¹⁾ sub-layer, the surface is aerodynamically smooth, but if such a sub-layer is not present the surface is aerodynamically rough. In the latter case the motion of the air is turbulent down to the surface itself. Sutton remarks that the depth of the viscous sub-layer depends on the magnitude of the Reynolds number; so the classification of the surface is determined not only by the characteristics of the boundary layer, but also by the magnitude of the mean wind speed. Hence, a surface which is "smooth" at low velocities may become "rough" if the mean velocity increases.

Generally speaking all natural surfaces are aerodynamically rough, and certainly in the case of neutral and unstable stratification. Only in stable situations and with low wind speeds a viscous sub-layer might be formed, in which case the large z_0 values might be explained in this way. This would mean that these z_0 values are not solely related to the roughness of the surface, but also to a certain extent to the depth of the viscous sub-layer.

1) SUTTON writes laminar, but according to modern ideas such a layer cannot be laminar in the absolute sense, certainly not under natural conditions.

APPENDICES

I. Standard deviation of $V = \frac{u_3 - u_2}{u_3 - u_1}$

(par. 2.2.1)

We introduce:

$$y \stackrel{d}{=} u_3 - u_2 \text{ and } x \stackrel{d}{=} u_3 - u_1$$

and we write:

$$u_i = Eu_i + \delta_i$$

where Eu_i is the statistical expectation of u_i and hence $E\delta_i = 0$. The standard deviation σ_{δ_i} of δ_i is assumed to be 0.015 m/s. (see p. 62).

We may assume: $E\delta_i\delta_j = 0 ; i \neq j$
 whereas
 and also: $E(u_i - u_j) = Eu_i - Eu_j$.

Let us now define:

$$\eta \stackrel{d}{=} Eu_3 - Eu_2 \text{ and } \xi \stackrel{d}{=} Eu_3 - Eu_1.$$

Then the following expression is valid as a first approximation:

$$EV \approx \frac{\eta}{\xi} \left\{ 1 + \frac{\sigma_x^2}{\xi^2} - \frac{\text{cov } x,y}{\eta \cdot \xi} \right\}$$

and:

$$\sigma_V^2 \approx \frac{\sigma_y^2}{\xi^2} + \frac{\eta^2 \sigma_x^2}{\xi^4} - \frac{2\eta \text{ cov } x,y}{\xi^3}$$

where cov stands for covariance viz.: $\text{cov } x,y = E(x - \xi)(y - \eta)$. (see KENDALL and STUART I, 1963 p. 232 or YULE and KENDALL 1965 p. 329). The values σ_y^2 , σ_x^2 and $\text{cov } x,y$ can be calculated as follows:

$$\sigma_y^2 = E(y - \eta)^2 = E\delta_3^2 + E\delta_2^2 - E\delta_3\delta_2 =$$

$$(0.015)^2 + (0.015)^2 - 0 = 0.00045$$

$$\sigma_x^2 = E(x - \xi)^2 = E\delta_3^2 + E\delta_1^2 - E\delta_3\delta_1 =$$

$$(0.015)^2 + (0.015)^2 - 0 = 0.00045$$

$$\text{cov } x,y = E(x - \xi)(y - \eta) = E\delta_3^2 - E\delta_2\delta_3 - E\delta_1\delta_3 + E\delta_1\delta_2 =$$

$$(0.015)^2 - 0 - 0 + 0 = 0.000225.$$

$$\text{So } \sigma_V^2 = 0.0045 \left\{ \frac{\xi^2 + \eta^2 - \xi \eta}{\xi^4} \right\}$$

Because ξ and η are unknown, we have to use x and y as estimates, hence:

$$EV \approx \frac{y}{x} \left\{ 1 + \frac{\sigma_x^2}{x^2} - \frac{\text{cov } x, y}{xy} \right\} = \frac{y}{x} \left\{ 1 + 0.0045 \left(\frac{1}{x^2} - \frac{1}{2xy} \right) \right\}.$$

$\frac{1}{x^2} - \frac{1}{2xy}$ proves to be of the order of magnitude of 1, and therefore $0.0045 \left(\frac{1}{x^2} - \frac{1}{2xy} \right)$

can be ignored, and $EV \approx \frac{y}{x}$.

For the variance of V we have as an estimator:

$$s_V^2 = 0.0045 \left(\frac{x^2 + y^2 - xy}{x^4} \right).$$

The s_V values of table 2.2.1 have been calculated according to this result.

II. Regression lines for the ($\zeta, z/L$) relation

(par. 2.2.1)

A method of determining a linear regression line if both variables have been measured with errors showing a given standard deviation is due to LINDLEY (1947).

For a simplified case we have the following derivation:

Suppose there are a number of observations (x_i, y_i) where $i = 1, \dots, n$, with $Ex_i = \xi_i$ and $Ey_i = \eta_i$.

Let us introduce:

$$u_i = x_i - \xi_i \text{ and } v_i = y_i - \eta_i \text{ and hence } Eu_i = Ev_i = 0.$$

It is postulated that:

$$1^\circ \eta_i = a\xi_i + \beta$$

$$2^\circ \text{ for every } i: \sigma_{u_i} = \sigma_1 \text{ (independent of } i)$$

$$3^\circ \text{ for every } i: \sigma_{v_i} = \sigma_2 \text{ (independent of } i)$$

$$4^\circ \text{ for every } i: Eu_i v_i = 0$$

The main problem is to find estimates $\tilde{\alpha}$ and $\tilde{\beta}$ for a and β from the n observation pairs (x_i, y_i) , each pair being observed only once.

The variance of $y_i - ax_i - \beta$ for a given i , is given by:

$$E(y_i - ax_i - \beta)^2 = E(v_i - au_i)^2 = \sigma_2^2 + a^2\sigma_1^2$$

and hence this variance does not depend on i .

The estimates $\tilde{\alpha}$ and $\tilde{\beta}$ can now be determined by minimizing with regard to a and β a weighted sum of n square deviations:

$$A = \sum_{i=1}^n \frac{(y_i - ax_i - \beta)^2}{\sigma_2^2 + a^2\sigma_1^2}.$$

Differentiation to β and requiring $\frac{dA}{d\beta} = 0$ yields:

$$\Sigma y_i - \tilde{\alpha} \Sigma x_i - \tilde{\beta} n = 0$$

or

$$\bar{y} = \tilde{\alpha} \bar{x} + \tilde{\beta} \quad (\text{II-1})$$

where $\bar{y} = \frac{1}{n} \Sigma y_i$ and $\bar{x} = \frac{1}{n} \Sigma x_i$.

Differentiation to a and requiring $\frac{dA}{da} = 0$ yields:

$$\frac{-2(\sigma_2^2 + \tilde{\alpha}^2 \sigma_1^2) \Sigma x_i (y_i - \tilde{\alpha} x_i - \tilde{\beta}) - 2\tilde{\alpha} \sigma_2^2 \Sigma (y_i - \tilde{\alpha} x_i - \tilde{\beta})^2}{(\sigma_2^2 + \tilde{\alpha}^2 \sigma_1^2)} = 0$$

or

$$\Sigma (y_i - \tilde{\alpha} x_i - \tilde{\beta}) (k x_i + \tilde{\alpha} y_i - \tilde{\alpha} \tilde{\beta}) = 0 \quad (\text{II-2})$$

where $k = \sigma_2^2 / \sigma_1^2$.

Substitution of (II-1) into (II-2) gives:

$$\Sigma (y_i - \tilde{\alpha} x_i - \bar{y} + \tilde{\alpha} \bar{x}) (k x_i + \tilde{\alpha} y_i - \tilde{\alpha} \bar{y} + \tilde{\alpha}^2 \bar{x}) = 0$$

or with $\tilde{y}_i = y_i - \bar{y}$ and $\tilde{x}_i = x_i - \bar{x}$:

$$\Sigma (\tilde{y}_i - \tilde{\alpha} \tilde{x}_i) (k \tilde{x}_i + \tilde{\alpha} \tilde{y}_i + (k + \tilde{\alpha}^2) \bar{x}) = 0.$$

If we now introduce $K_x = \Sigma \tilde{x}_i^2$; $K_y = \Sigma \tilde{y}_i^2$ and $K_{x,y} = \Sigma \tilde{x}_i \tilde{y}_i$ we can write:

$$\tilde{\alpha}^2 K_{x,y} + \tilde{\alpha} (k K_x - K_y) - k K_{x,y} = 0. \quad (\text{II-3})$$

From (II-1) and (II-2) $\tilde{\alpha}$ and $\tilde{\beta}$ can be solved if k is given. Unfortunately no completely satisfying theory has yet been developed for this regression problem. The accuracies of the estimates $\tilde{\alpha}$ and $\tilde{\beta}$, for instance, cannot be determined without special assumptions being made about the distributions of u_i and v_i .

III. Normality test by means of the χ^2 test

(par. 2.2.2)

Let us state the hypothesis that the distribution of V is normal. The hypothesis can be verified as follows:

The sample of 37 V -values is divided into 5 classes wide enough to contain n_i (= 7 or 8) elements each. The mean value of V is $\bar{V} = 0.500$ and the standard deviation $s_V = 0.040$. The class limits of t corresponding with those of V can be calculated by the introduction of $t = (V - \bar{V}) / s_V$, where t stands for the standardized normally distributed variable. The expectation of the number of V -values within the different intervals can be found with the aid of a table of the standardized normal distribution.

The result is as follows:

V	< 0.470	$0.470 \dots 0.484$	$0.484 \dots 0.502$	$0.502 \dots 0.520$	> 0.520
n_i	7	7	8	7	8
t	< -0.75	$-0.75 \dots -0.40$	$-0.40 \dots +0.05$	$+0.05 + 0.50$	$> +0.50$
P_i	0.227	0.118	0.175	0.172	0.308
En_i	8.4	4.4	6.5	6.3	11.4

The χ^2 sum $\Sigma \{(n_i - En_i)^2 / En_i\} = 4.28$. The number of degrees of freedom $\nu = 5 - 2 - 1 = 2$. Since the 5% level of the χ^2 distribution with $\nu = 2$ is 5.99, there is no reason to reject the null hypothesis that the V values are normally distributed.

IV. Testing whether V is dependent on height or not with the aid of the binomial distribution (par. 2.3.2)

The test used in 2.3.2, to decide whether V is dependent on height is based on the binomial distribution, which is a common tool in statistics and amply discussed in all elementary books on the subject.

If some event A has a probability p of occurrence, and the alternative event \bar{A} a probability $1 - p$, the probability $\mathbf{P}(k)$ that in N independent experiments k events A occur, can be written:

$$\mathbf{P}(k) = \binom{N}{k} p^k (1-p)^{N-k}. \quad (\text{IV}-1)$$

In 2.3.2 the inequality $V_5 > V_{1,2}$ is used and this can be considered as the event A . The probability \mathbf{P} of this event was stated to be $\frac{1}{2}$. In the stable case we had $N = 11$ and we found 9 cases A . The probability of finding 9 or more cases, according to (IV-1) is:

$$\sum_{k=9}^{11} \binom{11}{k} \left(\frac{1}{2}\right)^{11} = 0.033.$$

The other probabilities in 2.3.2 have been found by analogous means.

V. The method of least squares (par. 2.3.3)

The determination of a linear regression between two variables ξ and η , assuming that ξ is observed without error, whereas η is measured with error, is a classical statistical problem which has been solved completely. The resulting linear regression line is in fact the same as that given by the Lindley's method from II, if one substitutes $\sigma_{u_i} = \sigma_1 = 0$ and $k = \infty$.

In this case (II—3) changes into:

$$\tilde{\alpha} = \frac{S_{x,y}}{S_x^2}$$

and (II—1) will be left unchanged.

VI. The method of m -rankings

(par. 2.3.4)

The method of m -rankings is one of the older non-parametric methods and was developed by Friedman (M. G. Kendall, 1955).

If m series of k objects are available and the k objects in each series are ordered according to some property, the method of m -rankings can be used to test whether there is some significant agreement in the m -rankings or not. Let us introduce the null hypothesis that the rank orders of the m series are independent of each other. If the sum of the m rank numbers of the i^{th} object is called t_i , the expectation of t_i under the null hypothesis is $E t_i = \frac{1}{2}m(k + 1)$.

Now $h = \frac{\sum_{i=1}^k \{t_i - \frac{1}{2}m(k + 1)\}^2 - 1}{k(k - 1)}$ is introduced as a statistic.

$h = 0$ if all t_i 's are equal. The more the t_i -values differ, the larger h ; h reaches a maximum as soon as the rankings in the m series are completely equal.

TABLE VI—1 s values and rank numbers for the stable group

	KEYPS	Holzman	MO	Swinbank	Goptarev	Deacon	Power
I	14.7(7)	13.4(4)	13.9(5)	13.2(3)	14.1(6)	7.2(1)	10.4(2)
II	13.2(7)	11.9(4)	10.7(2)	11.6(3)	12.9(6)	5.8(1)	12.5(5)
III	12.7(2)	10.6(1)	20.4(5)	18.4(4)	14.0(3)	24.0(6)	33.6(7)
IV	5.8(7)	4.6(4)	3.6(3)	4.7(5)	5.5(6)	3.1(2)	3.0(1)
V	9.4(7)	7.0(4)	5.7(3)	2.3(1)	8.0(6)	3.0(2)	7.9(5)
VI	3.5(5)	2.1(2½)	1.8(1)	2.1(2½)	3.0(4)	6.2(6)	8.5(7)
VII	3.7(5)	2.6(3)	1.9(1)	2.3(2)	2.9(4)	5.7(6)	5.9(7)
VIII	2.4(1)	3.4(3)	4.6(5)	3.9(4)	2.7(2)	8.9(6)	9.0(7)
IX	3.7(1½)	4.0(4)	3.9(3)	3.7(1½)	4.2(5)	6.0(6)	9.0(7)
X	3.5(3)	3.6(4)	3.3(1½)	3.3(1½)	3.7(5)	4.2(6)	12.5(7)
XI	3.9(2)	3.1(1)	4.2(3½)	4.3(5½)	4.3(5½)	4.2(3½)	15.6(7)
t_i	47½	34½	33	33	52½	45½	62

TABLE VI—2 *s* values and rank numbers for the unstable group

	KEYPS	Holzman	MO	Swinbank	Goptarev	Deacon	Power
XII	4.7(2)	4.8(3)	5.4(5)	5.0(4)	5.6(6)	4.0(1)	23.8(7)
XIII	4.5(3)	4.7(4)	5.3(5)	4.4(1½)	6.0(6)	4.4(1½)	24.3(7)
XIV	3.8(3)	3.8(3)	4.0(6)	3.8(3)	4.4(3)	3.8(3)	18.9(7)
XV	2.5(2)	2.9(3½)	3.4(6)	3.2(5)	2.9(3½)	2.4(1)	15.4(7)
XVI	1.9(1)	2.5(3)	3.1(6)	2.6(4)	2.8(5)	2.2(2)	15.1(7)
XVII	3.1(2½)	3.1(2½)	4.3(6)	3.4(4½)	3.4(4½)	1.7(1)	11.2(7)
t_i	13½	19	34	22	28	9½	42

The frequency distribution of h has been derived exactly for a number of small m and k values and approximately for larger m and k values. Tables and nomograms are available.

For the eleven series I . . . XI ($m_1 = 11$) of seven s values ($k_1 = 7$) from table 2.3.3 and the six series XII . . . XVII ($m_2 = 6$) of seven s values ($k_2 = 7$) respectively, we give the s values and the corresponding rank numbers in table VI—1 and table VI—2 respectively.

Since $\frac{1}{2}m_1(k_1 + 1) = 44$ and $\frac{1}{2}m_2(k_2 + 1) = 24$ we find $h_1 = 13,25$ and $h_2 = 14,08$. The probability (\mathbf{P}) of finding such values or higher ones, if the null hypothesis is true, is, according to the nomogram (Statistische tabellen en nomogrammen, Stenfert Kroese N.V. - Leiden), $\approx 0,02$ and $< 0,01$ respectively. So on the 5% level of significance the null hypothesis has to be rejected; a significant agreement between the rankings exists. In other words: there is some real difference between the s values for the different formulae, or: one or more formulae seem to be better or worse than the others. As is stated in 2.3.4, this result is assumed to be due primarily to the power profile values of s , because in both cases the t_i values are the largest. The application of the test to the six cases that remain when the power profile is excluded leads to acceptance of the null hypothesis, even on the 10% level of significance for the stable group, and again rejection of the null hypothesis for the unstable group ($\mathbf{P} \leq 0,01$).

VII. Kendall's rank correlation test

(par. 2.3.7)

Kendall's rank correlation test is a test for rank order agreement of two series (x_i, y_i) of n observation pairs.

The application is very simple. Suppose that the x_i 's are ordered according to increasing size, that is $x_1 < x_2 < \dots < x_n$. Ranks r_i are assigned to the corresponding y_i 's. If complete "correlation" existed the rank numbers r_i would form the

series $1, 2, \dots, n$. If no correlation exists the ranks are a random permutation of the numbers $1, 2, \dots, n$. Let us introduce a statistic T : the number of pairs with $r_i > r_j$ minus the number of pairs with $r_i < r_j$. Under the null hypothesis (x and y are independent) T has a symmetrical distribution around zero. The exact distribution has been calculated for small values of $n (< 40)$. Tables are available. (Statistische Tabellen en Nomogrammen, Stenfert Kroese, Leiden.)

VIII. Fitting theoretical p curves to power profile exponent values from Lopik wind speed observations (par. 3.2.2)

p -values calculated according to (3.1.1) are available for seven mean wind speed groups and corresponding values of γ according to (3.1.2).

From figure 3.2.1 different values of ζ were determined for each p -value, denoted by $\zeta_i, i = 1, \dots, 9$. Here the index i denotes the value of ζ/ζ_0 , in such a way that $i = 1$ denotes $\zeta/\zeta_0 = 10, i = 2$ denotes $\zeta/\zeta_0 = 20$ etc.

ζ_1, \dots, ζ_4 was determined for each p in the wind speed group $u = 2.0 \dots 2.9$ (containing 48 p, γ pairs). For the other groups ζ_2, \dots, ζ_9 was determined, because from a rough graphical estimation it is clear that in the first case $\zeta/\zeta_0 \leq 100$ holds good and in the other $\zeta/\zeta_0 \geq 20$.

The next step was the determination of linear regression lines ζ_i on $x (= \gamma + 1)$ ($\gamma = -1$ is the adiabatic temperature lapse rate, and because of (3.3.5) we want to have $\zeta = 0$ for $\gamma = -1$).

The regression lines $\zeta_i = a_i x + b_i$ were determined for different i cases by the method of least squares. For this case we have assumed that the standard deviation of the measuring error of x is small compared to the standard deviation of the measuring error of ζ_i .

The values of b within each \bar{u} group prove to form a clearly increasing function of $\ln \zeta/\zeta_0$. So it is easy to determine graphically that value $(\zeta/\zeta_0)^*$ of ζ/ζ_0 for which $b = 0$. In this way we obtained 7 values $(\zeta/\zeta_0)^*$. A corresponding graph of a_i against $\ln(\zeta/\zeta_0)_i$ within each \bar{u} group yields the value a^* for $(\zeta/\zeta_0)^*$ corresponding to $b = 0$. In this way the 7 values of $\zeta/\zeta_0 = z/z_0$ and a , mentioned in table 3.2.1, have been found. The * is omitted.

For the least squares estimates \tilde{a}_i and \tilde{b}_i the standard deviations are determined according to the well-known formulae which can be found in most textbooks on statistics (viz. Pfanzagl, 1962).

REFERENCES

- Barad, M. L. 1958 Project Prairie Grass. A Field Program in Diffusion. Geoph. Res. Pap. No. 59. G. R. D. Bedford, Mass. U.S.A.
- Barry, P. J. 1966 The wind profile. Paper presented at Nat. Met. Congress, Sherbrooke, P.Q. June 8-10. AECL 2574.
- Benard, A. and Bos-Levenbach, E. C. 1953 Het uitzetten van waarnemingen op waarschijnlijkheidspapier. *Statistica (Neerlandica)* 7, p. 163-173.
- Businger, J. A. 1954 Some aspects of the influence of the earth's surface on the atmosphere. *Med. en Verh.* 61. Royal Neth. Met. Inst. De Bilt.
- Businger, J. A. 1959 A generalization of the mixing length concept. *Journ. of Met.* 16-5, p. 516-523.
- Businger, J. A. 1961 On the relation between the spectrum and the diabatic wind profile. *Journ. Geoph. Res.* 66-8, p 2405-2409.
- Calder, K. L. 1949 The criterion of turbulence in a field of variable density with particular reference to conditions in the atmosphere. *Q. J. Roy. Met. Soc.* 75, p 71-88.
- Deacon, E. L. 1949 Vertical diffusion in the lower layer of the atmosphere. *Q. J. Roy. Met. Soc.* 75, p 89-103.
- Ellison, T. H. 1957 Turbulent transport of heat and momentum from an infinite rough plane. *Journ. Fluid Mech.* 2-5, p 456-466.
- Frost, R. 1947 The velocity profile in the lowest 400 ft. *Met. Mag.* 76, p 14-17.
- Goptarev, N. P. 1960 On the influence of dynamic and thermal factors on the wind speed above the sea and on the motion at the sea surface. (In Russian.) *Trudy Gosp. Okean. Inst.* 51, p 5-23.
- Hollmann, G. 1961 Die Abhängigkeit des Anisotropiegrades der Turbulenz von der Schichtung. *V.D.I. Forschungsheft* 483-27, p. 29-32.
- Holzman, B. 1943 The influence of stability on evaporation. *Ann. N.Y. Ac. Sc.* 44, p 13-18.

- Ito S. 1966 Atmospheric diffusion in the earth's boundary layer.
The Geoph. Mag. 33-1, p. 1-70.
- Kazansky, A. B. and Monin, A. S. 1956 Turbulence in the inversion layer near the surface. (In Russian.)
Izv. Ak. Nauk. S.S.S.R. ser. Geoph. No. 1.
- Kendall, M. G. 1955 Rank correlation methods.
Griffin and Co. London.
- Klug, W. 1963 Zum vertikalen Windprofil.
Beitr. Phys. Atm. 36-3/4, p. 226-253.
- Kondo, J. 1962 Observations on wind and temperature profiles near the ground.
Sc. Rep. Tôhoku Univ. 14-2, p. 41-56.
- Lake, H. 1952 A comparison of the power law and a generalized logarithmic formula in micrometeorology.
Trans. Am. Geoph. Union. 33-5, p. 661-668.
- Lettau, H. H. 1949 Isotropic and nonisotropic turbulence in the atmospheric surface layer.
Geoph. Res. Pap. No 1 G.R.D. U.S. Air Force, Cambridge, Mass. (U.S.A.)
- Lettau, H. H. and Davidson, B. 1957 Exploring the atmosphere's first mile.
Pergamon Press, London etc.
- Levert, C. 1959 Een nomogram voor betrouwbaarheids grenzen van quantielen in overschrijdingskansen bij normaal verdeelde grootheden.
Statistica (Neerlandica) 13, p. 3-14.
- Lindley, D. V. 1947 Regression lines and the linear functional relationship.
Suppl. Journ. Roy. Stat. Soc. 9-II, p. 218-244.
- Monin, A. S. and Obukhov, A. M. 1954 Fundamentale Gesetzmäßigkeiten der turbulenten Vermischung in der bodennahen Schicht der Atmosphäre. (German transl. from Ak. Nauk. S.S.S.R. Trudy. Geof. Inst. 24 (151), 1954.)
Sammelband zur statistischen Theorie der Turbulenz. Akad. Verlag Berlin 1958, p. 199-224.
- Naito, K. 1964 Some remarks on the Monin-Obukhov function in the atmosphere near the ground.
Journ. Met. Soc. Japan 42-1, p. 53-63.

- Pandolfo, J. P. 1966 Wind and temperature profiles for constant flux boundary layers in lapse conditions with a variable eddy conductivity to eddy viscosity ratio. *Journ. Atm. Sc.* 23-5, p. 495-502.
- Panofsky, H. A., Blackadar, A. K. and McVehill, G. E. 1960 The diabatic wind profile. *Q. J. Roy. Met. Soc.* 86, p. 390-398.
- Panofsky, H. A. 1961 Alternative derivation of the diabatic wind profile. *Q. J. Roy. Met. Soc.* 87, p. 109-110.
- Pfanzagl, J. 1962 *Algemeine Methodenlehre der Statistik. II Höhere Methoden.* Sammlung Göschen Bd. 747/747a.
- Roll, H. U. 1965 *Physics of the marine atmosphere.* Int. Geoph. Ser. 7, New York-London.
- Rosby, C. G. and Montgomery, R. B. 1935 The layer of frictional influence in wind and ocean currents. *Pap. in Phys. Ocean and Met. M.I.T. and Woods Hole Inst.* 3, No 3.
- Saïssac, J. 1960 *Profil du vent et gradient vertical de température.* Notes de l'Étab. d'Études et de Rech. No 50. Dir. de la Mét. Nat. de France.
- Schubauer, G. B. and Tchen, C. M. 1961 *Turbulent Flow.* Princeton Aeronautical Paperbacks No 9. Princeton Univ. Press, Princeton N.J.
- Sellers, W. D. 1962 A simplified derivation of the diabatic wind profile. *Journ. Atm. Sc.* 19-2, p. 180-181.
- Shiotani, M. 1962 The relationship between wind profiles and stabilities of the layer in the outskirts of the city. *Journ. Met. Soc. Japan* 40-6, p. 315-329.
- Singer, I. A. and Nagle, C. M. 1962 A study of the wind profile in the lowest 400 ft. of the atmosphere. Brookhaven Nat. Lab. BNL 718. Final Report. Upton, N.Y.
- Su, Tsung-Shian 1958 The turbulence in the surface layer of the stratified atmosphere. *Acta Met. Sinica.* 29-2, p. 73-82.

- Sutton, O. G. 1953 Micrometeorology.
McGraw-Hill Publ. Co. Ltd., New York.
- Swinbank, W. C. 1964 The exponential wind profile.
Q. J. Roy. Met. Soc. 90, p. 119-153.
- (Swinbank, W. C.) 1966 Discussion on a paper of . . .
The exponential wind profile.
Q. J. Roy. Met. Soc. 92, p. 416-426.
- Townsend, A. A. 1965 The response of a turbulent boundary layer to
abrupt changes in surface conditions
Journ. Fluid. Mech. 22-4, p. 799-822.
- Udny Yule, G. and
Kendall, M. G. 1965 An introduction to the theory of statistics.
Griffin and Co., London.
- Yamamoto, G. 1959 Theory of turbulent transfer in non-neutral condi-
tions.
Journ. Met. Soc. Japan 37-2, p. 60-67.
- Vereniging voor Statistiek Statistische Tabellen en Nomogrammen.
Stenfert Kroese N.V., Leiden.

SUMMARY

The literature on meteorology contains a large number of formulae worked out to describe the increase of wind speed with height under non-adiabatic atmospheric conditions.

A few of the formulae proposed have a purely mathematical significance and the only requirement they fulfil is that they shall transform into the logarithmic profile in neutral conditions. The formulae based on a physical reasoning rest solely on a simplified balance equation. This equation contains, on one side, terms which refer to mechanical and convective turbulence respectively, and on the other side a term representing the total turbulent energy or energy dissipation. A generally accepted mathematical expression in the characteristic basic quantities can be found for the first two terms, but unfortunately this is not the case for the last term. Various authors have attempted to find an analytical form for this term. The attempts are based mainly on dimensional considerations.

In the present study the formulae have been combined as far as possible to form one mathematical system, whereby one manageable whole has been obtained.

The study is divided into three parts. Chapter 1 gives the derivation of the general system and a number of mathematical particulars. Chapter 2 gives applications with the aid of observations made in O'Neill, Nebraska (USA) in 1953 and 1956. These applications must be regarded as examples only, because the accuracy of the observations is not quite sufficient. Finally, the so-called power law is dealt with in a short third chapter.

The basic quantities and symbols having been defined in section 1.1, a number of wind profile formulae are reviewed in section 1.2, where also a few particulars of the derivations are given.

In 1.3 two derivations (KEYPS and Businger) are generalized. Two groups of equations then appear (Plus and Minus groups) for logarithmic non-dimensional wind gradient as a function of the stability parameter ζ . These groups prove to transform into one another by a simple mathematical transformation. For the sake of simplicity the two groups are brought together in one general formula, while a general solution in parameter form is given for the wind profile.

In 1.4 a number of special cases from the various groups are dealt with, including of course, the KEYPS and Businger formulae.

Two well-known empirical formulae, the power law and the Deacon profile, do not fit into the system. The Swinbank formula, however, which is not directly included in the system, can be made to relate to the system. (par. 1.5).

In the majority of articles on the subject it is customary to use the quantity S as a function of ζ , and to present in the form of a graph not only the „theoretical” function,

but also estimated values of S and ζ from observations, in order to test the formulae in this way. One objection to this method is the fact that both S and ζ contain the friction-velocity u_* and the measuring error in u_* affects the shape of the graph. (This is investigated more thoroughly in Chapter 2.) In Section 1.6, a wind speed difference ratio V is introduced. This is also a function of ζ , but the same objection does not arise. The mathematical properties of V in the various profile formulae are further investigated.

Chapter 2 makes use in the first place of a number of observations from the 1953 experiments at O'Neill (Great Plains Turbulence Field Program). These are wind speed measurements at four levels and measurements of heat flux and friction velocity at three levels.

The objection to the S - ζ graph is demonstrated in Section 2.1.

The usefulness of a number of formulae is investigated by means of the V - ζ graph in par. 2.2. The tentative conclusion (taking into account the unreliability of the observations) is that there is no difference in usability between the Swinbank, Goptarev and Holzman profile formulae. All three are probably usable for a fairly large range of stability. Others, such as KEYPS and MO, are certainly as they stand not usable for a large range of ζ values.

In par. 2.3 use is made of a series of measurements of wind speed at seven levels between $\frac{1}{4}$ and 16 m. taken from the Project Prairie Grass (O'Neill 1956). No measurements of u_* and H are available here, so there can be no question of testing, but only of fitting.

The Deacon and power law formulae have been used for fitting as well as five formulae from the system. The KEYPS, Holzman, Swinbank and Goptarev formulae were found to fit almost equally well.

The power law proves to fit considerably less well in unstable situations, and the reasons for this are explained; while MO seems to be slightly less favourable in stable situations.

A reasonable fit can be obtained with Deacon, but in stable situations it was found that a serious objection attached to the formula, is that negative u_* and complex z_0 values appear.

The mathematical explanation for this phenomenon is found.

A notable result of the fitting process is the fact that large z_0 values occur in stable situations. This variation of z_0 proves to be connected with the average wind speed.

The third chapter is devoted entirely to the power law. Although this formula has no physical basis whatever, it is useful to investigate what can be done with it; the fact is that the formula is often applied because of its simplicity.

The investigation conducted here is based on observations at Lopik (central Netherlands). The power law exponent p was found to vary as a function of tempera-

ture and mean speed. It also proved possible to derive this variation from the Holzman formula. (In theory it should be possible to select a different formula instead of Holzman.)

A secondary result was that here too z_0 was found to increase with decreasing wind speeds. An attempt is made to explain this z_0 variation in physical terms.

Explanatory notes to the statistical methods employed are given in appendices.

SAMENVATTING

In de meteorologische literatuur is een groot aantal formules ontwikkeld om de toename van de windsnelheid met de hoogte in niet-adiabatische atmosferische omstandigheden te beschrijven.

Enkele van de voorgestelde formules hebben uitsluitend een mathematische betekenis en voldoen alleen aan de eis dat ze voor neutrale omstandigheden in het logaritmische profiel overgaan. De formules die een enigszins fysische basis bezitten berusten alle op een vereenvoudigde balans-vergelijking, waarin enerzijds termen voorkomen die respectievelijk betrekking hebben op de mechanische en de convectieve turbulentie en anderzijds een term die de totale turbulente energie of energiedissipatie voorstelt. Voor de eerste twee termen is een algemeen aanvaarde mathematische uitdrukking te geven in de karakteristieke basisgrootheden. Voor de laatste term is dit helaas niet het geval. Diverse auteurs hebben gepoogd voor deze term een analytische vorm te vinden. Deze pogingen berusten hoofdzakelijk op dimensiebeschouwingen.

In deze studie worden deze formules voor zover mogelijk in een mathematisch systeem samengevat, waardoor een overzichtelijk geheel wordt verkregen.

De studie bestaat uit drie gedeelten. Hoofdstuk 1 geeft de afleiding van het algemene systeem en een aantal mathematische bijzonderheden. Hoofdstuk 2 geeft toepassingen met behulp van waarnemingen die in 1953 resp. 1956 in O'Neill-Nebraska-U.S.A. werden verricht. Deze toepassingen moeten gezien worden als voorbeelden omdat de kwaliteit van de waarnemingen vrij matig is. In een klein 3de hoofdstuk werd tenslotte de z.g. machtwet behandeld.

Nadat in 1.1 de basisgrootheden en symbolen zijn gedefinieerd, wordt in 1.2 een overzicht gegeven van een aantal windprofiel formules en enkele bijzonderheden van de afleidingen.

In 1.3 worden twee afleidingen (KEYPS en Businger) gegeneraliseerd. Er ontstaan dan twee groepen vergelijkingen (Plus en Minus groepen) voor de logaritmische dimensieloze windgradiënt als functie van de hoogte-stabiliteits parameter ζ . Deze groepen blijken door een eenvoudige mathematische transformatie in elkaar over te gaan. Gemakshalve worden beide groepen in één algemene formule samengevat, terwijl een algemene oplossing in parametervorm voor het windprofiel gegeven wordt.

In 1.4 worden een aantal bijzondere gevallen van de verschillende groepen behandeld, waaronder uiteraard de KEYPS formule en die van Businger.

Een tweetal bekende empirische formules nl. de machtwet en het Deacon profiel passen niet in het systeem. Wel kan de formule van Swinbank, die niet rechtstreeks in het systeem is ingesloten, met dit systeem in relatie worden gebracht (par. 1.5).

In de meeste artikelen in de literatuur is het gebruikelijk de grootheid S als functie van ζ te gebruiken en in grafiek te brengen (zowel de "theoretische" functie, als ook

schattingen van S en ζ uit waarnemingen) om op deze wijze de formules te toetsen. Een bezwaar van deze methode is het feit dat zowel S als ζ de schuifspanningssnelheid u_* bevatten, en de meetfout in deze u_* beïnvloedt het beeld van de grafiek. (Hierop wordt in het 2de hoofdstuk nader ingegaan.) In 1.6 wordt een windsnelheidsverschilverhouding V ingevoerd, die eveneens een functie van ζ is, maar genoemd bezwaar niet heeft. De mathematische eigenschappen van V worden nader onderzocht.

In het tweede hoofdstuk worden in de eerste plaats uit het 1953 onderzoek te O'Neill (Great Plains Turbulence Field Program) een aantal waarnemingen gebruikt nl. windsnelheidsmetingen van vier niveaus en metingen van warmteflux en schuifspanningssnelheid van drie niveaus.

In 2.1 wordt het bezwaar van de (S, ζ) grafiek aangetoond.

In 2.2 wordt de bruikbaarheid van een aantal formules via de (V, ζ) grafiek onderzocht. De voorlopige conclusie (in verband met de onbetrouwbaarheid van de waarnemingen) is dat tussen de Swinbank, Goptarev en Holzman profielformules geen verschil in bruikbaarheid is te constateren. Alle drie zijn waarschijnlijk voor een vrij groot stabiliteitsgebied bruikbaar. Enkele andere, b.v. KEYPS en MO, zijn bepaald niet zonder meer voor een groot gebied van ζ waarden bruikbaar.

In 2.3 worden uit het materiaal van het Project Prairie Grass (O'Neill 1956) series metingen van de windsnelheid op zeven niveaus tussen $\frac{1}{4}$ en 16 m gebruikt. Er zijn hierbij geen metingen van u_* en H beschikbaar, zodat van toetsing geen sprake kan zijn, maar slechts van aanpassing.

Naast vijf formules uit het systeem werden de Deacon en machtwet formules gebruikt voor de aanpassing. Het blijkt hierbij dat de aanpassingsmogelijkheden voor de KEYPS, Holzman, Swinbank en Goptarev formules nagenoeg gelijk zijn.

De machtwet blijkt in onstabiele situaties aanzienlijk minder goed aan te sluiten, dan de overige formules. Dit is plausibel te maken. In stabiele situaties is MO misschien iets ongunstiger dan de overige formules.

Met Deacon kan een redelijke aanpassing worden verkregen, echter blijkt er in stabiele situaties een ernstig bezwaar aan de formule te kleven; er kunnen dan n.l. negatieve u_* en complexe z_0 waarden ontstaan. De mathematische verklaring van dit effect is nagegaan.

Een opmerkelijk resultaat van de aanpassing is nog het feit dat in stabiele situaties grotere z_0 waarden voorkomen dan in onstabiele. Deze variatie van z_0 blijkt met de gemiddelde windsnelheid samen te hangen.

Het derde hoofdstuk is speciaal aan de machtwet gewijd. Hoewel deze formule in het geheel geen fysische basis heeft is het toch nuttig na te gaan wat er mee gedaan kan worden; het is tenslotte zo dat de formule wegens zijn eenvoud vaak toegepast wordt.

Het hier uitgevoerde onderzoek is gebaseerd op waarnemingen te Lopik (centrum

Nederland). Het bleek dat de machtwetexponent p varieert als functie van de temperatuur en de gemiddelde snelheid. Verder bleek het mogelijk dit verloop af te leiden uit b.v. de Holzman formule.

Als bijkomstig resultaat kon ook hier een toename van z_0 bij afnemende wind worden geconstateerd. Getracht is deze z_0 variatie fysisch plausibel te maken.

In een aanhangsel zijn tenslotte de toegepaste statistische methoden nader toegelicht.

Van de reeks MEDEDELINGEN EN VERHANDELINGEN zijn bij het Staatsdrukkerij- en Uitgeverij-bedrijf nog verkrijgbaar de volgende nummers:

23, 25, 26, 27, 29b, 30, 31, 34b, 35, 36, 37, 38, 39, 40, 42, 43, 44, 45, 46, 47, 48, 49, 50, 51, 52, 53, 54, 55, 56, 57, 58, 59,

alsmede

60. C. Kramer, J. J. Post en J. P. M. Woudenberg. Nauwkeurigheid en betrouwbaarheid van temperatuur- en vochtigheidsbepalingen in buitenlucht met behulp van kwikthermometers. 1954. (60 blz. met 11 fig.)	3,50
62. C. Levert. Regens. Een statistische studie. 1954. (246 blz. met 67 fig. en 143 tab.)	10,00
63. P. Groen. On the behaviour of gravity waves in a turbulent medium, with application to the decay and apparent period increase of swell. 1954. (23 blz.)	1,50
64. H. M. de Jong. Theoretical aspects of aeronavigation and its application in aviation meteorology. 1956. (124 blz. met 80 fig., 9 krt. en 3 tab.)	4,50
65. J. G. J. Scholte. On seismic waves in a spherical earth. 1956. (55 blz. met 24 fig.)	5,00
66. G. Verploegh. The equivalent velocities for the Beaufort estimates of the wind force at sea. 1956. (38 blz. met 17 tab.)	1,75
67. G. Verploegh. Klimatologische gegevens van de Nederlandse lichtschepen over de periode 1910—1940.	
Deel I: Stormstatistieken. — Climatological data of the Netherlands light-vessels over the period 1920—1940. P. I.: Statistics of gales. 1956. (68 blz. met tabellen)	3,50
Deel II: Luchtdruk en wind; zeevang. — Climatological data of the Netherlands light-vessels over the period 1910—1940. P. II: Air pressure and wind; state of the sea. 1958. (91 blz. met tabellen.)	7,50
Deel III: Temperaturen en hydrometeoren; onweer. — Climatological data of the Netherlands light-vessels over the period 1910—1940. P. III: temperatures and hydrometeors; thunderstorms. 1959. (146 blz. met tabellen.)	8,00
68. F. H. Schmidt. On the diffusion of stack gases in the atmosphere. 1957. (60 blz., 12 fig. en tab.)	5,00
69. H. P. Berlage. Fluctuations of the general atmospheric circulation of more than one year; their nature and prognostic values. 1957	7,50
70. C. Kramer. Berekening van de gemiddelde grootte van de verdamping voor verschillende delen van Nederland volgens de methode van Penman. 1957. (85 blz., fig. en tab.)	7,00
71. H. C. Bijvoet. A new overlay for the determination of the surface wind over sea from surface weather charts. 1957. (35 blz., fig. en tab.)	2,50
72. J. G. J. Scholte. Rayleigh waves in isotropic and anisotropic elastic media. 1958. (43 blz., fig. en tab.)	3,00
73. M. P. H. Weenink. A theory and method of calculation of wind effects on sea levels in a partly-enclosed sea, with special application to the southern coast of the North Sea. 1958. (111 blz. met 28 fig. en tab.)	8,00
74. H. M. de Jong. Geostrophic flow. Geostrophic approximation in the upper air flow with application to aeronavigation and air trajectories. 1959. (100 blz. met 17 fig., 14 krt. en 2 tab.)	5,00
75. S. W. Visser. A new analysis of some features of the 11-year and 27-day cycles in solar activity and their reflection in geophysical phenomena. 1959. (65 blz. met 16 fig. en 12 tab.)	3,50
76. A. R. Ritsema and J. Veldkamp. Fault plane mechanisms of South East Asian earthquakes. 1960. (63 blz. met 26 fig. en 11 tab.)	4,00

77. G. Verploegh. On the annual variation of climatic elements of the Indian Ocean. P. I: text. P. II: charts. 1960. (64 blz., 15 fig., 28 krt.)	6,00
78. J. A. As. Instruments and measuring methods in paleomagnetic research. 1960. (56 blz., 20 fig.)	2,50
79. D. J. Bouman. Consistency of approximations in discontinuous fields of motion in the atmosphere with an introduction to the use of generalized functions or distributions in meteorology. 1961. (94 blz., 6 fig.)	6,50
80. H. Timmerman. The influence of topography and orography on the precipitation patterns in the Netherlands. 1963. (49 blz., 37 fig. en 5 tab.)	6,50
81. A. W. Hanssen & W. J. A. Kuipers: On the relationship between the frequency of rain and various meteorological parameters (with reference to the problem of objective forecasting). 1965. (77 blz., 18 fig. en 12 tab.)	10,00
82. G. A. de Weille: Forecasting crop infection by the potato blight fungus. A fundamental approach to the ecology of a parasite — host relationship. 1964. (144 blz., 37 fig. en 37 tab.)	14,50
83. H. J. de Fluiter, P. H. van de Pol, J. P. M. Woudenberg (redactie) e.a. Fenologisch en faunistisch onderzoek over boomgaardinsekten. Phenological and faunistic investigations on orchard insects. 1964. (226 blz., 84 fig. en 59 tab.)	9,25
84. D. J. Bouman & H. J. de Jong: Generalized theory of adjustment of observations with applications in meteorology. 1964. (89 blz., 8 fig. en 1 tab.)	11,00
85. L. Otto: Results of current observations at the Netherlands lightvessels over the period 1910—1939. P. 1. Tidal analysis and the mean residual currents. 1964. (56 blz. en 8 tab.)	6,25
86. F. H. Schmidt: An analysis of dust measurements in three cities in the Netherlands. 1964. (68 blz., 14 fig. en 22 tab.)	5,50
87. Commissie Meteorologische Voorlichting van Straalvliegtuigen: Climatology of Amsterdam Airport (Schiphol). 1966. (145 blz., 6 fig., 10 tab.)	16,50
88. H.P. Berlage: The southern oscillation and world weather. 1966. (152 blz., 46 fig., 34 tab.)	15,50
89. G. Verploegh: Observation and analysis of the surface wind over the ocean. 1967. (67 blz., 14 tab., 4 krtn.)	6,50
90. R. Dorrestein: Wind and wave data of Netherlands lightvessels since 1949. 1967. (123 blz., 22 tab.)	15,50